

Copyright Warning & Restrictions

The copyright law of the United States (Title 17, United States Code) governs the making of photocopies or other reproductions of copyrighted material.

Under certain conditions specified in the law, libraries and archives are authorized to furnish a photocopy or other reproduction. One of these specified conditions is that the photocopy or reproduction is not to be “used for any purpose other than private study, scholarship, or research.” If a user makes a request for, or later uses, a photocopy or reproduction for purposes in excess of “fair use” that user may be liable for copyright infringement,

This institution reserves the right to refuse to accept a copying order if, in its judgment, fulfillment of the order would involve violation of copyright law.

Please Note: The author retains the copyright while the New Jersey Institute of Technology reserves the right to distribute this thesis or dissertation

Printing note: If you do not wish to print this page, then select “Pages from: first page # to: last page #” on the print dialog screen

The Van Houten library has removed some of the personal information and all signatures from the approval page and biographical sketches of theses and dissertations in order to protect the identity of NJIT graduates and faculty.

ABSTRACT

FUNCTIONALIZED CARBON NANOTUBES IN HYDROPHOBIC DRUG DELIVERY

**by
Kun Chen**

The direct incorporation of carboxylated carbon nanotubes (f-CNTs) into hydrophobic drug particles during their formation via anti-solvent precipitation is presented. The approach is tested using two drugs namely antifungal agent Griseofulvin (GF) and antibiotic Sulfamethoxazole (SMZ) that have very different aqueous solubility. It is observed that the f-CNTs dispersed in the water serve as nucleating sites for crystallization and are readily incorporated into the drug particles without altering crystal structure or other properties. The results show that the hydrophilic f-CNTs dramatically enhance dissolution rate for both drugs. The increased degree of functionalization leads to higher hydrophilicity and therefore faster dissolution rate. The enhanced dissolution is attributed to the fact that the hydrophilic f-CNTs serve as conduits for bringing in water in close contact with the drug crystals. Particle size and sedimentation monitoring studies show incorporation of f-CNTs reduces hydrophobic particle size and slows sedimentation. Increased carboxylation of f-CNTs results in smaller particle sizes and slower sedimentation rates.

**FUNCTIONALIZED CARBON NANOTUBES IN
HYDROPHOBIC DRUG DELIVERY**

**by
Kun Chen**

**A Dissertation
Submitted to the Faculty of
New Jersey Institute of Technology
in Partial Fulfillment of the Requirements for the Degree of
Doctor of Philosophy in Chemistry**

Department of Chemistry and Environmental Science

December 2018

Copyright © 2018 by Kun Chen

ALL RIGHTS RESERVED

APPROVAL PAGE

**FUNCTIONALIZED CARBON NANOTUBES IN
HYDROPHOBIC DRUG DELIVERY**

Kun Chen

Dr. Somenath Mitra, Dissertation Advisor
Distinguished Professor of Chemistry and Environmental Science, NJIT

Date

Dr. Tamara Gund, Committee Member
Professor of Chemistry and Environmental Science, NJIT

Date

Dr. Edgardo T. Farinas, Committee Member
Associate Professor of Chemistry and Environmental Science, NJIT

Date

Dr. Yong I. Kim, Committee Member
Assistant Professor of Chemistry and Environmental Science, NJIT

Date

Dr. Robert B. Barat, Committee Member
Professor of Chemical and Materials Engineering, NJIT

Date

BIOGRAPHICAL SKETCH

Author: Kun Chen

Degree: Doctor of Philosophy

Date: December 2018

Undergraduate and Graduate Education:

- Doctor of Philosophy in Chemistry,
New Jersey Institute of Technology, Newark, NJ, 2018
- Master of Science in Pharmaceutical Chemistry,
New Jersey Institute of Technology, Newark, NJ, 2012
- Bachelor of Science in Pharmaceutical Science,
China Pharmaceutical University, Nanjing, Jiangsu, P. R. China, 2010

Major: Chemistry

Presentations and Publications:

Chen, K. and Mitra, S., Incorporation of functionalized carbon nanotubes into hydrophobic drug crystals for enhancing aqueous dissolution, *Colloids and Surfaces B: Biointerfaces* **2019**, 173, 386-391

Chen, K. and Mitra, S., Controlling the dissolution rate of hydrophobic drugs by incorporating carbon nanotubes with different levels of carboxylation, *Journal of Drug Delivery Science and Technology*, under review

Wang, Z., Meng, X., Chen, K. and Mitra, S., Development of high-capacity periodate battery with three-dimensional-printed casing accommodating replaceable flexible electrodes, *ACS Applied Materials & Interfaces* **2018**, 10 (36), 30257-30264

Zhu, Y., Chen, K., Yi, C., Mitra, S. & Barat, R., Dry reforming of methane over palladium–platinum on carbon nanotube catalyst, *Chemical Engineering Communications* **2018**, 205 (7), 888-896

Wang, Z., Meng, X., Chen, K. and Mitra, S., Synthesis of carbon nanotube incorporated metal oxides for the fabrication of printable, flexible nickel-zinc batteries, *Advanced Materials Interfaces* **2017**, 5 (4), 1701036

Desai, C., Chen, K. and Mitra, S., Aggregation behavior of nanodiamonds and their functionalized analogs in an aqueous environment, *Environmental Science: Processes and Impacts* **2014**, 16 (3), 518-523

I would like to dedication this dissertation to my wife, Qianqian Liu who has provide enormous support for my research all these years and to my newborn son, Jason Xiaofan Chen who has been my motivation to surmount any obstacles.

ACKNOWLEDGMENT

I would like to thank Dr. Somenath Mitra for his support and guidance in my research, I would also like to thank Dr. Edgardo Farinas, Dr. Tamara Gund, Dr. Yong-Ick Kim and Dr. Robert B. Barat for providing valuable suggestions as committee members.

Thank to the National Institute of Environmental Health Sciences (NIEHS: R01ES023209) for funding my research and the Department of Chemistry and Environmental Science for financial support.

My appreciation to Dr. Larisa Krishtopa, Dr. Xueyan Zhang, Dr. Jeong Seop Shim, Mr. Yogesh Gandhi for experiment support.

Thanks also to the former Mrs. Gayle Katz, Mrs. Sylvana L. Brito and Mrs. Genti M. Price for all their administrative help.

Finally thanks to my research group members: Dr. Zhiqian Wang, Dr. Zheqiong Wu, Dr. Megha Thakkar, Dr. Roy Sagar, as well as Xianyang Meng, Samar Azizighannad, Emine Songul Karaman and Worawit Intrchom.

TABLE OF CONTENTS

Chapter	Page
1 INTRODUCTION.....	1
1.1 Objective	1
1.2 Drug Delivery System	1
1.3 Hydrophobic Drugs	5
1.4 Size Reduction of Drug Particles	7
1.4.1 Dissolution Enhancement through Size Reduction	7
1.4.2 Drug Particle Formation Techniques	8
1.4.2.1 Top-down Techniques	9
1.4.2.2 Bottom-up Techniques	10
1.5 Functionalized Carbon Nanotubes	13
1.5.1 Covalent Functionalization.....	14
1.5.2 Non-covalent Functionalization	16
1.6 CNT-Loaded Drug for Drug Delivery	18
2 INCORPORATION OF FUNCTIONALIZED CARBON NANOTUBES INTO HYDROPHOBIC DRUG CRYSTALS FOR ENHANCING AQUEOUS DISSOLUTION	23
2.1 Introduction	23
2.2 Materials and Methods	26
2.2.1 Materials	26
2.2.2 Methods	26
2.3 Results and Discussion	28

TABLE OF CONTENTS
(Continued)

Chapter	Page
2.4 Conclusion.....	39
3 CONTROLLING THE DISSOLUTION RATE OF HYDROPHOBIC DRUGS BY INCORPORATING CARBON NANOTUBES WITH DIFFERENT LEVELS OF CARBOXYLATION.....	40
3.1 Introduction	40
3.2 Materials and Methods	42
3.2.1 Materials	42
3.2.2 Methods	43
3.3 Results and Discussion	44
3.4 Conclusions.....	54
4 COLLOIDAL BEHAVIOR OF DRUG/CNTS COMPOSITE PARTICLES	55
4.1 Introduction	55
4.2 Materials and Methods	56
4.2.1 Materials	56
4.2.2 Methods	57
4.3 Results and Discussion	59
4.3.1 Characterizations	59
4.3.2 Particle Size Analysis for Drug Suspensions	61
4.3.3 Sedimentation Rate	65
4.4 Conclusions.....	67
REFERENCES	68

LIST OF TABLES

Table	Page
1.1 Biopharmaceutics Classification System	6
2.1 Dissolution and Melting Point of SMZ-CNTs and GF-CNTs	37
3.1 Analysis of f-CNTs with Different Levels of Functionalization.....	45
3.2 Dissolution and Melting Point of SMZ-CNT _x and GF-CNT _x	52
4.1 I _D /I _G of Raw CNTs and f-CNTs with Different Treatment Time	60
4.2 Stabilizing SMZ with f-CNTs	63

LIST OF FIGURES

Figure	Page
1.1 Routes of Administration.....	2
1.2 Process of anti-solvent precipitation.....	11
1.3 Mechanism of anti-solvent precipitation.....	12
2.1 (a) SEM image of f-CNTs, (b) Incorporation of f-CNTs in drug composites as a function of concentration of f-CNTs in the dispersion, (c) XRD spectra of f-CNTs, RAMAN spectra of (d) Raw CNTs and (e) f-CNTs.....	28
2.2 TGA curve of drug and drug incorporated with different amount of f-CNTs: (a) GF-CNT and (b) SMZ-CNT.	31
2.3 SEM images of (a) Pure GF and (b) GF-CNT-2.4	32
2.4 SEM images of (a) Pure SMZ and (b) SMZ-CNT-1.4	32
2.5 TEM images of (a) GF-CNT-4.0 and (b) GF-CNT-2.7	33
2.6 RAMAN spectra of pure GF and GF incorporated with different amount of f-CNTs.....	34
2.7 RAMAN spectra of pure SMZ and SMZ incorporated with different amount of f-CNTs.....	34
2.8 XRD spectra of pure GF and GF incorporated with different amount of f-CNTs.	35
2.9 XRD spectra of pure SMZ and SMZ incorporated with different amount of f-CNTs.....	36
2.10 Dissolution of (a) SMZ-CNTs and (b) GF-CNTs showed enhanced dissolution with the incorporation of f-CNTs in drug crystals.....	38
3.1 TGA of different GF-CNT _x	46
3.2 SEM image of (a) GF-CNT _{23.2} , (b) GF-CNT _{19.8} , (c) GF-CNT ₁₆ , (d) SMZ-CNT _{23.2} , (e) SMZ-CNT _{19.8} , (f) SMZ-CNT ₁₆ , (g) Pure GF, (h) Pure SMZ, TEM image of (i) GF-CNT ₁₆	47

LIST OF FIGURES
(Continued)

Figure	Page
3.3 RAMN spectra of f-CNT _{23.2} and (a) GF- CNT _x , (b) SMZ- CNT _x	49
3.4 XRD spectrum of (a) GF- CNT _x and (b) SMZ- CNT _x	50
3.5 (a) Dissolution of GF-CNT _x , (b) Dissolution of SMZ-CNT _x (c) Time to reach 80% dissolved for drug with degree of functionalization of f-CNTs.....	52
4.1 Anti-solvent precipitation of drug/f-CNTs.....	58
4.2 EDX of carbon and oxygen ration of raw CNTs and f-CNTs with different treatment time	59
4.3 Raman spectroscopy of raw CNTs and f-CNTs with different treatment time	60
4.4 FTIR spectroscopy of pure SMZ, SMZ-CNT _{23.2} , SMZ-CNT _{19.8} , SMZ-CNT _{18.5} and SMZ-CNT _{16.0}	61
4.5 Size distribution of pure SMZ, SMZ-CNT _{23.2} , SMZ-CNT _{19.8} , SMZ-CNT _{18.5} and SMZ-CNT _{16.0}	62
4.6 (a) Mean radius of pure SMZ and SMZ-CNT _{23.2} as a function of time, (b) Mean radius of SMZ-CNT _x as a function of time	64
4.7 Electrostatic double layers of drug/f-CNTs composites	65
4.8 Weight percentage of stabilized drug particles in suspension for Pure SMZ, SMZ-CNT _{23.2} , SMZ-CNT _{19.8} , SMZ-CNT _{18.5} and SMZ-CNT _{16.0}	66
4.9 Rate of settling as a function of time for Pure SMZ, SMZ-CNT _{23.2} , SMZ-CNT _{19.8} , SMZ-CNT _{18.5} and SMZ-CNT _{16.0}	67

CHAPTER 1

INTRODUCTION

1.1 Objective

The low aqueous solubility and dissolution rate of hydrophobic drugs is one of the major obstacles in drug delivery development. The dissolution rate and the bioavailability of hydrophobic drug are dependent on the particle size. The smaller particles have more surface area, which lead to an increase in dissolution rate. Utilize carriers can also control dissolution rate.

The objective of this research is micron-scale drug particles formation, their incorporation into carriers for drug delivery and colloid behaviors of drug/carriers. Biopharmaceutics Classification System (BCS) class II drugs such as Griseofulvin and Sulfamethoxazole were used as the model drugs in this project. The objectives of this project are listed as follows:

- Study of micro-scale drug particle formation with anti-solvent precipitation;
- Incorporation of functionalized carbon nanotubes (f-CNTs) into drug crystals;
- Characterization of drug/f-CNTs composites;
- Drug release study for drug/f-CNTs composites.
- Understanding of colloidal stability of drug/f-CNTs suspension based on the characterization for different suspension systems;

1.2 Drug Delivery System

Drug follows absorption, distribution, metabolism, and excretion (ADME) after being administered. A drug compound needs to enter bloodstream to be distributed to reach target

site. Drugs can be introduced into the human body by various administration routes based on the disease, the effect desired and the product available, such as oral, buccal, sublingual, ocular, intravenous, intramuscular, subcutaneous, transdermal, pulmonary/nasal and vaginal/rectal routes (Figure 1.1) ([1-2](#)). The solubility, chemical stability and permeability critically affect the bioavailability of the drug. Distribution of drug compound can be hindered by some natural barriers like blood-brain barrier.

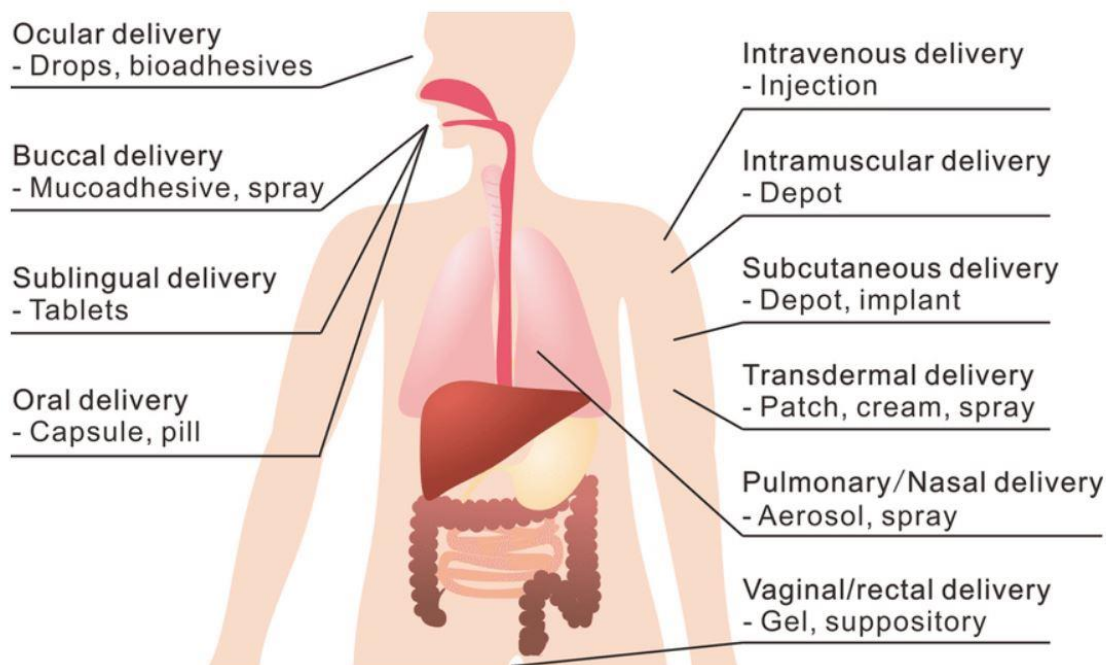


Figure 1.1 Routes of Administration.

Source: National Pain Centers, Routes of Administration.

<http://www.nationalpain.com/routes-of-administration>, accessed Oct 12, 2018

Drug delivery system (DDS) is the formulation designed to combat various obstacles for a pharmaceutical compound to successfully achieve a therapeutic effect once administered in humans or animals. The drug delivery process includes the administration of the drug product, the release of the active pharmaceutical ingredients by the products, and the transport of the active ingredients across the biological membranes to the site of

action. Drug delivery system is an interface between the patient and the drug (3). Well-designed DDS should increase the bioavailability of the drug molecule, improve bio-distribution, improve therapeutic efficacy and reduce toxicity.

Oral drug delivery has been the mostly used route of administration for decades. It is very easy to administrate as most of them can be taken with water or simply chewed. The coating on the outside of tablet or flavor of gummy improve the compliances especially for younger patients. Drugs designed for oral delivery include immediate-release, sustained- release and controlled-release products. Immediate-release (IR) products provide immediate release of drug for rapid absorption, normally used to treat acute diseases. While sustained release (SR) products provide long acting or delayed release for chronic diseases. Controlled release has been recognized as new generation of pharmaceutical products recently (4) because different drug compounds have variable absorption rates and serum concentrations are unpredictable. Controlled release delivery aims at delivering the drug at the specific rate for a certain period of time. All the pharmaceutical products designed for oral administration must be developed based on the thorough understanding of the anatomy and physiology of the gastrointestinal tract (GI). This includes the fundamental understanding of various disciplines of drug absorption, GI transit, microenvironment of GI tract, pharmacokinetics and pharmacodynamics (4). The biggest disadvantage for oral drug delivery is the bioavailability of drug can be negatively affected by first pass metabolism which refers to greatly reduced drug concentration mainly by liver and gut (5).

Intravenous drug delivery has been established as an effective alternative to the commonly used oral administration routes. It involves of injection of drug substance

through the skin or mucous membrane. It bypassed the first pass metabolism as drugs enter the bloodstream circulation directly. Although it has the advantage of fast drug action and high bioavailability, the pain associated with intravenous injection reduces patient compliance. However, patients who are not able to ingest anything orally can use it as the alternative administration route.

Transdermal drug delivery system is another alternative delivery method to oral administration as it delivers drugs through the skin to achieve the desired therapeutic effect locally. Drug candidates need to have certain lipophilicity and small molecular weight (usually less than 500 Da) which limited the commercial applications of transdermal delivery (6). Penetration enhancers and prodrugs are often necessary in order to enhance the poor permeability of drug across the skin. Use of physical techniques such as electroporation, reverse iontophoresis, iontophoresis and sonophoresis have emerged recently to improve transdermal permeability of drugs of different lipophilicity and large molecular weight, such as proteins and peptides (7).

The pulmonary administration is another attractive route for drug delivery because it provides local lung effects and possibly high systemic bioavailability. The local pulmonary deposition and delivery of the drug substances facilitates a targeted treatment of many acute and chronic medical conditions (8). Recent advances of inhalation systems for pulmonary delivery include pressurized metered-dose inhalers (MDIs), dry powder inhalers (DPIs) and nebulizers (9).

The development of drug delivery has changed dramatically in the past few decades and even more promising changes are expected in the near future. Our understanding of the physiological barriers to efficient drug delivery, such as transport in the circulatory

system and drug movement through cells and tissues have improved substantially; and many new designs of drug delivery systems have entered clinical practice. There are 30 main drug delivery products on the market now and the number of those products has significantly increased in the past few years. This growth is expected to continue in the near future ([10](#)).

Yet, with all of this progress, many drugs, even those discovered using the most advanced molecular biology strategies, have unacceptable side effects due to the drug interacting with healthy tissues that are not the target of the drug. Pharmaceutical industry needs to continue developing innovative drug delivery technologies to keep up with drug discovery technologies, to improve patient compliance, to shorten drug development cycle in order to lower drug cost.

1.3 Hydrophobic Drugs

Drug is hydrophobic when it is poorly soluble in water but are typically soluble in various organic solvents. The drug solubility in water can be categorized as slightly soluble (1-10mg/ml), very slightly soluble (0.1-1 mg/ml), and practically insoluble (<0.1mg/ml) ([11](#)). Based on the aqueous solubility related to dose at three relevant pHs and intestinal permeability ([12](#)), U.S. Food and Drug Administration provides the Biopharmaceutics Classification System (BCS) to serve as guide for predicting the intestinal absorption of the Active Pharmaceutical Ingredients (API). BCS classifies APIs into four groups: class I APIs have high solubility and high permeability, class II APIs have low solubility and high permeability, class III APIs have high solubility and low permeability, and class IV APIs have low solubility and low permeability (Table 1.1). Low solubility in water may cause

low dissolution rate, thus lead to low bioavailability and suboptimal drug delivery. It has been reported that about 40% of the market approval drugs and 90% of drug molecules in the pipeline are hydrophobic. The oral bioavailability of these drug compounds is limited due to slow drug dissolution in the gastrointestinal tract and many drugs suffer from poor solubility, low permeability, rapid metabolism and elimination from the body along with poor safety and tolerability (13). Therefore, various pharmaceutical technologies have been developed to improve the solubility of these drug compounds (14).

Table 1.1 Biopharmaceutics Classification System

		Permeability	
		High	Low
Solubility	High	Class I	Class III
	Low	Class II	Class IV

The development of innovative drugs without compromising on safety and efficacy is always a challenge. In spite of significant advances in recent years such as various prodrug technologies have been employed to modify drug structure, discovery and development of new drugs alone are not sufficient to achieve therapeutic as it is not always practical to change the chemical structure of the drug compound after development of compound structure. Therefore, many studies have focused on formulation design to improve hydrophobic drug delivery. Many ionizable drugs are weakly basic and exhibit a pH-dependent solubility. Ciprofloxacin is practically insoluble in water at neutral pH but has higher solubility at acidic condition. Most of its intravenous formulations use lactic acid as pH modifier to improve the solubility of Ciprofloxacin (15). Formulation of hydrophobic drugs using co-solvents is another widely used technique, especially for liquid

formulation intended for oral or intravenous administration. One of the formulations of anticancer drug docetaxel contains ethanol and Tween 80 to solubilize the drug (16). Among the various formulation approaches that have been developed to increase the solubility of drug molecules, size reduction and nanonization for the formation of fine drug particles have been proved to be effective techniques to improve solubility and enhance bioavailability (17).

1.4 Size Reduction of Drug Particles

1.4.1 Dissolution Enhancement through Size Reduction

Dissolution is the process of a drug particle dissolves in the medium at the absorption site. During dissolution, the drug molecules on the surface enter into solution, creating a diffusion layer. The drug molecules from diffusion layer pass throughout the dissolving fluid and contact with the biologic membranes, and absorption occurs (18), which according to Noyes-Whitney equation (19), dissolution rate of hydrophobic drugs can be enhanced by formulated as micro- or nano-particles with high surface area:

$$dc / dt = kS(Cs - Ct) \quad (1.1)$$

where dc/dt is the rate of dissolution, k is the dissolution rate constant, S is the surface area of the dissolving solid, Cs is the saturation concentration of drug in the diffusion layer, Ct is the concentration of the drug in the dissolution medium at time. Based on this equation, increasing surface area can result in considerable improvement in dissolution rate and

bioavailability. And the increase of surface area can usually be achieved by reducing particle size.

In addition to the dissolution rate enhancement described above, particle size reduction also improves the saturation solubility of drug substances. According to the Ostwald-Freundlich equation, the solubility increases exponentially as a function of particle size (17):

$$S = S_{\infty} \exp\left(\frac{2\gamma M}{r\rho RT}\right) \quad (1.2)$$

where S is the saturation solubility of the drug substance, S_{∞} is the saturation solubility of an infinitely large drug crystal, γ is the crystal medium interfacial tension, M is the compound molecular weight, r is the particle radius, ρ is the density, R is a gas constant and T is the temperature. The increase in solubility further increases the dissolution rate. Therefore, size reduction of drug particles can effectively enhance the bioavailability of drug compound (20).

1.4.2 Size Reduction Techniques

Micro- or nano-particles can be produced by bottom-up or top-down techniques. Top-down techniques typically apply forces in various ways to break down coarse materials into micro- or nano-particles. Bottom-up techniques usually start with the molecules in solution and the molecules are aggregated to form the solid particles (21).

1.4.2.1 Top-down Techniques Two traditional top-down methods for size reduction of large quantities of materials are high-pressure homogenization and milling. High-pressure homogenization has been used for many years to produce emulsions and suspensions. Its advantage is easy to scale up, even for very large amounts. Piston-gap and jet-stream are the two basic technologies for most homogenizers. In a typical piston-gap homogenizer, the macro suspension coming from the sample container is forced to pass through a tiny gap and particle diminution is affected by shear force, cavitation and impaction. While in jet-stream homogenizers, the collision of two streams leads to particle diminution mainly by impact forces. Intralipid® and Lipofundin® are the two commercial products which have mean droplet diameters within the range of 200-400nm (22).

During the milling operation, the stress is applied on the materials to break the particles. Ball/Pearl milling is a popular technique used by many pharmaceutical development team to produce of fine drug particles. For instance, commercial use of the ball-milling technology to produce Rapamune® coated tablet showed improved bioavailability than the solution form (23). Surfactants or stabilizers were used to stable the structure of the produced drug nanoparticles during milling process. Sodium dodecyl sulfate (SDS) has excellent dispersion properties and can adsorb on the particle surface. It was widely used as surfactant in various formulations (23). Despite milling process is an effective means to produce micro or nano- particles, one of its disadvantages is the potential contamination of the products caused by erosion of the milling material. The other downside is some milling processes require very long operation time in order to reach the targeted particle size range (24) which may adversely cause the formation of amorphous product by prolonged milling (25).

1.4.2.2 Bottom-up Techniques Bottom-up processes such as emulsification and precipitation methods have emerged in recent researches to synthesize submicron or micro-particles from the liquids. Emulsification is a simple method to form drug particles as most hydrophobic drugs are soluble in various water immiscible organic solvents. It has been used to form fine particles for a large number of drug compounds ([26-27](#)). During a typical emulsification process, the drug and polymer are dissolved in a water immiscible organic solvent and then are added into an emulsifier containing aqueous solution. The solvent is removed by evaporation to a gas phase or by extraction to the continuous phase ([28](#)).

Precipitation methods such as anti-solvent precipitation have gathered lots of interest recently to prepare fine drug particles ([29-30](#)). In a typical anti-solvent precipitation process, the drug is first dissolved in an organic solvent and then mixed with a miscible anti-solvent. Water is widely used as an anti-solvent because its low solubility toward most drug compounds and the relatively high miscibility with few of polar solvents. The use of the anti-solvent in precipitation reduces the solubility of the drug in the solution and induces rapid crystallization to precipitate the drug particles (Figure 1.2). The ultrasonic agitation is used during precipitation to assist rapid and uniform nucleation which leads to smaller and uniform sized drug particles ([31](#)). Sonication also helps reduce the agglomeration of drug particles ([31](#)). The advantage of precipitation processes is that forming particles directly provides more control of particle size distribution and morphology. Recent studies have reported sonication assisted anti-solvent precipitation for the formation of submicron and micro-particles of hydrophobic drugs, and the use of cellulose ethers and surfactants during anti-solvent precipitation to enhance the rate of

particle formation and to reduce overall particle size ([32-35](#)). The stabilization of these suspensions is also important for both controlling the particle size and developing manufacturing processes, which can include conventional methods such as spray drying or incorporation into drug delivery vehicles like polymer films or other control release formulations.

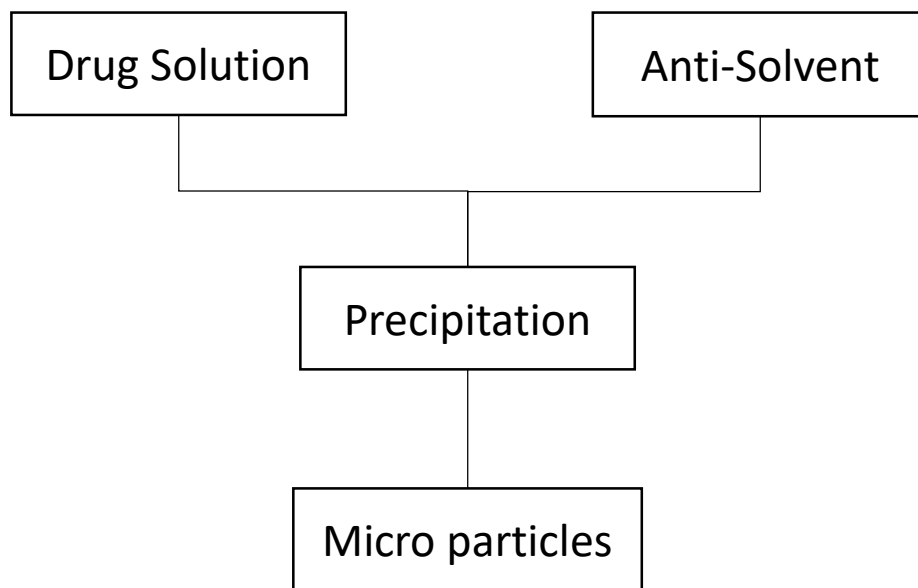


Figure 1.2 Process of anti-solvent precipitation.

The particle precipitation and growth involve nucleation, condensation of solute molecules, and coagulation of particles. (Figure 1.3) Nucleation happens when a critical number of molecules join together to form nuclei. The nucleation rate depends on the degree of supersaturation when anti-solvent is mixed with drug solution. The increase of supersaturation leads to a significant increase of nucleation rate. Condensation occurs when single molecules are absorbed onto the surface of the formed small nuclei and results in growth of the particle size. Nucleation and condensation also compete with each other and affect the particle size during the precipitation process because both of them are consuming

the solute molecules. Generally, high nucleation rate results in small particles and low nucleation rate leads to large particles ([36-37](#)). After particle precipitation, coagulation process occurs which resulting in particles collide and stick together to form bigger particles. However, since coagulation does not consume solute molecules, the total precipitated particle mass remains unchanged ([38](#)). Coagulation favors nucleation and competes with condensation by reducing the number of particles thus reduces the condensation rate ([37](#), [39-40](#)).

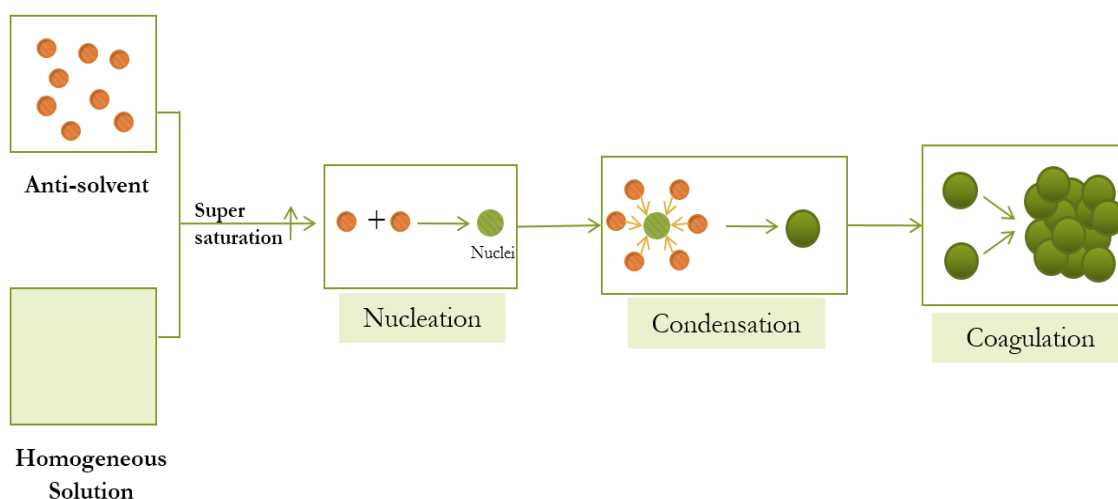


Figure 1.3 Mechanism of anti-solvent precipitation.

Combining top-down and bottom-up techniques is also possible. Rapid precipitation has also been used with high shear processing such as high-pressure homogenization ([23](#)). During this process, sudden supersaturation is achieved by rapid addition of drug solution into an anti-solvent which leads to fine crystalline or amorphous solids. Due to supersaturation favors nucleation rather than crystal growth, high supersaturation often results in the formation of needle like crystals. Other techniques like supercritical technology has been combined with anti-solvent precipitation method for

particle formation which uses the high diffusive supercritical fluid to rapidly extract the solvent and precipitate the drug particles ([41-42](#)).

1.5 Functionalized Carbon Nanotubes

As drug carriers, the solubility of CNTs in aqueous solvent is an important parameter for drugs to achieve good gastrointestinal absorption, blood transportation, secretion and biocompatibility. CNT dispersions should also be uniform and stable in a sufficient degree to obtain accurate concentration data. The hydrophobicity of the graphene side walls and the strong π - π interactions between the individual tubes lead to low solubility of pristine CNTs in aqueous solvents. These properties cause aggregation of CNTs into bundles which affects the uniformity of CNTs suspensions.

In order to successfully disperse CNTs for drug carrier purpose, four basic approaches ([43](#)) have been proposed: surfactant-assisted dispersion, solvent dispersion, functionalization of side walls and bio molecular dispersion. Among the above described approaches, functionalization of side walls has been the most effective and widely used approach. Functionalization has been shown the ability to reduce cytotoxicity, improve biocompatibility and provide possibilities to attach drug molecules, proteins or genes for drug delivery systems designs ([44](#)). The functionalization of CNTs can be divided into two main subcategories: covalent functionalization and non-covalent functionalization.

1.5.1 Covalent Functionalization

Covalent functionalization refers to linking CNTs and functional groups with chemical bond which leads to more secure conjunction of functional molecules. CNTs can be oxidized to give CNTs hydrophilic groups such as carboxylate, hydroxyl and amine groups. After treating with strong acid under microwave radiation (45), defects can be created on the side walls of CNTs where the carboxylate groups are generated. Excessive surface defects can possibly change the electronic properties of CNTs and shorten CNTs to fit the need of certain drug carriers. The functional groups on the oxidized CNTs can further react with SOCl or carbodiimide to extend functionalization possibilities with other compounds (46-47).

Acyl peroxides can be used to generate carbon-centered free radicals for functionalization of CNTs (48), which unlike treating CNTs with strong acid, allows the chemical attachment of a variety of functional groups to the wall or end-cap of CNTs covalently without destroying their wall or end-cap structure (49). Organic groups with terminal carboxylic acid functionality can further react with acyl chloride and amine to form amide. The functional groups attached to CNTs improve the solvent dispersibility and offers reaction sites for monomers to incorporate in polymeric structures. Free radicals for functionalization can also be produced by organic sulfoxides with a reasonable choice of radical generating compounds (50).

Polymers was covalently attached to CNTs to produce polymer/CNTs composites (51). The resulting composites exhibited good colloidal stabilities for prolonged periods when dispersed in liquid media. The polymer functionalized CNTs can also be dispersed into the parent polymer. The method has been effectively and conveniently used in the functionalization, and solubilization of CNTs. Another method to produce polymer/CNTs

composites was carried out by blending derivatized carbon nanotubes into polymer matrices (52). Modification with suitable chemical groups using diazonium chemistry improved chemical compatibility of CNTs with polymer matrix, which allows the properties of CNTs to transfer to the composites.

Functionalization of CNTs can be achieved in strong acidic solution which is easily scalable and produces sidewall-functionalized CNTs in large industrial quantities (49). CNTs can be separated by dispersing them in an acidic medium under sonication. This exposes the sidewalls of CNTs to facilitate the functionalization. Once CNTs are dispersed in unbundled state, the functionalization occurs. CNTs can be shortened in acidic solutions which is sometimes necessary for certain purposes such as in the development of oral drug carriers (53).

A nondestructive covalent functionalization of CNTs by selective oxidation of the defects was proposed (54). Fe (VI) successfully oxidized CNTs under mild conditions and resulted in highly carboxylated CNTs. Unlike acid treatment that has poor selectivity that inevitably consumes the carbon bonds in tube structure, Fe (VI) selectively oxidized only sp^3 -hybridized carbons while kept the tube structure unchanged.

In the studies on the use of CNTs in neurology, an implant system was constructed (55) in which CNTs and neurons were growing. CNTs were functionalized with neuronal growth promoting agents to promote the growth of neurons. This system provided possibility for stroke patients to recover from their paralyzed states.

CNTs was quite inert due to the seamless arrangement of hexagon rings without any dangling bonds on their sidewalls. The method of asymmetric end-functionalization has been tried by employing physicochemical process to produce asymmetric end-

functionalization of CNTs (56) which successfully functionalized CNTs with each of their two end tips attached by different chemical reagents.

SWCNTs were covalently functionalized with polytyrosine to disperse glassy carbon electrodes (57). The proposed sensor was highly sensitive in quantification of polyphenols in tea extracts. Bimetallic Palladium- platinum supported CNTs were prepared by microwave irradiation process. The catalyst showed excellent activity in dry reforming of methane to synthesis gas using carbon dioxide (58).

1.5.2 Non-covalent Functionalization

Many small drug molecules and large polymeric drugs can be adsorbed non-covalently onto the surface of pristine CNTs through hydrophobic and π - π stacking interactions between the chains of the adsorbed molecules and the surface of CNTs. Hydrophobic forces are the main driving forces for the loading of drugs that are hydrophobic in nature or have hydrophobic moieties into or onto CNTs. Ionic interactions from the presence of charge on the nanotube surface due to chemical treatment can enable the adsorption of the charged molecules (59-60). Compared to covalent functionalization, non-covalent functionalization of CNTs is very attractive because it offers the possibility of attaching chemical groups without affecting the electronic network of the tubes.

SWCNTs were non-covalently functionalized with oxide surfaces modified with pyrene through π - π stacking interactions (61). Pyrenecarboxylic acid derivative served as chemical cross-linker to attached alkyl-modified iron oxide nanoparticles onto CNTs (62). The chemical functions of the inorganic nanoparticles in the resulting product showed increased solubility in organic media.

Phthalocyanines and porphyrin derivatives have been non-covalently functionalized on SWNTs with a dispersion technique (63). The resulting hybrid materials are used as sensing layers for the detection of toluene. The high surface area of the hybrid material leads to improvement of the sensor responses.

Surface functionalized CNTs can be achieved by simply exposing CNTs to vapors containing functionalization species. This process not only non-covalently bonds functionalization species to the CNTs surface but also provides chemically functional groups (64). The resulting functionalized CNTs surface can be exposed further to another layer precursor species to expand functionalization possibilities.

A convenient and nondestructive one-pot co-deposition of tannic acid (TA) and polyethyleneimine (PEI) to the MWCNTs was proposed (65). The TA-PEI modified MWCNTs showed good dispersibility in various solvents as well as epoxy resin. Epoxy composites reinforced with the above mentioned CNTs exhibited significantly improved impact strength and tensile strength, increased glass transition temperature and enhanced electrical conductivity.

A process involves CNTs treated with polymers and their derivatives for noncovalent functionalization of the nanotubes showed increased solubility and enhancement of other properties of interest (66). A new non-wrapping approach to functionalizing CNTs has been introduced (67), where the functionalization can be carried out in both organic and inorganic solvents. CNT surfaces can be functionalized in a non-wrapping or non-packaging fashion with a functionally conjugated polymer that included functional groups. Dispersions of CNTs in a host polymer or copolymer with delocalized

electron orbitals was patented (68). In this method, a dispersion interaction occurred between the host polymer or copolymer and the CNTs dispersed in that matrix.

Various large molecules can be non-covalently functionalized on CNTs. Dimethyl sulfoxide/water mixtures was used to solubilize nanotubes with amylose (69). Metallothionein proteins were adsorbed onto the surface of MWCNTs (70). DNA strands was reported to interact strongly with CNT to form stable hybrids which can disperse in aqueous solutions effectively (71-72).

1.6 CNT-Loaded Drug for Drug Delivery

The performance of drug compound can be significantly improved by incorporating into a drug delivery system. Drug delivery systems have been improved over the years by various of designs that increase bioavailability, reduce toxicity, controlled release of drug molecules and enable precision drug targeting (73). The drug delivery system can be applied not only for common oral delivery but also for other delivery routes such as intravenous, transdermal or pulmonary. The interaction between the fine particles and skin at cellular level can be used to enhance immune reactivity for topical vaccine applications (74). In a typical drug delivery system, drug carriers are needed to incorporate those drug compounds. The biodegradability, biocompatibility and functionalization capability make biopolymer materials good candidates as drug carriers to be widely used in the pharmaceutical industry (75). Drug molecules can be entrapped or encapsulated within the polymer matrix, which can be customized to protect active ingredients before they reach site of target, and provides the modified release of the drug molecules through the matrix

to the onsite of action. The drug delivery system also provides the possibility to deliver drug compound through different dosage forms based on route of administration and solubility and stability of drug compounds, including solids (tablets, capsules and thin films), semi-solids (gels and creams) and liquids (solutions, colloids and emulsions).

Over the years, CNTs has gained much interest as drug delivery vehicles in drug formulation designs. The unique tubular structure of carbon nanotubes can have very high drug loading efficiency due to their large length/diameter ratio (76). Their cylinder shape provides great permeability which shows advantage in crossing blood-brain barrier (BBB) (77). Functionalization of CNTs with different chemical groups also shows potential targeting capabilities. Many anti-cancer drugs can be functionalized on the external walls of carbon nanotubes (78). And CNTs can deliver drugs selectively and effectively into the tumor cells with functionalization of specific ligands on their surface to recognize cancer-specific receptors on the cell surface (79).

MWCNTs can be covalently conjugated with hyaluronic acid for targeted delivery of DOX to cancer cells that overexpress CD44 receptors, with fluorescein isothiocyanate to image the distribution of MWCNTs (80). In this study, DOX was encapsulated into the inner cavities of MWCNTs for controlled release and targeted delivery. DOX released faster under acidic environment and slower at a physiological pH condition. The drug delivery system also achieved a high DOX loading efficiency and exhibited good biocompatibility to HeLa cells.

Folic acid (FA) receptors are well known overexpressed in cancer cells, and several research groups have designed drug carriers to include FA derivatives for targeting purposes. For example, single wall CNTs was functionalized with PEG and FA to deliver

5-fluorouracil into MCF-7 human breast cancer cells (81). The conjugation of PEG increased the hydrophilicity and improved the biological compatibility of drug delivery system. And folic acid improved drug accumulation in the target tissue thus elevated the efficacy of antitumor activities to MCF-7 human breast cancer cells. Moreover, non-spherical nano carriers CNTs have been reported to have longer retention time in the lymph nodes than spherical nano carriers (82), which provides targeting abilities for CNTs to treat lymph node cancers (83-85). In these studies, magnetic nanoparticles containing the anticancer drug cisplatin were entrapped into folic acid-functionalized CNTs. The CNTs were dragged by an external magnet to the lymph nodes where the drug was shown to be released over several days to selectively inhibit the tumor. These results clearly demonstrated that CNTs have great potential in dual-targeting drug delivery applications.

CNTs can also be used to conjugate with antibodies to assist the targeted drug delivery. For example, SWCNTs attached with SNX-2112 were functionalized with chitosan antibodies fluorescein (86). Compared to SWCNTs, SWCNTs-chitosan exhibited higher drug-loading capability and caused higher cell apoptosis.

Noncovalent π - π stacking of DOX and PEG-functionalized SWCNTs was designed and the drug delivery system was injected via the tail vein into mice (87). The results showed greatly enhanced therapeutic efficacy of SWCNT-DOX complex compared with free DOX due to prolonged blood circulation time of drug molecules by PEG. In another study, mice was intravenously injected with MWCNT_{OX} and MWCNT_{TEG} to investigate the effects of the CNT surface functionalization on the *in vivo* bio distribution of platinum-based drug delivery system (88). The results showed enhanced tissues uptake of platinum compared with those injected with pristine MWCNTs. The bio distribution of platinum-

based molecules was not affected by functionalized CNTs despite CNTs initiated the abnormal immune response.

Another area where CNTs have advantage as drug carriers is to facilitate drugs to cross the relative impermeable Blood Brain Barrier (BBB), which has tight junctions formed by endothelial cells of the brain capillaries. Many small and large therapeutic compounds were reportedly having difficulty to cross the BBB (89). Recent studies have shown that CNTs could effectively penetrate the BBB (90).

Functionalized SWCNT-COOH was used to attach levodopa (LD) into PC12 cells (91). The results showed the release of LD was pH dependent and the drug delivery system did not compromise the viability of PC12 cells. Some *in vivo* studies showed after the endothelin-1-induced stroke, rats injected with functionalized CNT-siRNA had reduced apoptosis and the increased cognitive ability (92).

PEG functionalized CNTs attached with an immune adjuvant were fluorescently labeled and then injected into an intracranial GL261 glioma (93). The results showed improved uptake of immune adjuvant by PEG-CNTs and pro-inflammatory cytokines were then released to inhibit tumor growth.

Acetylcholine (Ach) conjugated SWCNTs were developed to deliver Ach into the brain of mice with Alzheimer disease (53). In this drug delivery system, SWCNTs provide lysosomes targeting capabilities while Ach was released with the environmental pH change. The results showed Ach-loaded SWCNTs improved the learning and memory capability of mice with Alzheimer disease. These studies suggested that CNTs-based drug delivery was a promising drug delivery system for the delivery of drugs to the nervous

system. The application of CNTs in drug delivery system for various routes of administration are expected to gain more interest in the near future.

CHAPTER 2

INCORPORATION OF FUNCTIONALIZED CARBON NANOTUBES INTO HYDROPHOBIC DRUG CRYSTALS FOR ENHANCING AQUEOUS DISSOLUTION

2.1 Introduction

The high aspect ratio, potential for unique functionalization via covalent and non-covalent means have made carbon nanotubes (CNTs) attractive in many medical, therapeutic and nano medicine applications ([94](#)). The CNTs have demonstrated excellent potential in tissue engineering, scaffolding, as material for bone, neuron and cell growth, thermal ablation and photo-thermal therapy, and as materials that promote differentiation of stem cells into specific lineages ([95-107](#)). They have been used to deliver a wide range of small molecules such as chemotherapeutic drugs ([108-114](#)), anti-inflammatory and antimicrobials agents ([115-116](#)), and as carriers for controlled release ([117](#)). They have also been used to deliver complex molecules such as peptide based vaccines ([118-119](#)), antibodies ([120](#)), nucleic acids proteins and genes ([121](#)). CNTs have been particularly attractive in targeted delivery because they have shown enhanced permeability and retention in tumor tissues, their needle-like shape can facilitate trans-membrane penetration and they have been shown to enter cells via endocytosis ([122](#)).

Drug loadings on CNTs have been addressed via covalent and noncovalent functionalization. Functionalization by a hydrophilic group also improves aqueous dispensability and reduces cytotoxicity ([123-124](#)). Varieties of small and large molecules have been covalently attached to CNTs and it remains a popular approach to drug loading ([125](#)). Besides direct conjugation of the active molecule, functionalization of CNTs with

carboxylic, amine and polymer molecules have been used to facilitate the physical adsorption of drugs on CNTs surface. Non-covalent coating of CNTs for the purpose of drug delivery include amphiphilic macromolecules like lipid and polymers ([125](#)), cancer drug ([126-127](#)) and anti-Alzheimer drug ([128](#)). CNTs have also been used for controlled release. For example, drugs encapsulated into oxidized CNTs with the open ends capped with thiol modified gold nanoparticles have shown controlled release activity ([129](#)), Heparin attachment to carbodiimide functionalized CNTs have shown prolonged anticoagulant activity ([130](#)), a dual-targeted drug carrier for prolonged release has been designed by combining CNTs with folic acid and iron nanoparticles ([131](#)). Electrical properties of CNTs have been utilized to design hydrogel systems to electro-responsive drug release ([132](#)), and nano precipitation technique has been reported where water soluble drugs have been incubated with CNTs followed by solvent evaporation where the drug adsorbed in the interstitial spaces in the CNTs to show slow release ([117](#)). While there is much ongoing effort for using CNTs in drug delivery and biomedical applications, it is worth noting that there have been concerns about the toxicity of CNTs and numerous *in vitro* and *in vivo* studies have been carried out with conflicting reports ([133-141](#)). However, functionalization with carboxyl group has shown to be an effective way to mitigate MWCNTs toxicity ([142-143](#)).

A large number of pharmaceutically active molecules have low aqueous solubility, reduced dissolution rate and these lead to poor absorption and therapeutic failures ([144-145](#)) of oral drugs. The inability to hydrogen bond in an aqueous medium is among the main reasons behind low aqueous solubility ([23](#)). Biopharmaceutical classification system (BCS) highlights the fact that dissolution as a rate-limiting step for oral absorption of BCS

class 2 and class 4 drugs, which have low solubility. About 70% of active pharmaceutical ingredients and new chemical entities are considered as poorly soluble which is great obstacle for drug development ([146](#)). Increasing solubility can not only improve drug absorption but also potentially reduces dosage needed to achieve the same therapeutic effect while reducing side effects. Typically, dissolution can be improved by size reduction or incorporating into drug carriers ([147](#)). Methods such as dry and wet milling and homogenization are conventional methods for the synthesis of micron/nano-scale drug particles where the control of particle size, morphology, and surface properties can be relatively challenging ([147](#)). Precipitation processes are also effective methods for synthesizing micron and submicron hydrophobic drug particles ([148](#)).

Anti-solvent crystallization is a functionally simple and rapid precipitation process ([149](#)) where a drug is dissolved in a solvent and then contacted with a miscible anti-solvent to precipitate micro/nano particles. The physio-chemical properties of the anti-solvent can alter the rate of nucleation, crystal growth and colloidal behavior of the crystallizing molecule ([149](#)). In the case of hydrophobic molecules, water which has relatively high miscibility with many polar solvents can serve as an anti-solvent ([149](#)). Ultra-sonication is known to bring about uniform nucleation, rapid crystallization. Narrow size distribution can be obtained by carrying out the process in the presence of additives that prevent agglomeration ([31](#)).

An interesting possibility in anti-solvent precipitation is that the drug particles can also be directly incorporated into a drug delivery vehicle such as CNTs. Carboxylated CNTs which are highly water dispersible offer the potential to serve as nucleating sites for a hydrophobic drug during its anti-solvent synthesis. This could be a way to incorporate

CNTs into the drug structure where some specific sites on the CNTs may provide targeting capabilities. Also, the hydrophilic CNTs incorporated into a hydrophobic drug could potentially enhance hydrogen bonding with the aqueous medium leading to faster dissolution. The objective of this work was to study the possibility of incorporation of hydrophilic CNTs during anti-solvent synthesis of micron-scale drug particles and see if the CNTs would enhance dissolution. Of particular interest to this study were antifungal agent Griseofulvin (GF) and antibiotic Sulfamethoxazole (SMZ).

2.2 Materials and Methods

2.2.1 Materials

Griseofulvin (GF), Sulfamethoxazole (SMZ), Sulfuric acid (95-98%), Nitric acid (70%), Methanol ($\geq 99.9\%$) and Acetone ($\geq 99.9\%$) were purchased from Sigma Aldrich, USA. Sodium dodecyl sulphate (SDS) was purchased from GFS Chemicals. Hydrochloride acid was purchased from Fisher Scientific. Sodium dodecyl sulphate (SDS) was purchased from GFS Chemicals. Raw multiwall carbon nanotubes (20-30 nm diameter, 10-30 μm length, Purity > 95 wt%) was purchased from Cheap Tubes. The water used in the experiments was purified with a Milli-Q Plus system.

2.2.2 Methods

Carboxylated multiwall carbon nanotubes (f-CNTs) were synthesized following a previously published methodology ([142](#), [150-151](#)). In short, pre-weighed amounts of purified CNTs were treated in a microwave reactor (Model: CEM Mars) with a mixture of concentrated H_2SO_4 and HNO_3 at 140°C for 20 min. This led to the formation of carboxylic

groups on the CNTs surface leading to high aqueous dispersibility. The f-CNTs were filtered through a 10 μ m membrane filter, washed with water to a neutral pH and dried under vacuum at 65°C to a constant weight.

Drug/CNTs composite were prepared by anti-solvent precipitation. At room temperature, GF or SMZ was saturately dissolved in acetone. Antisolvent was prepared by disperse f-CNTs in water under sonication for 10 min. The antisolvent was added dropwise into the drug solution under sonication and the solution turned cloudy immediately after the addition of f-CNTs suspension which indicated crystal formation of the f-CNTs/drug composites. The resulting solution was filtered through a 10 μ m PTFE membrane filter, washed and dried in a vacuum oven to a constant weight.

The resulting drug/CNTs composites were characterized with SEM, TEM, TGA, DSC, Raman, XRD and the release behavior was examined by dissolution testing. TGA was performed with PerkinElmer Pyris 1 thermogravimetric analyzer. Samples were heated from 30 to 1200°C under a 10ml/min air flow at 10°C per minutes. SEM was performed with LEO 1530VP. Samples were mounted on aluminum stubs with adhesive tape and coated with carbon using Quorrum EMS 150T ES sputtering coater to improve conductivity. Raman spectroscopy was carried out with DXR Raman Microscope from Thermo Scientific with 532 nm filter. XRD was carried out with PANalytical EMPYREAN XRD. Melting point was measured with PerkinElmer DSC 6000.

Dissolution measurements were carried out based on standard US Pharmacopeia Method (USP 41) with Symphony 7100 dissolution system. Since GF is absorbed in the lower intestine and SMZ in the stomach, the dissolution tests were carried out at different pH. For GF-CNTs, the composite was added to 40mg/ml sodium dodecyl sulfate (pH 5.2)

and stirred at 75 rpm at 37°C. Samples were withdrawn at different points in time, filtered through PTFE membrane to remove f-CNTs and then analyzed with UV at 291 nm to determine the amount of GF dissolved. For SMZ-CNTs samples, the composite was added in 0.1 N hydrochloric acid (pH 1.4) and stirred at 75 rpm at 37°C. Once again, the samples were withdrawn at different times, filtered and analyzed with UV at 265 nm to determine the amount of SMZ dissolved.

2.3 Results and Discussion

The aqueous solubility of Griseofulvin (GF) and Sulfamethoxazole (SMZ) were 12 µg/ml and 0.61 mg/ml, respectively. It was possible to form excellent crystals of both these drugs in the presence of f-CNTs.

The SEM image of functionalized carbon nanotubes are shown on Figure 2.1 a. It shows that the structure of carbon nanotubes was not altered after microwave treatment. XRD spectra of f-CNTs is showed in Figure 2.1 c. The RAMAN spectra of raw CNTs and f-CNTs are shown on Figure 2.1 d and e.

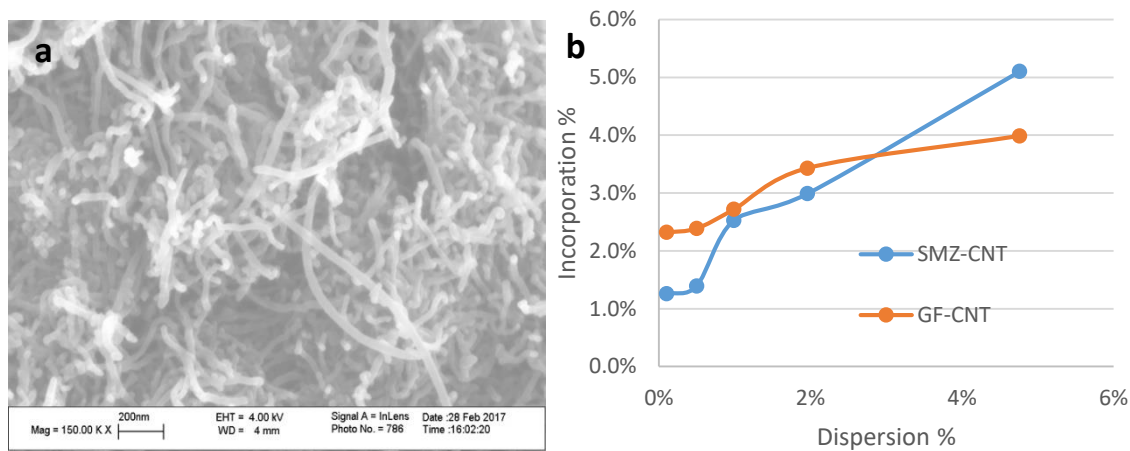


Figure 2.1 (a) SEM image of f-CNTs, (b) Incorporation of CNTs in drug composites as a function of concentration of f-CNTs in the dispersion, (c) XRD spectra of f-CNTs, RAMAN spectra of (d) Raw CNTs and (e) f-CNTs.

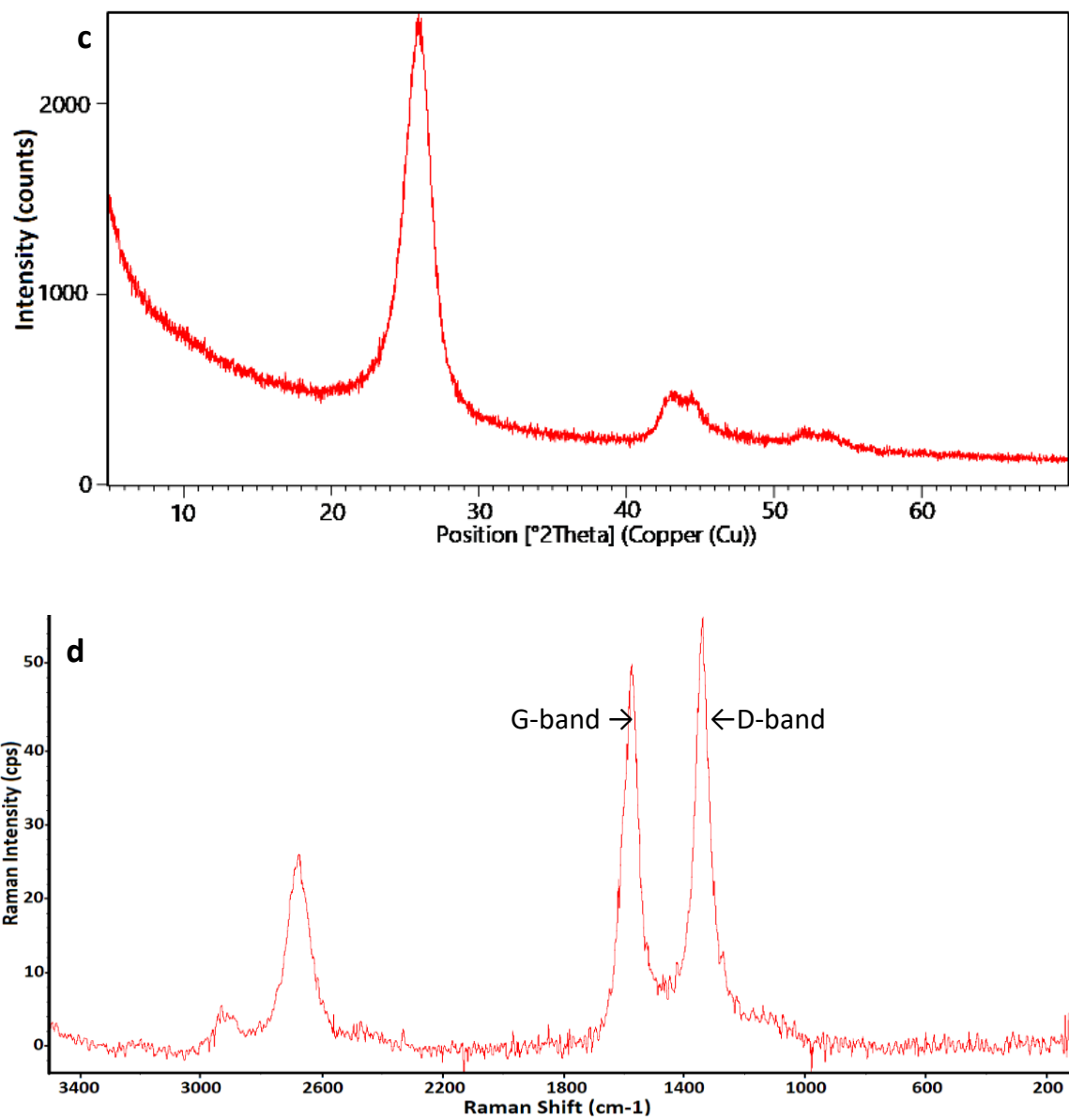


Figure 2.1 (Continued) (a) SEM image of f-CNTs, (b) Incorporation of f-CNTs in drug composites as a function of concentration of f-CNTs in the dispersion, (c) XRD spectra of f-CNTs, RAMAN spectra of (d) raw CNTs and (e) f-CNTs.

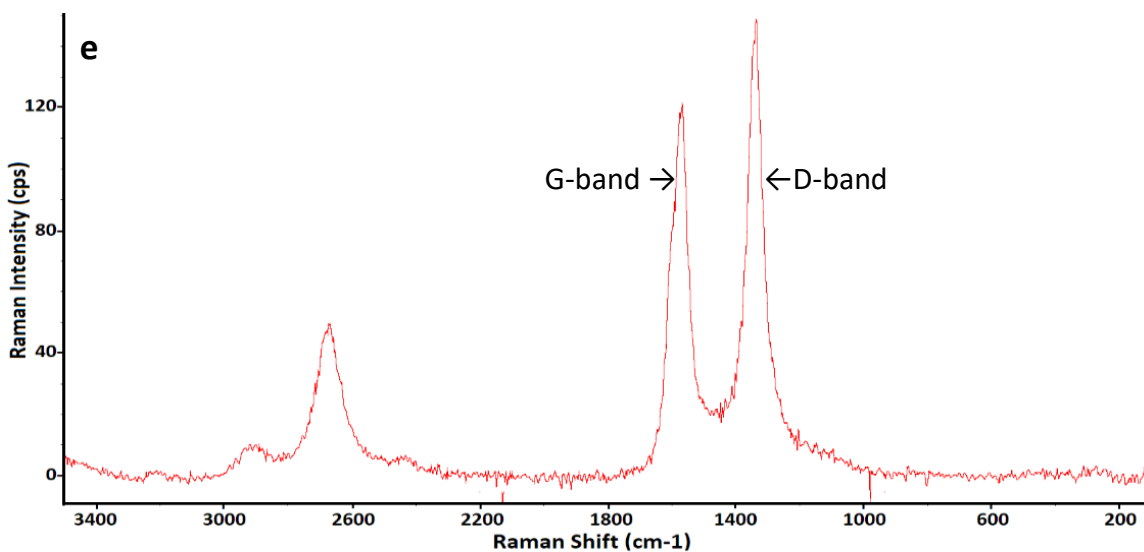


Figure 2.1. (Continued) (a) SEM image of f-CNTs, (b) Incorporation of CNTs in drug composites as a function of concentration of f-CNTs in the dispersion, (c) XRD spectra of f-CNTs, RAMAN spectra of (d) raw CNTs and (e) f-CNTs.

The amount of f-CNTs in the anti-solvent was varied to make drug/CNT composites. The incorporated concentrations of f-CNTs in each composite were measured using TGA (Figure 2.2 a and b). The amount of f-CNTs incorporated in the GF crystals prepared from f-CNTs suspension containing 0.1, 0.5, 1.0, 2.0 and 5.0% were 2.3, 2.4, 2.7, 3.4 and 4.0% respectively. For SMZ-CNTs, the corresponding values for the same f-CNTs suspensions were 1.3, 1.4, 2.5, 3.0 and 5.1%, respectively. These are referred to as SMZ-CNT-X or GF-CNT-X where X represents the incorporation concentration of f-CNTs. Figure 2.1 b is a plot of incorporation concentration of f-CNTs in the drug as a function of f-CNTs in the original suspension. The f-CNTs served as nucleation point for drug crystallization.

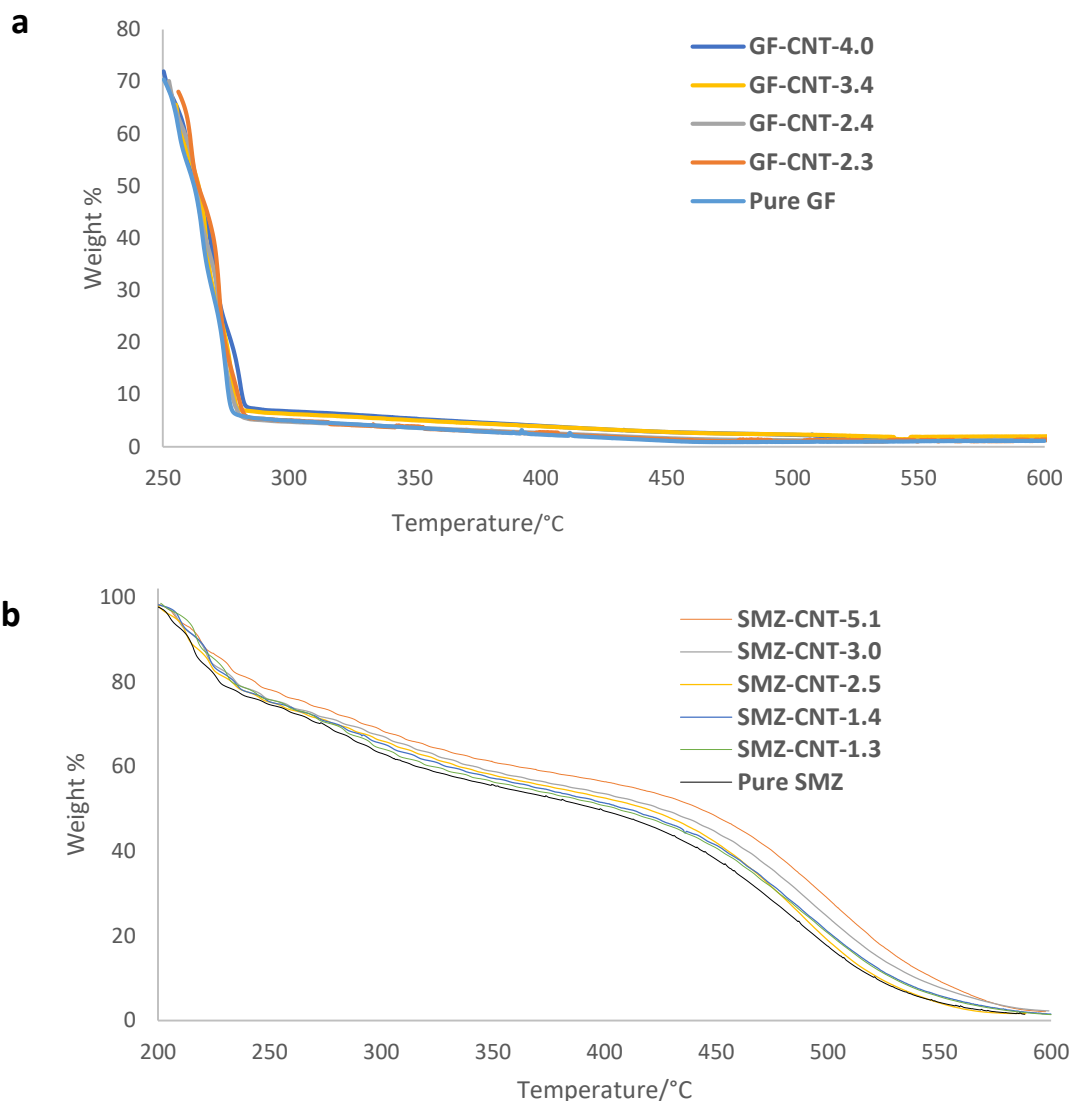


Figure 2.2 TGA curve of drug and drug incorporated with different amount of f-CNTs: (a) GF-CNTs and (b) SMZ-CNTs.

The morphology of GF-CNTs and SMZ-CNTs samples was studied using SEM. Figure 2.3 a, b showed SEM images of pure GF and GF-CNTs composites while Figure 2.4 a, b showed respective images of SMZ-CNTs. The crystal shape and size did not depend on f-CNTs incorporation. All the samples showed the presence of the f-CNTs on the crystal surface. The TEM images (Figures 2.5 a, b) clearly indicate that the f-CNTs were also embedded inside the drug crystals, the tubes were partially incorporated into the crystal

while some portion remained outside. The section remaining outside was effective in increasing the composite's interactions with the aqueous phase during dissolution studies.

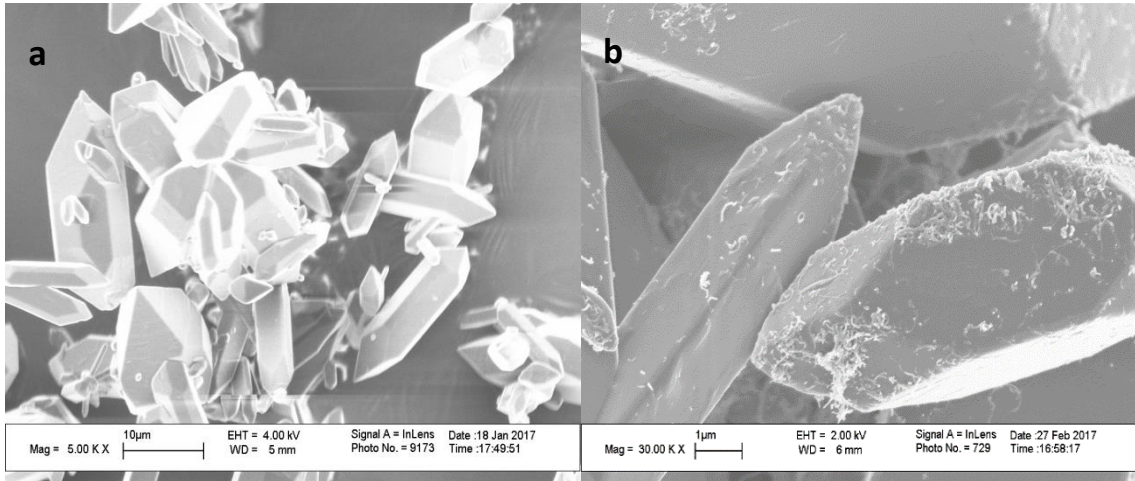


Figure 2.3 SEM images of (a) Pure GF and (b) GF-CNT-2.4.

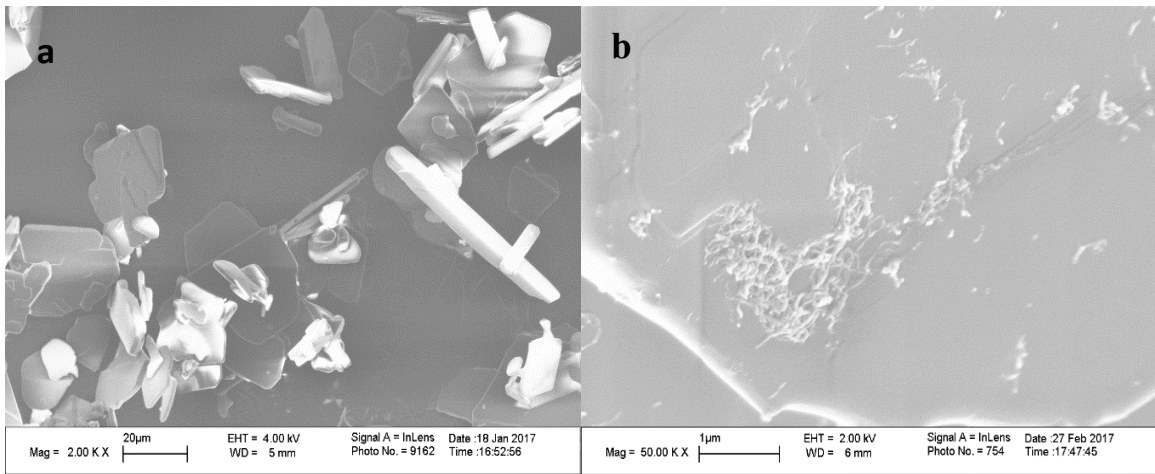


Figure 2.4 SEM images of (a) Pure SMZ and (b) SMZ-CNT-1.4.

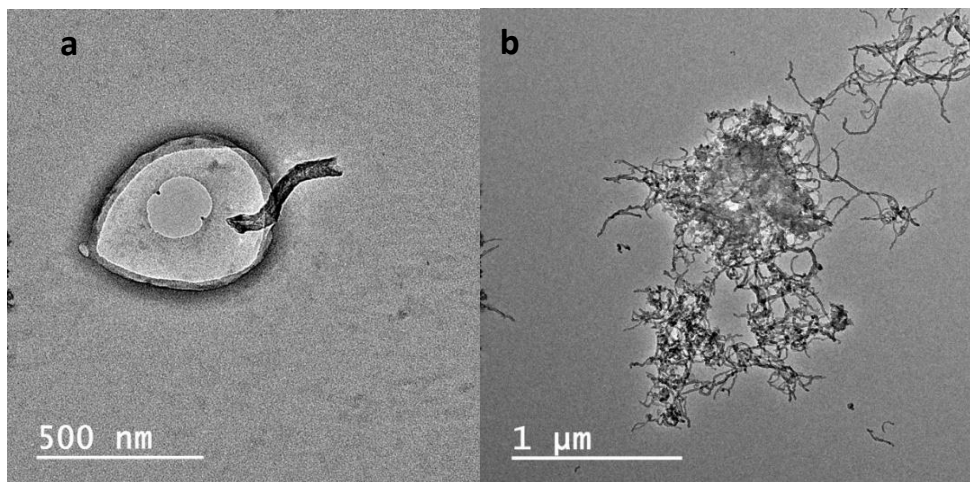


Figure 2.5 TEM images of (a) GF-CNT-4.0 and (b) GF-CNT-2.7.

Figure 2.6 showed the RAMAN spectra of pure GF and GF-CNTs of various composition. The D-band at 1350 cm^{-1} and G-band at 1580 cm^{-1} from the f-CNTs were overlaid with peaks from SMZ and GF. The GF spectra showed strong peaks in the region $1550\text{-}1800\text{ cm}^{-1}$ and $2800\text{-}3200\text{ cm}^{-1}$ which were attributed to the C=O stretching of benzo furan ring and C-H stretching of GF respectively([152](#)). The same characteristic peaks were also observed in all samples, which indicated that the presence of the f-CNTs didn't change the chemical structure of GF. The similar observation was found in Figure 2.7 which showed RAMAN spectra of pure SMZ and SMZ-CNTs of various f-CNTs concentration.

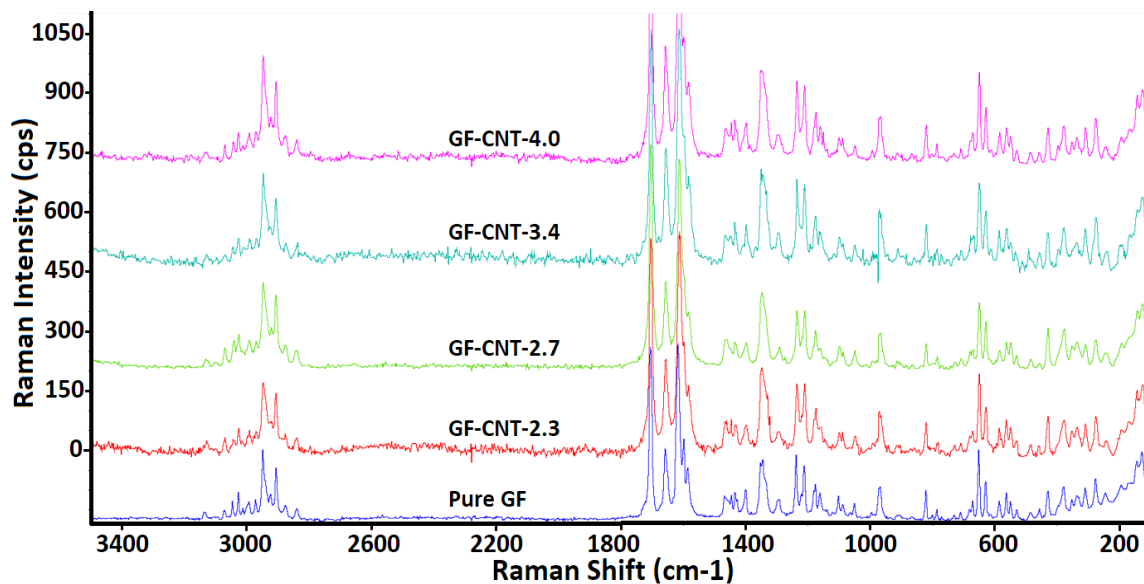


Figure 2.6 RAMAN spectra of pure GF and GF incorporated with different amount of f-CNTs.

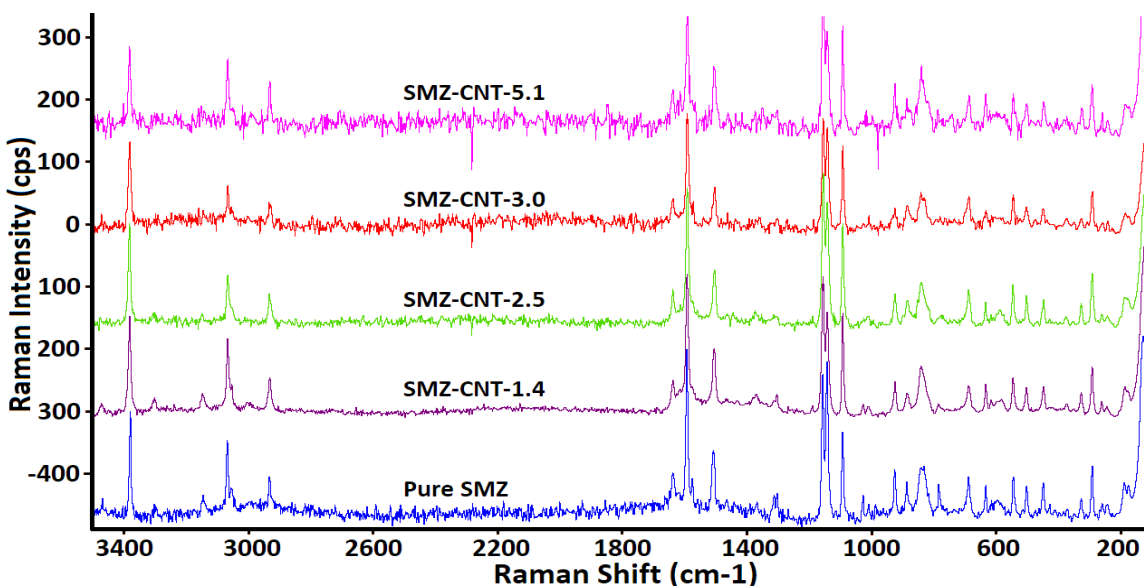


Figure 2.7 RAMAN spectra of pure SMZ and SMZ incorporated with different amount of f-CNTs.

XRD was used to study the crystal structure of the GF-CNTs and SMZ-CNTs composites. The scanning range for GF was 5 to 70 degrees and 5 to 50 degrees for SMZ. Figure 2.8 shows XRD spectra of pure GF, GF-CNT-2.7, GF-CNT-4.0. It was seen that the

crystal structure did not change in the presence of f-CNTs. The spectra of pure drug and drug-CNTs composites were identical, and neither splitting nor shifting of the peak was observed for the drug-CNTs composites. This indicated that there was no change in polymorphism, which is an important consideration in drug synthesis. The similar observation was found in Figure 2.9 which showed XRD spectra of pure SMZ, SMZ-CNT-2.5 and SMZ-CNT-5.1.

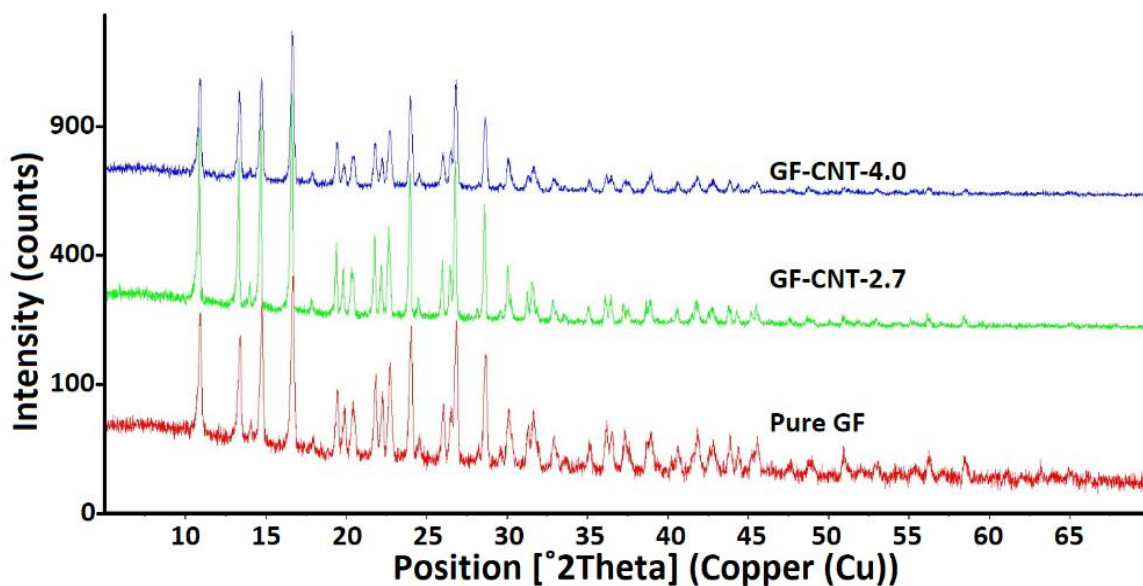


Figure 2.8 XRD spectra of pure GF and GF incorporated with different amount of f-CNTs.

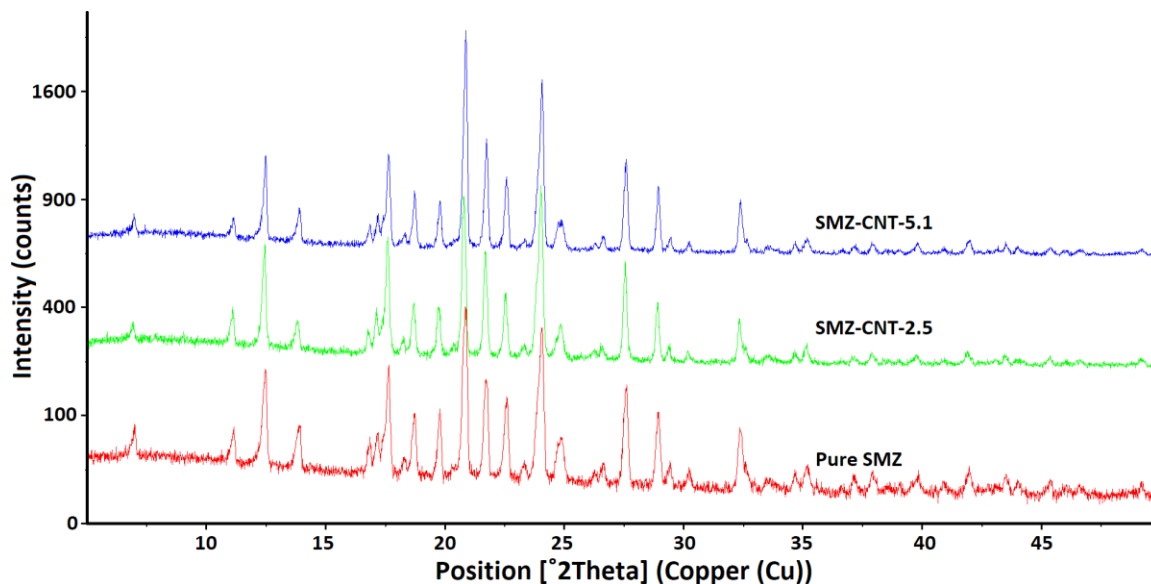


Figure 2.9 XRD spectra of pure SMZ and SMZ incorporated with different amount of f-CNTs.

The melting point were analyzed by DSC where the SMZ-CNTs samples were heated from 25°C to 200°C, and GF was heated from 25°C to 250°C. Both samples were programed to cool down and reheated for the second time. The results are presented in Table 2.1. No significant change in melting point was observed between pure GF, SMZ and their respective composites with different f-CNTs concentrations indicating the drug structure weren't altered with incorporation of f-CNTs.

Dissolution profiles for SMZ-CNTs and GF-CNTs are presented in Figure 2.10. It is evident from both profiles that the f-CNTs helped enhance the release of the drugs. It also showed that increasing concentration of f-CNTs in the composite increased the release rate quite dramatically. Table 2.1 shows the t_{50} and t_{80} , or the time necessary to reach 50 and 80% dissolution. Both t_{50} and t_{80} reduced with the increased concentration of f-CNTs. With the incorporation of 1.4% f-CNTs, the t_{50} and t_{80} of SMZ dropped from 22 to 10 min and from 67 to 29 min respectively. Corresponding drop for GF with 2.4% f-CNTs incorporation were from 27 to 12 min and from 66 to 48 min respectively. Simple mixtures

of the drugs with 5% f-CNTs were prepared and dissolution data are shown in Figure 2.10. The results showed that simply adding f-CNTs to the drug did not improve the dissolution. This demonstrated that the enhanced dissolution was brought about by incorporation into the crystal structure. The mediums used in the dissolution of both drugs are considered resemble to gastrointestinal environment, thus the dissolution behavior is relevant to human biology.

Table 2.1 Dissolution and Melting Point of SMZ-CNTs and GF-CNTs

	Amount of CNT in Composite (%)	T ₅₀ (min)	T ₈₀ (min)	M _p (°C)
SMZ	0	22	67	170.37
	1.3	20	38	170.31
	1.4	10	29	170
	3.0	8	21	170.38
	5.1	5	10	169.96
GF	0	27	66	221.25
	2.3	22	56	221.3
	2.4	12	48	221.08
	2.7	11	33	221.04
	4.0	6	18	220.38

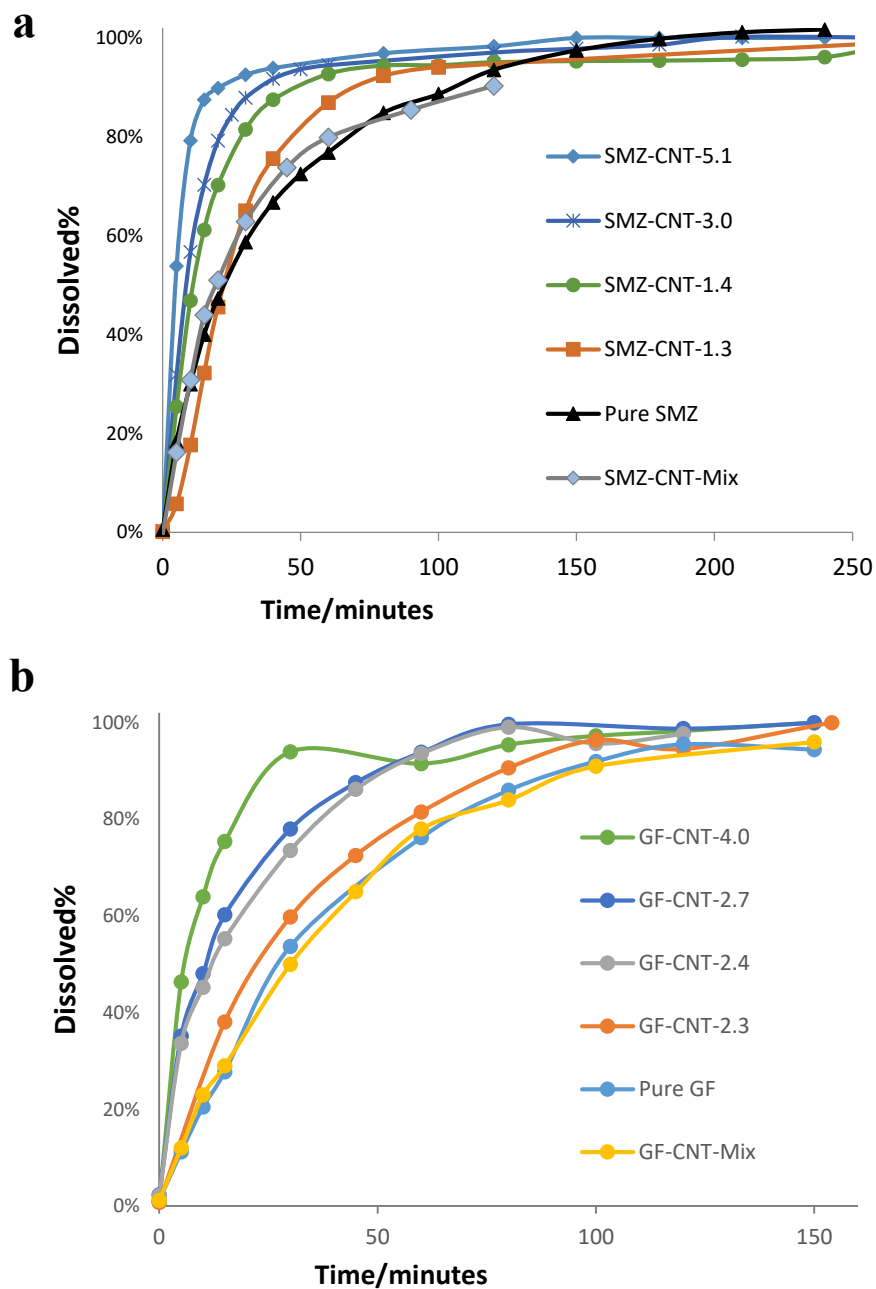


Figure 2.10 Dissolution of (a) SMZ-CNTs and (b) GF-CNTs showed enhanced dissolution with the incorporation of f-CNTs in drug crystals.

The increased dissolution was attributed to the two factors. The carboxylated CNTs were hydrophilic and hydrogen bonded well with water molecules and brought the latter

into close contact with the drug crystals. The TEM image in Figure 2.5 shows that some f-CNTs were incorporated into the crystals. A water molecule could potentially adsorb on the hydrophilic f-CNTs and use it as a conduit to enter the crystal thus enhancing the dissolution.

2.4 Conclusion

The f-CNTs dispersed in the water served as nucleating sites for crystallization and were readily incorporated into both GF and SMZ during their formation via anti-solvent precipitation. The SEM and TEM images show f-CNTs incorporation and their presence inside as well as outside the crystals. Raman, XRD and DSC showed presence of f-CNTs didn't change the crystal structure and melting point with the incorporation of as much as 5.1% f-CNTs by weight. The increase in dissolution rate was dramatic with t_{50} and t_{80} reducing by 78 for and 73% respectively for GF, and the corresponding increase for SMZ were 77 and 85%. This project presents a novel approach to f-CNTs incorporation that can go beyond enhancing dissolution and opens the door to targeting and other forms of drug delivery.

CHAPTER 3

CONTROLLING THE DISSOLUTION RATE OF HYDROPHOBIC DRUGS BY INCORPORATING CARBON NANOTUBES WITH DIFFERENT LEVELS OF CARBOXYLATION

3.1 Introduction

There has been much interest in using carbon nanotubes (CNTs) in nanomedicine and tissue engineering applications ([96](#), [99](#), [101](#), [104](#), [107](#), [153-155](#)). The CNTs have been used to deliver a wide range of small, large molecules and their controlled release. Small drug molecules as well as peptides, vaccines, antibodies, nucleic acids, proteins and genes have been attached to CNTs ([118-121](#)). Targeted drug delivery using CNTs have been successful ([156](#)), and they have shown permeability into tumor tissues via endocytosis ([122](#)).

The key to the applications of CNTs in drug delivery is its attachment to the drug molecules. Different molecules/species can be attached onto CNTs via covalent or non-covalent bonding. Covalent attachment to the CNT can provide secure loading of a molecule, and drugs such as paclitaxel, taxoid, doxorubicin, boron-bearing agents, methotrexate and 10-hydroxycamptothecin have been linked to CNTs via non-biodegradable or degradable linkages ([131](#), [157](#)). While the covalent approach can provide well-controlled targeting and delivery, it is only good for drugs whose functionality is not altered due to the bonding to CNTs. On the other hand, non-covalent approaches do not cause changes in the chemistry of drugs. Noncovalent approach to drug loading has been to load the molecule on the CNT surface by simple adsorption, π -stacking, hydrophobic interaction or capillarity-induced filling ([125](#), [158-159](#)). Both pure CNTs and functionalized CNTs (or f-CNTs) have been used in drug delivery, and in the case of noncovalent bonding, the advantages of f-CNTs can still be utilized.

Many drugs referred to as Class II and Class IV drugs have low solubility that limits their bioavailability and consequently their effectiveness as therapeutic agents (144). The solubility and bioavailability is typically improved by particle size reduction, which is described by the Noyes Whitney equation (29). Typically micro and nano drug particles are formed via mechanical size reduction such as dry/wet milling and homogenization (160), and also via precipitation techniques (148). Anti-solvent precipitation has been used to synthesize micro and nano particles of hydrophobic drugs (161-162). Here an antisolvent is used to precipitate crystals from a solution whose properties can be controlled by altering process conditions and the use of additives (163-164). Dissolution rate of hydrophobic drugs have been enhanced by the addition of hydrophilic moieties to the formulation. For example different cellulosic materials (165) have been used as co-precipitating agents and hydrophilic silica nanoparticles have been used to promote faster aqueous dissolution (166). Various polymers have been employed as peptide carriers in diabetes, oncology and cardiovascular drugs (167) and solid dispersion is an increasingly popular method that use HPMC, PVP, PEG and polymer micelles as carriers for insoluble drugs (168-169). Glucosamine hydrochloride has been used in solid dispersions (170) and hydrophobic molecules have been included in cyclodextrin (171) to enhance dissolution rates.

A drug carrier can be directly incorporated into the drug crystal during anti-solvent precipitation, and the latter can play multiple roles. For example, it can serve as a nucleation site for crystal formation, provide colloidal stability during crustal formation, and be a drug delivery vehicle such as a targeting agent or one that alters bioavailability by changing the dissolution rate. It is well known that functionalization is effective means to control aqueous behavior of nanotubes including colloidal stability as well as their solubilization

capacity towards hydrophobic molecules ([172-174](#)). The fiber like CNTs can actually be incorporated into drug crystals, and if the f-CNTs are hydrophilic, they can attract water molecules and bring them to drug crystal leading up to faster dissolution. The hydrophilicity of f-CNTs can also be altered to alter the dissolution rate; a phenomenon that can be used to control the release of the drug.

Among the f-CNTs, carboxylated CNTs are highly water dispersible and our studies have demonstrated its potential to enhance dissolution rates ([45](#)). The carboxylated CNTs can be synthesized such that the carbon to oxygen atomic ratio can be varied to have different hydrophilicity and it is conceivable that by varying the degree of functionalization, the drug can be released at different rates. Therefore, the level of functionalization is expected to be an important factor. The objective of this work was to study the effect of the degree of functionalization on the incorporation of hydrophobic drugs during anti-solvent synthesis of micron-scale drug particles as well as the dissolution rates. Of particular interest to this study were antifungal agent Griseofulvin (GF) and antibiotic Sulfamethoxazole (SMZ).

3.2 Materials and Methods

3.2.1 Materials

Sodium dodecyl sulphate (SDS) was purchased from GFS Chemicals, hydrochloride acid was purchased from Fisher Scientific, raw multiwall carbon nanotubes nanotube (20-30 nm diameter, 10-30 μm length, Purity > 95 wt%) was purchased from Cheap Tube, while Griseofulvin (GF), Sulfamethoxazole (SMZ), sulfuric acid (95-98%) and nitric acid (70%)

were purchased from Sigma Aldrich. Purified Milli-Q Plus water was used in all experiments.

3.2.2 Methods

Carboxylated multiwall carbon nanotubes (f-CNTs) were synthesized following a methodology published before (45). Raw CNTs were reacted with a mixture of concentrated H₂SO₄ and HNO₃ at 140 °C for 5, 10, 40 and 90 minutes respectively in a microwave reactor (Model: CEM Mars). This led to the formation of various amounts of carboxylic groups on the CNT surface that had different hydrophilicity (142). The carboxylated CNTs were filtered through a 10µm PTFE membrane filter, washed to a neutral pH and dried under vacuum at 65 °C. The resulting f-CNTs were characterized with EDX to determine the amount of carboxylated group added to CNTs.

Drug/f-CNTs composite were prepared by anti-solvent precipitation. At room temperature, GF or SMZ was satutely dissolved in acetone. Antisolvent was prepared by disperse f-CNTs in water under sonication for 10 minutes. The antisolvent was added dropwise into the drug solution under sonication and the solution turned cloudy immediately after the addition of f-CNTs suspension which indicated crystal formation of the f-CNTs/drug composites referred to as GF-CNT_x and SMZ-CNT_x, respectively. X represents the carbon to carboxylated group ratio. The resulting solution was filtered through a 10µm PTFE membrane filter, washed and dried in a vacuum oven to a constant weight.

The resulting drug/f-CNTs composites were characterized with SEM, TEM, DSC, XRD, TGA and elemental analysis. The dissolution was tested by dissolution testing apparatus 2.

SEM and EDX was performed with LEO 1530VP. TEM was performed with Hitachi H-7500 Tungsten/LaB6 with 100KV energy beam. TGA was performed with Perkin Elmer Pyris 1 thermogravimetric analyzer which heated the samples from 30 °C to 1200 °C at 10 °C/min under air environment. Elemental analysis was performed Perkin-Elmer 2400 Series II elemental analyzer.

Raman spectroscopy was performed with Thermo Scientific DXR Raman Microscope with 532 nm filter. Melting point was measured with Perkin Elmer DSC 6000. DSC was carried out under nitrogen where GF-CNT_x were heated from 30 °C to 250 °C at 20 °C/min while SMZ-CNT_x were heated from 30 °C to 200 °C at 20 °C/min. XRD was performed with PANalytical EMPYREAN XRD. Symphony 7100 dissolution system was used to study the dissolution behavior of the drug composites using standard USP method (USP 41).

3.3 Results and Discussion

EDX was used to examine the carbon and oxygen percentage in the functionalized CNTs. The degree of functionalization is shown on Table 3.1. As functionalization time increased, oxygen content and the C: COOH increased. After 40min of functionalization, the oxygen percentage did not increase significantly, therefore treatment time beyond 40 minutes were not studied. The oxygen content of the different f-CNTs varied from 6.1 to 13.6% while the carbon to carboxylic group ratio could be as low as 16:1. The f-CNTs were labeled based on the C: COOH ratio.

Table 3.1 Analysis of f-CNTs with Different Levels of Functionalization

Treatment Time(min)	% by Weight		C: COOH
	C	O	
0	92.7	6.1	39.5
5	89.3	10.4	23.2
10	87.9	11.2	19.8
40	86.3	13.6	16.0
90	83.7	13.7	15.2

The concentrations of f-CNTs in GF were calculated from the TGA (Figure 3.1). The amount of f-CNTs in the GF crystals prepared from f-CNT_{23.2}, f-CNT_{19.8}, f-CNT_{16.0} suspensions were found to be 3.9, 4.2 and 3.8%, respectively. The values were calculated based on the weight% at the temperature from which f-CNTs started to burn out (around 300°C) for each composite minus the corresponding weight% of pure GF at the same temperature. The concentrations of f-CNTs in SMZ-CNTs were measured based on the elemental analysis. The sulfur content was used to calculate the amount of SMZ in the composite from which the amount of f-CNTs could be predicted. The amount of f-CNTs in the SMZ crystals prepared from f-CNT_{23.2}, f-CNT_{19.8}, f-CNT_{16.0} suspensions were found to be 2.9, 1.3 and 1.4%, respectively. These are referred to as SMZ-CNT_x or GF-CNT_x where x is the C: COOH ratio. It appears that the degree of functionalization did not significantly affect the weight percent of f-CNTs in the drug crystals formed during the anti-solvent precipitation.

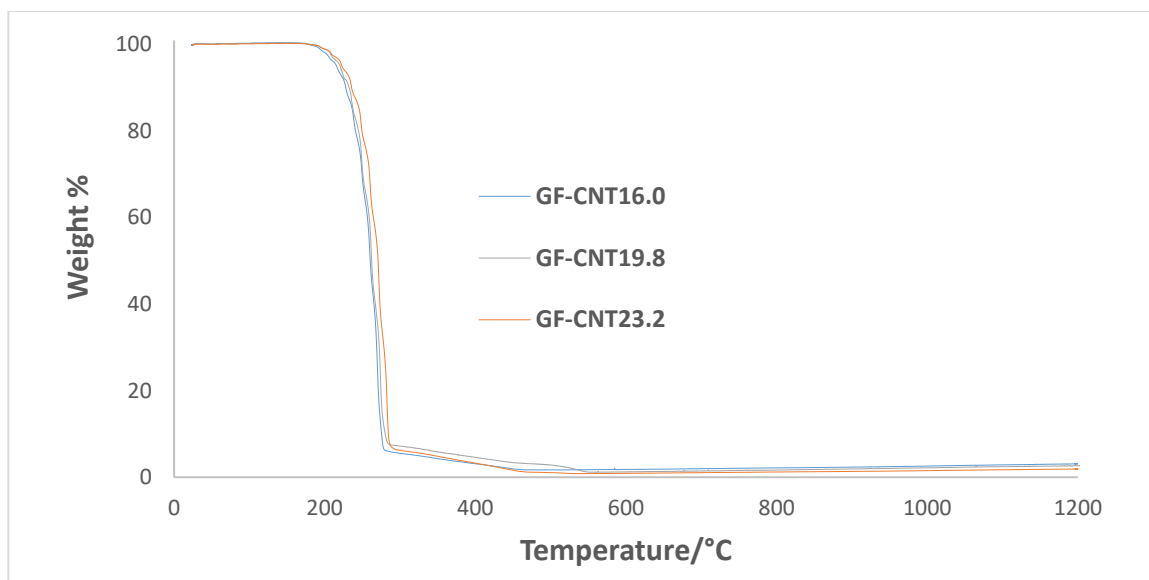


Figure 3.1 TGA of different GF-CNT_x.

The GF-CNTs and SMZ-CNTs sample morphology was studied using SEM. Figure 3.2 a, b, c show SEM images of GF-CNT_{23.2}, GF-CNT_{19.8}, GF-CNT₁₆ at 25K magnification. Figure 3.2 d, e, f show SEM images of SMZ-CNT_{23.2}, SMZ-CNT_{19.8} and SMZ-CNT₁₆ at the same magnification. SEM images showed the f-CNTs was present on the crystal surface. Compared to SEM images of pure GF and pure SMZ in figure 3.2 g and h, the crystals shape and size did not depend on f-CNTs functionalization or incorporation. The TEM images (Figures 3.2 i) showed that the f-CNTs were also partially embedded in the drug crystals.

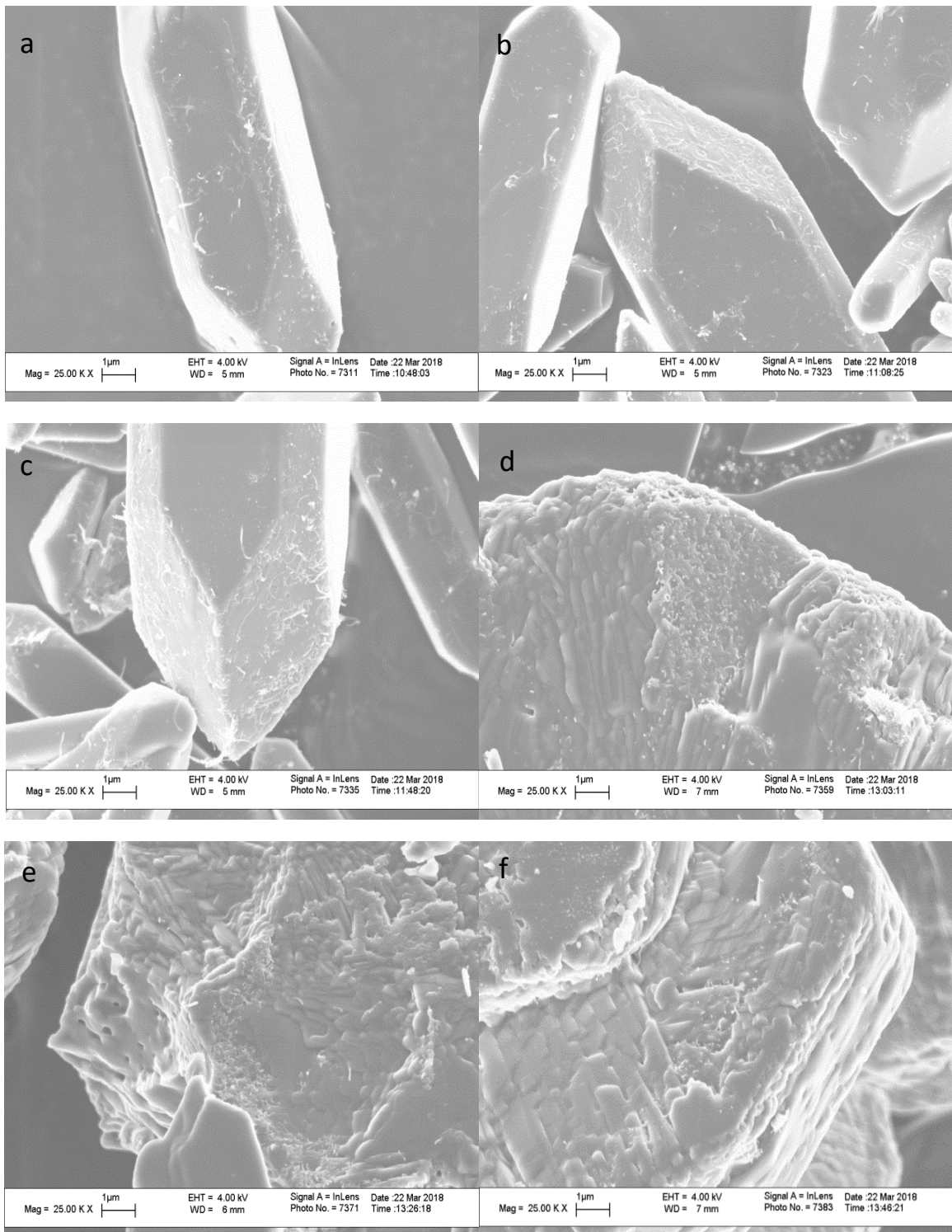


Figure 3.2 SEM image of (a) GF-CNT_{23.2}, (b) GF-CNT_{19.8}, (c) GF-CNT₁₆, (d) SMZ-CNT_{23.2}, (e) SMZ-CNT_{19.8}, (f) SMZ-CNT₁₆, (g) Pure GF, (h) Pure SMZ, TEM image of (i) GF-CNT₁₆.

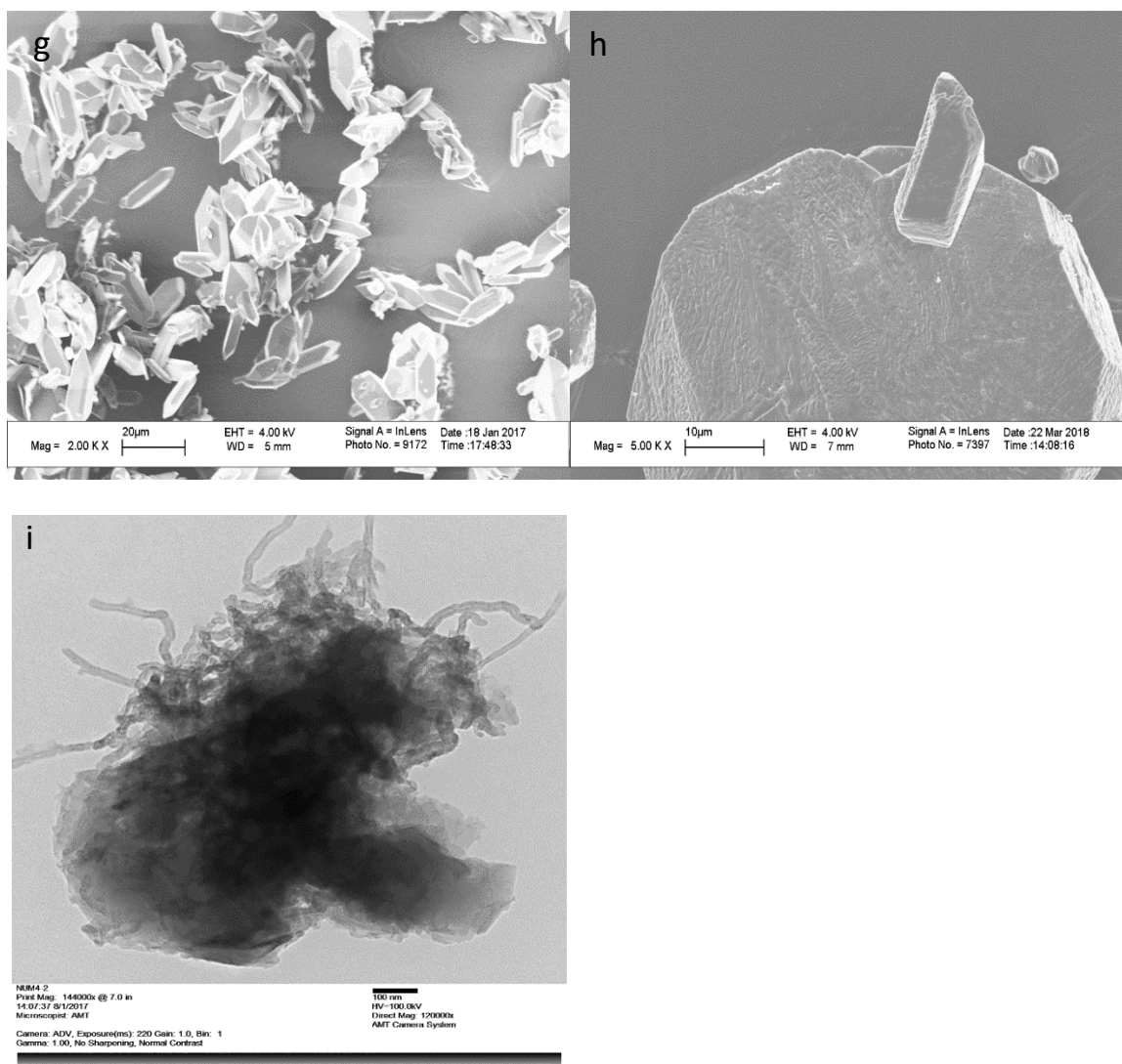


Figure 3.2 (Continued) SEM image of (a) GF-CNT_{23.2}, (b) GF-CNT_{19.8}, (c) GF-CNT₁₆, (d) SMZ-CNT_{23.2}, (e) SMZ-CNT_{19.8}, (f) SMZ-CNT₁₆, (g) Pure GF, (h) Pure SMZ, TEM image of (i) GF-CNT₁₆.

Figure 3.3 a showed the Raman spectra of f-CNTs, GF and GF-CNTs with various degree of functionalization. The typical spectral features of f-CNTs were overlaid with peaks from GF. The Raman spectra for GF and GF-CNTs composites remained the same indicating that the presence of the f-CNTs didn't change the chemical nature of the GF or its polymorphism, which are important considerations in drug development. The similar

observation was found in Figure 3.3 b which showed Raman spectra of f-CNTs, SMZ and SMZ-CNTs with various degree of functionalization.

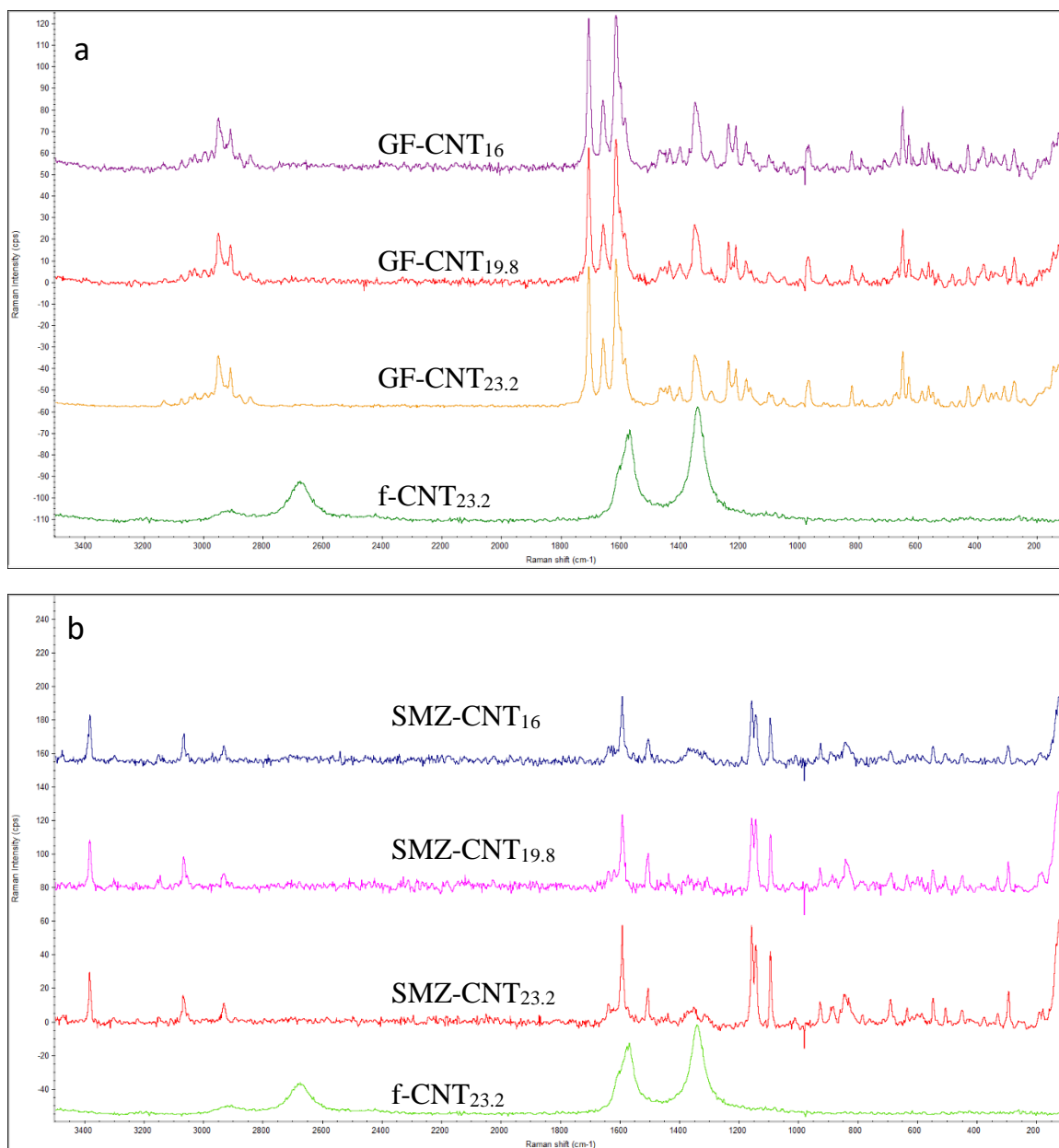


Figure 3.3 RAMN spectra of f-CNT_{23.2} and (a) GF- CNT_x, (b) SMZ- CNT_x.

Crystal structure of the GF-CNT_x and SMZ-CNT_x were also studied using XRD and Figure 3.4 shows the spectrum of GF-CNT_x and SMZ-CNT_x. It was seen that the crystal structure remained unchanged with the incorporation of the f-CNTs. The spectra of pure

drugs and drug/CNTs were identical. This implied that there were no changes in polymorphism.

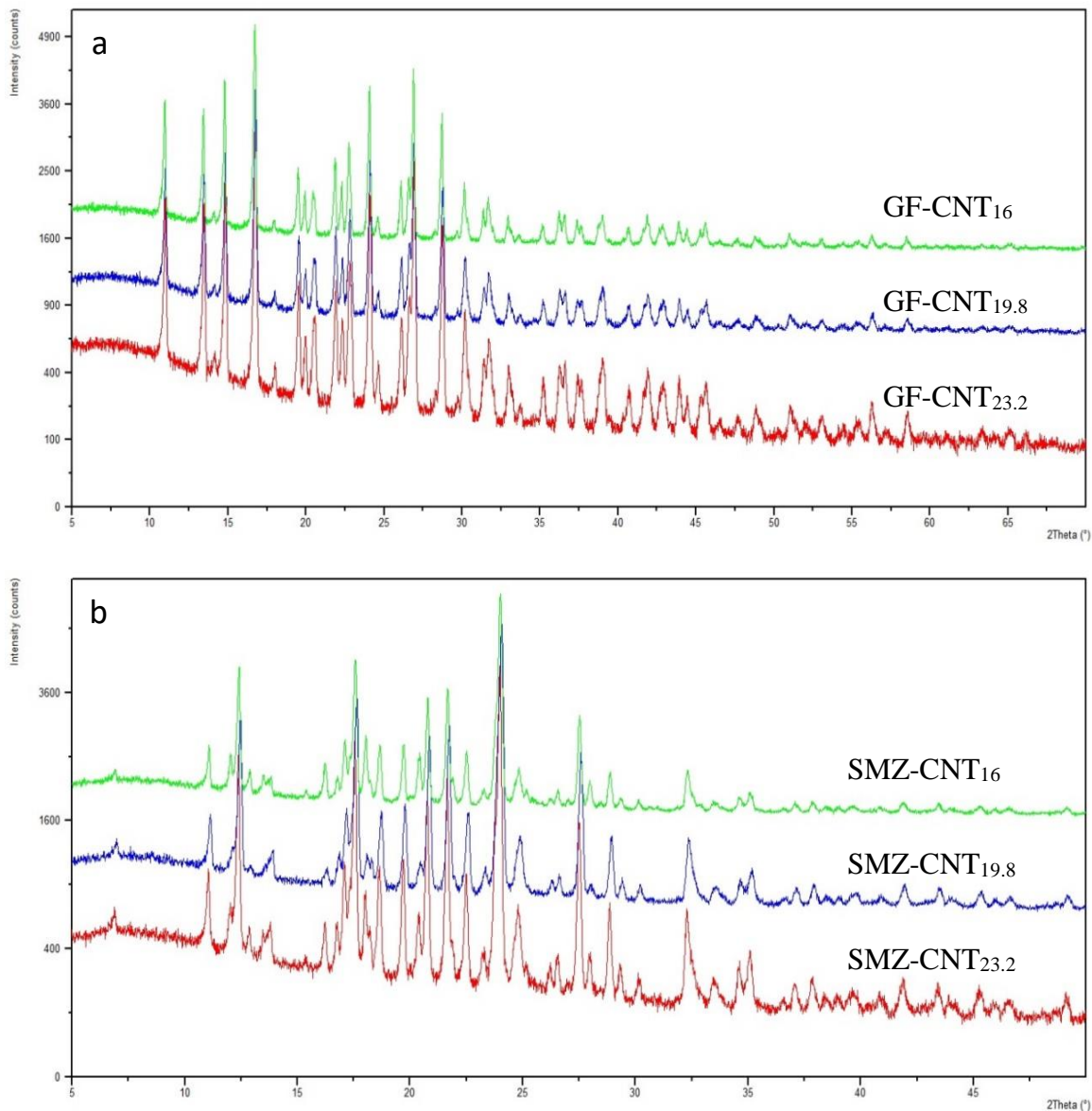


Figure 3.4 XRD spectrum of (a) GF-CNT_x and (b) SMZ-CNT_x.

The melting point of drug/CNTs composites were analyzed by DSC 6000. The results are presented in Table 3.2. It was seen that there was no significant change in melting point between the pure drug and their f-CNTs composites.

Dissolution measurements were carried out based on standard US Pharmacopeia Method (USP 41). GF-CNTs composites were added to 4mg/ml sodium dodecyl sulfate while SMZ-CNTs composites were added to 0.1 N hydrochloric acid. The samples were stirred with paddle at 75rpm and heated to keep temperature at 37°C. A small amount of medium was withdrawn at different times, filtered with PTFE membrane to remove f-CNTs and analyzed with UV-visible spectrophotometry to determine the amount of drug dissolved, 291 nm for GF and 265 nm for SMZ samples. The dissolution data is presented in Figure 3.5.

It is evident from both profiles that the increase in the level of functionalization in f-CNTs enhanced the release of the drugs. The carboxylated CNTs were hydrophilic and increased contact between the water and the drug crystals. The water molecules adsorbed on the hydrophilic carboxylic group, and then use it as a conduit to the drug crystal to increase dissolution.

The time necessary to reach 50% (t_{50}) and 80% (t_{80}) dissolution reduced with the incorporation of f-CNTs, and higher levels carboxylation showed lower values of these parameters. As the C: COOH ratio decreased from 23.2 to 16, the t_{50} and t_{80} of GF dropped from 6.0 to 4.0 min and from 60.0 to 30.5 min, respectively. Corresponding drop for SMZ were from 8.5 to 6.0 min and from 16.5 to 11 min, respectively. Therefore, it is evident that by varying the level of carboxylation, it is possible to control the dissolution rate of the hydrophobic drugs.

Table 3.2 Dissolution and Melting Point of SMZ-CNT_x and GF-CNT_x

	Incorporation %	C:COOH	T ₅₀ (min)	T ₈₀ (min)	M _p (°C)
GF-CNT _x	0	39.5	8.0	>120.0	221.25
	3.9	23.2	6.0	60.0	220.75
	4.2	19.8	4.5	44.0	220.92
	3.8	16	4.0	30.5	221.01
SMZ-CNT _x	0	39.5	23.5	52.5	170.37
	2.9	23.2	8.5	16.5	170.21
	1.3	19.8	7.5	15.0	170.06
	1.4	16	6.0	11.5	170.05

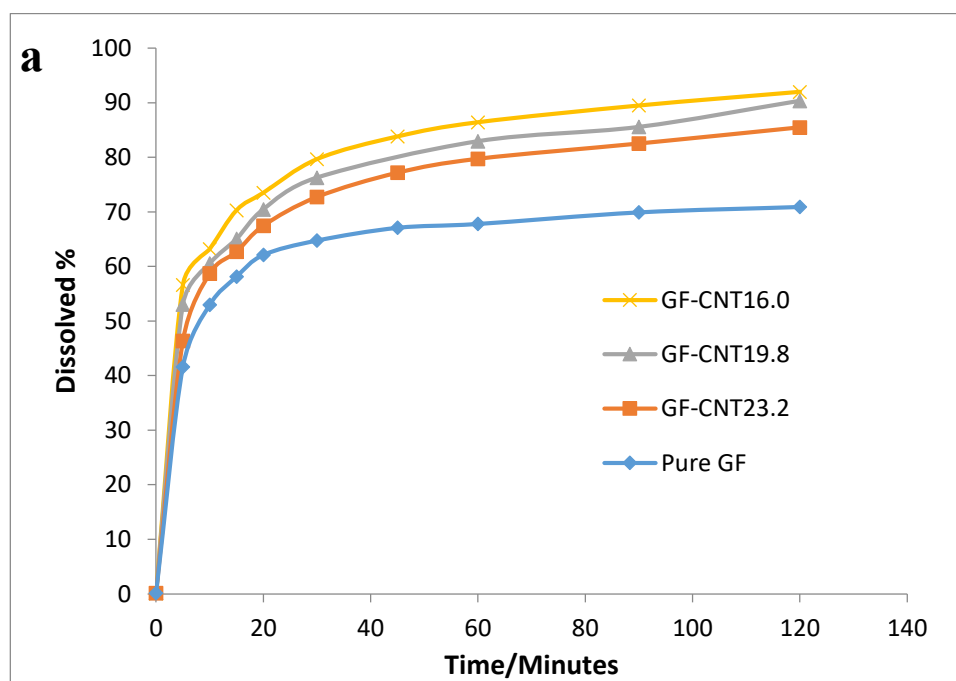


Figure 3.5 (a) Dissolution of GF-CNT_x, (b) Dissolution of SMZ-CNT_x (c) Time to reach 80% dissolved for drug with degree of functionalization of f-CNTs.

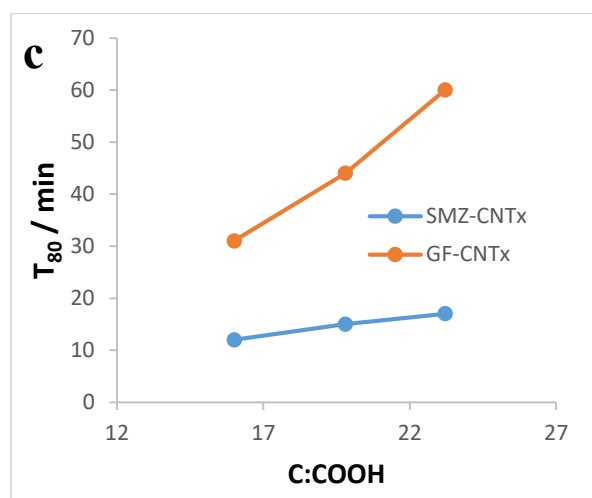
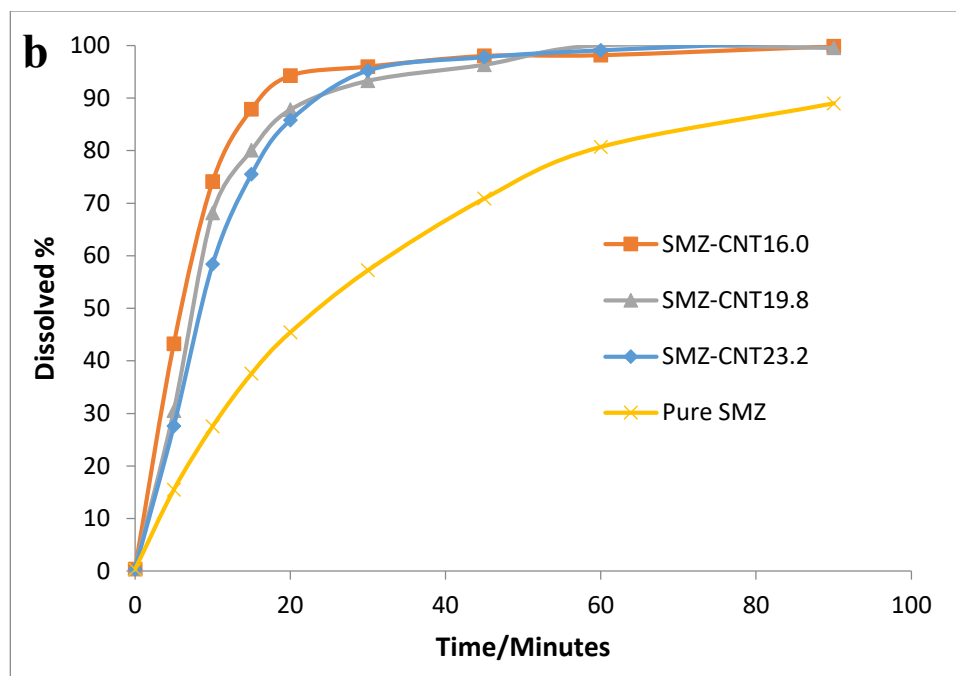


Figure 3.5 (Continued) (a) Dissolution of GF-CNT_x, (b) Dissolution of SMZ-CNT_x (c) Time to reach 80% dissolved for drug with degree of functionalization of f-CNTs.

3.4 Conclusion

The CNTs were oxidized to form f-CNTs with different levels of carboxylation. The SEM and TEM images show CNT incorporation into the drug crystals, and their presence was seen inside as well as outside the crystals. Based on Raman, XRD and DSC measurements, it was evident that the f-CNTs did not change the crystal structure or the melting point. The dissolution rate was significantly enhanced with the incorporation of f-CNTs, where t_{50} and t_{80} reduced by as much as 50 and 75% for GF and 74 and 78% for SMZ. By decreasing the C: COOH ratio in the f-CNTs, the t_{50} and t_{80} could be reduced by 33% for and 49% respectively for GF, and 31% and 33% for SMZ. This paper not only presents a novel approach to f-CNT incorporation into hydrophobic drugs, but goes beyond and opens the door to controlling the release rate by altering the level of CNT carboxylation.

CHAPTER 4

COLLOIDAL BEHAVIOR OF DRUG/CNTS COMPOSITE PARTICLES

4.1 Introduction

Poor water solubility has always been a key obstacle in achieving adequate bioavailability for many hydrophobic drug molecules being developed by the pharmaceutical industry ([14](#), [175](#)). Dissolution in the gastrointestinal (GI) tract is a limiting factor for these compounds and increasing their dissolution rate has been a great interest in drug development processes ([176](#)). Particle size and the morphology plays a key role in the dissolution rate and bioavailability of hydrophobic drug molecules. Finer particles have more surface area per unit mass that is exposed to fluids in the gastrointestinal tract, hence increase the dissolution rate of the drug ([177](#)).

Various techniques have been developed to reduce particle size. Chemical modification and self-emulsifying systems have the disadvantages of pharmacological activity change of active pharmaceutical ingredients due to chemical modification as well as physical and chemical instability ([178](#)).

Traditional top down methods for the synthesis of micron and submicron particles such as milling and homogenization presents challenges to control the size, morphology, surface properties and electrostatic charge of the drug particles ([147](#)). The chemical degradation and residual metal content are also concerns in top down methods ([179](#)).

Compared to top-down methods, bottom-up approaches such as anti-solvent precipitation has gain much interest in recent years. These approaches involve the formation of fine particles from molecular state by precipitation or evaporation of solvent. Anti-solvent precipitation has been considered as a simple and cost effective method to

prepare fine drug particles ([180](#)). It has been used to produce micron size particles for a long time and can be adjust to prepare nano size particles as well ([180](#)).

However, the disadvantage of precipitation process is that the drug particles produced are not stable in the suspension and precipitated particles tend to aggregate. Immediate spray drying has been shown as an effective method to maintain particle size after precipitation ([179](#)). Another approach is adding surfactant such as β -Cyclodextrin or High molecular weight hydroxypropyl methyl cellulose ([181](#)). In both cases, the anti-solvent was either water or homogeneous solution. There is potential that using different type of anti-solvent such as suspension can affect the aggregation behavior of drug particles as well.

The purpose of the present investigation is to study the effects of varies degree of carboxylated carbon nanotubes on the colloidal behavior of hydrophobic drug particles formed during anti-solvent synthesis. The Sulfamethoxazole particles were produced with anti-solvent precipitation, while varies degree of carboxylated carbon nanotubes were incorporated into drug crystals. The interaction between f-CNTs and Sulfamethoxazole has been investigated.

4.2 Materials and Methods

4.2.1 Materials

Raw multiwall carbon nanotubes nanotube (20-30 nm diameter, 10-30 μ m length, Purity >95 wt%) was purchased from Cheap Tube, Sulfamethoxazole (SMZ), Sulfuric acid (95-98%), Nitric acid (70%) and acetone (\geq 99.9%) were purchased from Sigma Aldrich. Purified Milli-Q Plus water was used in all experiments.

4.2.2 Methods

Carboxylated multiwall carbon nanotubes(f-CNT) were synthesized following a methodology published before ([45](#), [182](#)). CNTs were reacted with a mixture of concentrated H₂SO₄ and HNO₃ at 140 °C for 5, 10, 20 and 40 min respectively in a microwave reactor (Model: CEM Mars). This led to the formation of various amounts of carboxylic groups on the CNT surface that had different hydrophilicity ([142](#)). The carboxylated CNTs were diluted to reduce acidity and then filtered through 0.22 µm PES membrane filter, washed with water to a neutral pH and dried under vacuum at 65 °C to a constant weight.

Anti-solvent precipitation was carried out at room temperature as shown in Figure 4.1. The anti-solvent was prepared by suspending f-CNTs in water by sonication of 5 minutes. The solvent solution was prepared by dissolving SMZ in acetone to reach saturation. The mixing of anti-solvent and solvent (SMZ: f-CNTs = 100:1, w/w) was carried out under ultrasonic agitation for 3 min where anti-solvent was drop by drop added into solvent solution. For preparation of the solid complexes, the drug suspensions were filtered through 10 µm PTFE membrane filters and the water was removed from aqueous drug/f-CNTs solutions by evaporation.

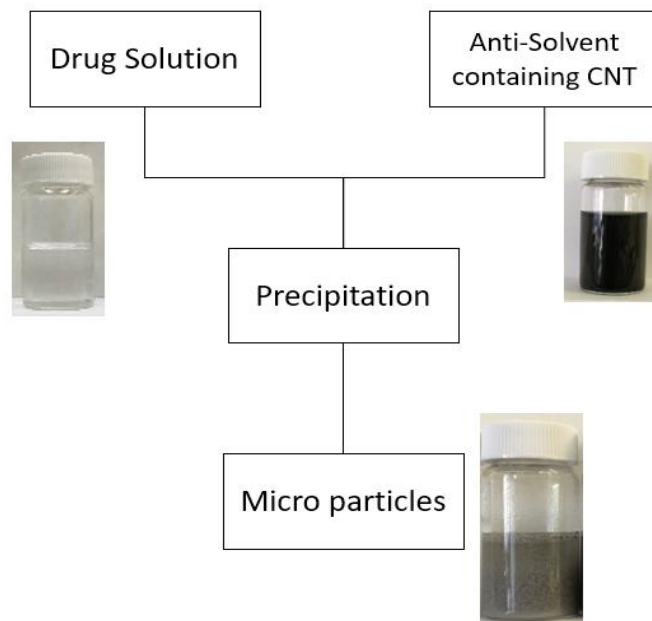


Figure 4.1 Anti-solvent precipitation of drug/f-CNTs.

f-CNTs were characterized with EDX and Raman. EDX was carried out with LEO 1530VP. Raman spectroscopy was tested with DXR Raman Microscope from Thermo Scientific with 532 nm filter. Drug/f-CNTs composites were characterized with FTIR using Agilent Cary 670 FTIR spectrometer with Diamond-ATR.

Particle size analysis and Zeta potential measurements were carried out by and dynamic light scattering using Zetasizer Nano series ZS90. Zeta potential was measured immediately following the complete of anti-solvent precipitation. Particle size of drug/f-CNTs suspension was measured at different time where the suspension was allowed to settle down.

Sedimentation was monitored as a function of time by measuring the weight percentage of the solid remaining in the suspension. This was accomplished as follows. Each suspension was prepared five times to be settled and measured after different time at

25 °C. The solid sediments were collected at 0.8, 2.3, 4.3 and 7.4 hour, dried in the oven at 65 °C in a vacuum to remove the solvent and weighed. The amount of solid remaining in the suspension was calculated by deducting the sediments weight from the combined weight of drug and f-CNTs before anti-solvent precipitation.

4.3 Results and Discussion

4.3.1 Characterizations

EDX data of raw CNTs and f-CNTs were measured and presented in Figure 4.2. The oxygen content increased with the treatment time from 5 to 40 min. The number of carboxylic per carbon (C: COOH) was calculated based on EDX data. The ratio decreased from 23.2 to 16.0 with treatment time 5 to 40 min. The functionalized CNTs with different treatment times were referred as f-CNT_{23.2}, f-CNT_{19.8}, f-CNT_{16.0} based on the C: COOH ratio.

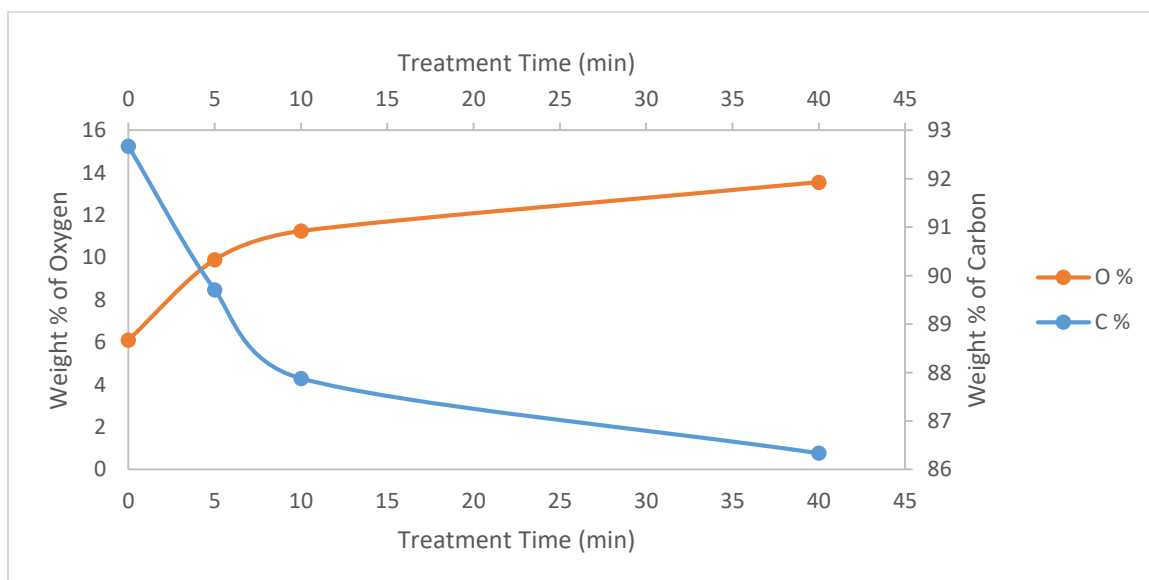


Figure 4.2 EDX of carbon and oxygen ration of raw CNTs and f-CNTs with different treatment time.

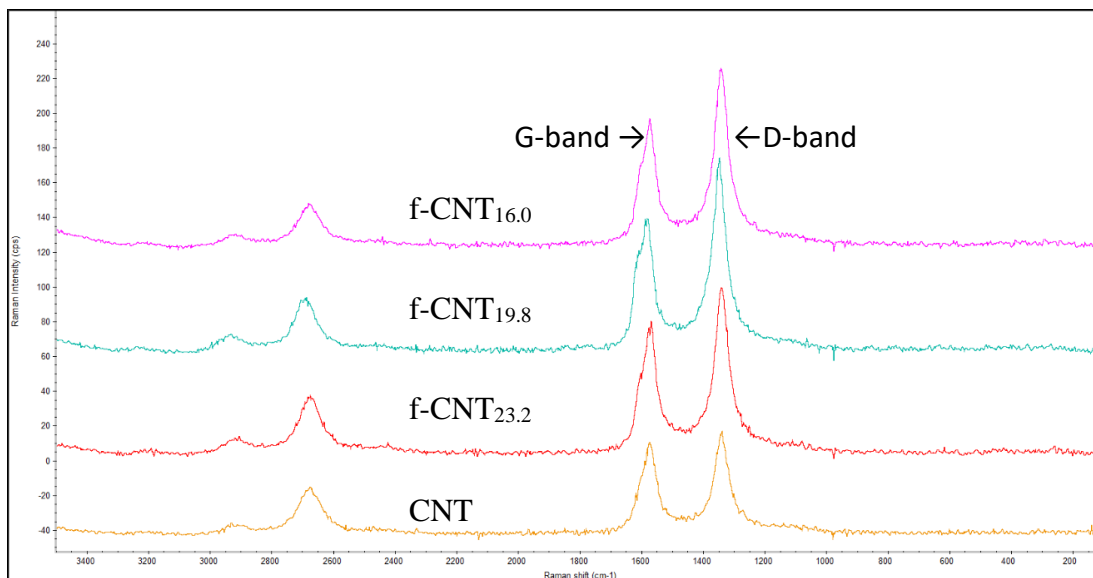


Figure 4.3 Raman spectroscopy of raw CNTs and f-CNTs with different treatment time.

Table 4.1 I_D/I_G of Raw CNTs and f-CNTs with Different Treatment Time

	I_D	I_G	I_D/I_G
F-CNT _{16.0}	180.32	113.91	1.58
F-CNT _{19.8}	117.01	81.80	1.43
F-CNT _{23.2}	99.06	79.72	1.24
Raw CNT	38.84	34.81	1.12

The Raman spectroscopy of raw CNTs and f-CNTs with different treatment time was presented in Figure 4.3. The intensity ratio of the D (defect band) and G band (graphite band) from Raman spectroscopy increased from raw CNT to f-CNT_{16.0}. The I_D/I_G ratio was calculated and presented in Table 4.1. The higher I_D/I_G ratio typically implies higher levels of defects associated with functionalization, which correlated the EDX results that longer treatment time leads to more carboxylated group in f-CNTs.

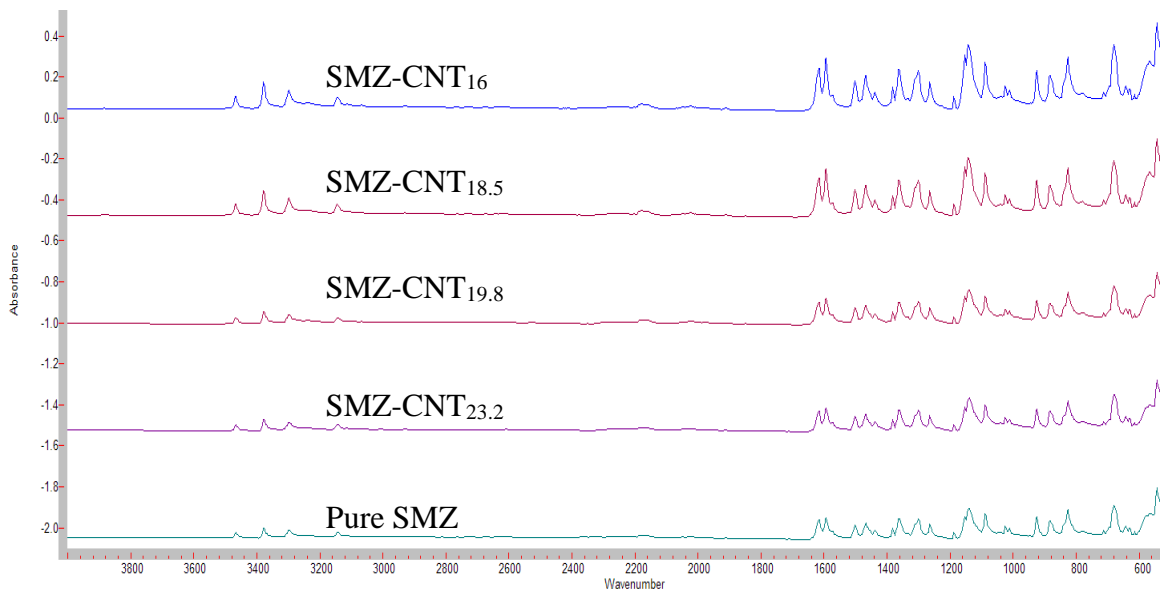


Figure 4.4 FTIR spectroscopy of pure SMZ, SMZ-CNT_{23.2}, SMZ-CNT_{19.8}, SMZ-CNT_{18.5} and SMZ-CNT_{16.0}.

Pure SMZ and SMZ incorporated with various degree of carboxylated CNTs were characterized with FTIR in Figure 4.4. The signature peaks of pure SMZ and SMZ-CNT_x were identical, indicating incorporation of f-CNTs did not change the structure of SMZ. The lack of peaks for carboxylated group was attributed to the low concentration of f-CNTs incorporated which leads to even lower concentration of carboxylated group in the drug/f-CNTs composites.

4.3.2 Particle Size Analysis for Drug Suspensions

It was observed that most of the SMZ underwent anti-solvent precipitation rather than be completely consumed in a soluble, aqueous complex. The precipitation occurred immediately after adding f-CNTs suspensions. The precipitation time was controlled to avoid temperature increasing due to prolonged sonication.

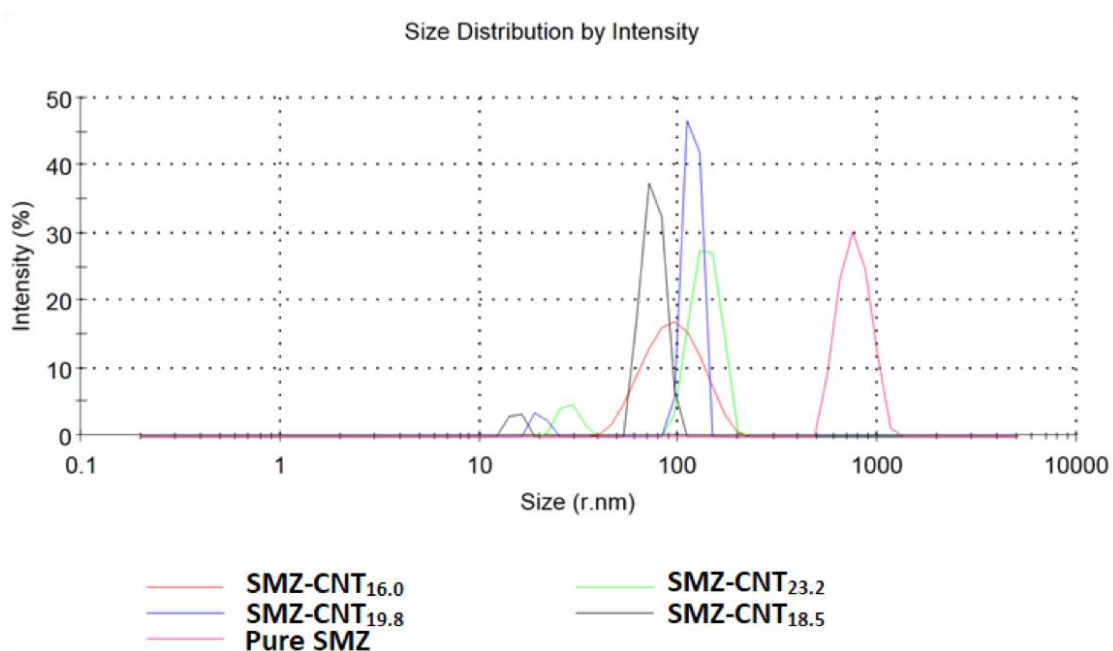


Figure 4.5 Size distribution of pure SMZ, SMZ-CNT_{23.2}, SMZ-CNT_{19.8}, SMZ-CNT_{18.5} and SMZ-CNT_{16.0}.

Typical particle size distribution (PSD) of pure SMZ and stabilized SMZ suspension with f-CNTs are measured immediately after precipitation and results are shown in Figure 4.5. The mean diameter of pure SMZ in the aqueous suspension was 667 nm with a broad size distribution. With anti-solvent precipitation and stabilization with f-CNTs, the mean particle diameter decreased to 149 nm with a significantly narrow particle size distribution. Bimodal distributions were achieved with stabilization with all the f-CNTs, which clearly showed the drug particles coagulated. The mean diameters of particle for different suspension systems are presented in Table 4.2 at the initiation of anti-solvent particle formation and 2.3 hours hence. All the f-CNTs used here were effective in reducing the particle size. It was observed that with the increase of carboxylated group in f-CNTs, the particle size decreases.

Table 4.2 Stabilizing SMZ with f-CNTs

Suspension	Mean Radius (nm)		Percentage of particles in suspension (%)		Sedimentation Rate (wt%/h)		Zeta Potential (mV)
	0 h	2.3 h	0.8 h	2.3 h	0.8 h	2.3 h	
Pure SMZ	667.6	133.0	29.2	21.1	88.5	38.9	-12.1
SMZ-CNT _{23.2}	322.1	117.8	37.5	23.8	73.5	32.8	4.6
SMZ-CNT _{19.8}	257.7	94.3	43.8	37	76.9	27.6	-7.8
SMZ-CNT _{18.5}	213.0	89.2	42.8	36.1	71.5	28.8	2.6
SMZ-CNT _{16.0}	149.3	89.0	59.9	48.1	41.4	22.3	-3.2

Also seen from Table 4.2 is that as the suspension was allowed to stand, the larger particles settled, reducing the average particle radius in the suspension. It is evident from Figure 4.6 that the presence of the f-CNTs had a stabilizing effect. Increased carboxylation leads to significantly less variation in average particle radius because the settling rate was slower. Incorporation of carboxylated group also provided steric stabilization to help maintain the distance between closely approaching solid particles in a suspension ([183](#)). Carboxylation group also provided electrostatic stabilization by forming electro double layer (Figure 4.7) and increased carboxylation provided increased electrostatic stabilization which lead to reduced particle size and settling rate.

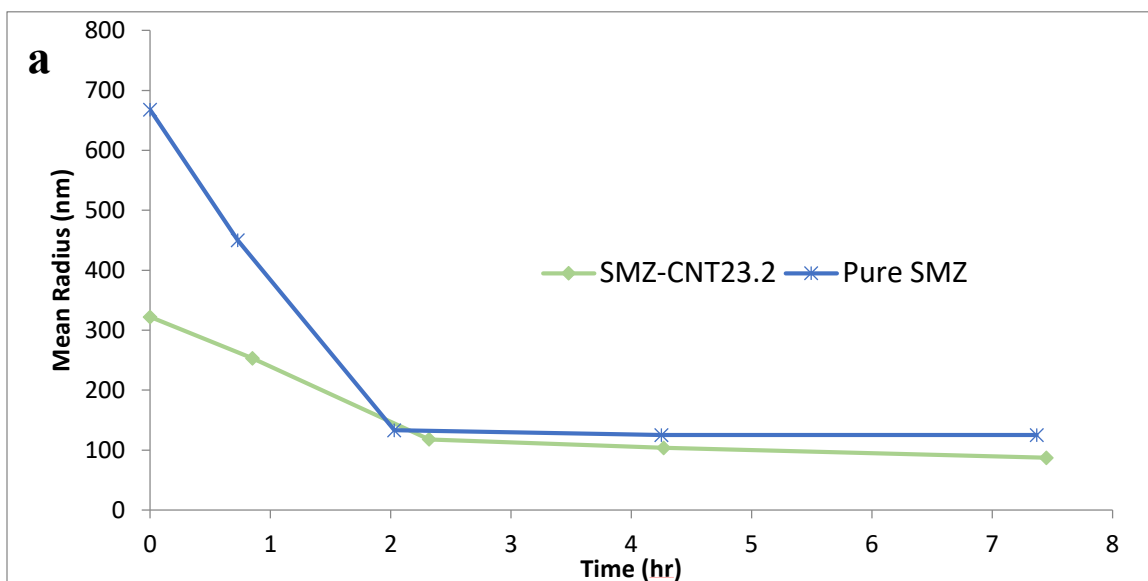


Figure 4.6 (a) Mean radius of pure SMZ and SMZ-CNT_{23.2} as a function of time, (b) Mean radius of SMZ-CNT_x as a function of time.

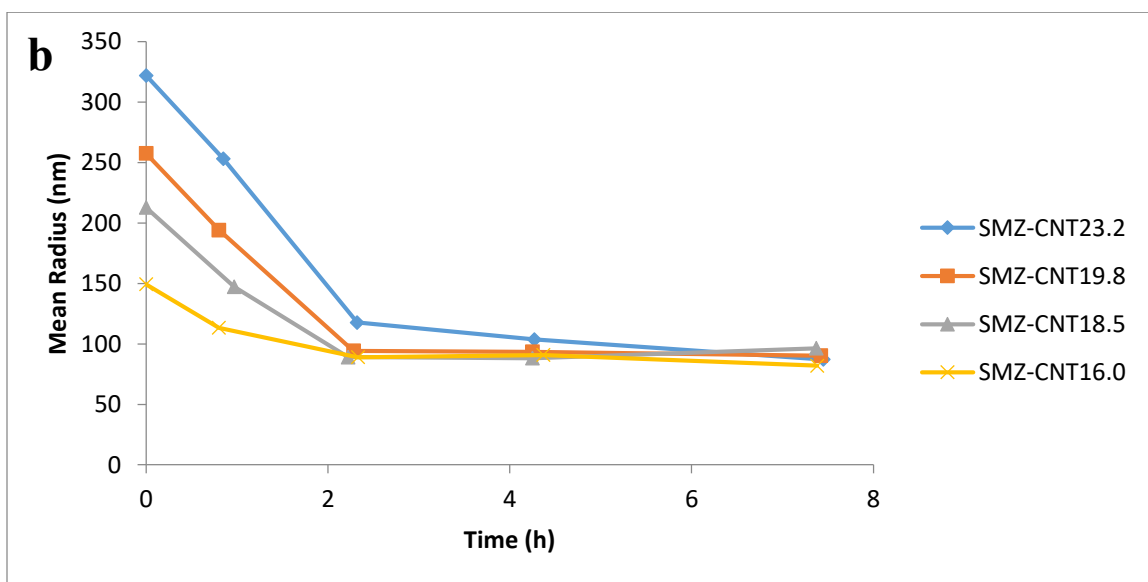


Figure 4.6 (Continued) (a) Mean radius of pure SMZ and SMZ-CNT_{23.2} as a function of time, (b) Mean radius of SMZ-CNT_x as a function of time.

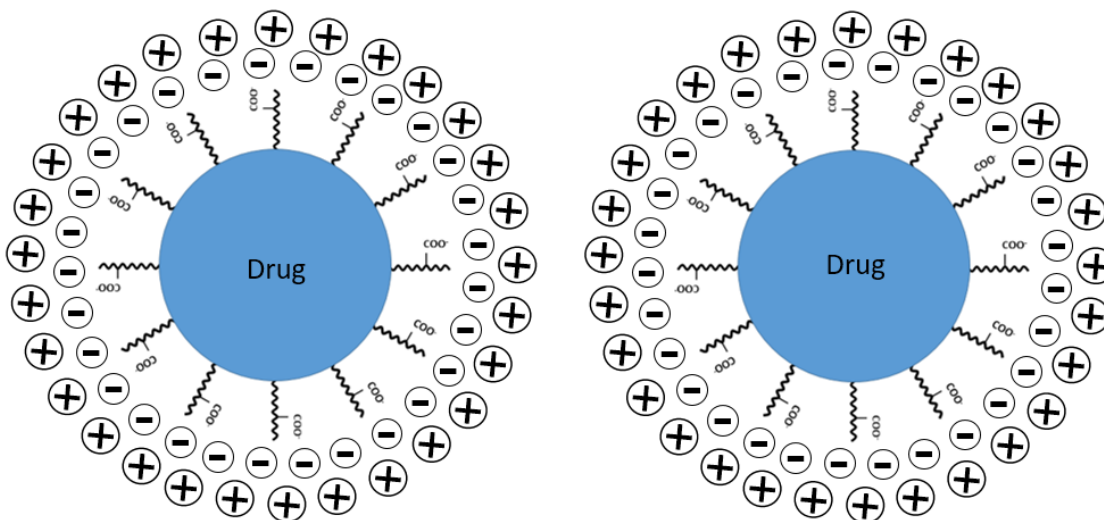


Figure 4.7 Electrostatic double layers of drug/f-CNTs composites.

Zeta-potential measurements were used to study the stability of the drug suspension. The zeta potential values were measured after the preparation of the drug suspensions. Dispersed SMZ particles showed zeta potential in the range of -19.8 to 4.6 mV in Table 4.2. The result indicated that the drug/f-CNTs suspension is not stable and tend to aggregate and settle down.

4.3.3 Sedimentation Rate

Sedimentation rate is an important parameter in determining long term stability of suspension ([184](#)). Typically, the particles tend to grow or aggregate to a larger size, which leads to increases of the overall setting rate. According to Stokes equation the rate of sedimentation depends upon the diameter of the dispersed particles, the density and the viscosity of the medium ([185](#)). Sedimentation rate was measured by calculating the weight percentage (wt%) of solid drug particles remaining in the suspension as a function of time.

The solid particles were uniformly distributed after the preparation of the suspension. The amount of the solid particles in the suspension decreased with time as they began to settle down. The data are presented in Figure 4.8. The results appear to be consistent with the Stokes Equation that the smaller diameter particles have slower settling rate, thus higher amount remaining in the suspension. It was found that the amount of particles in suspension of SMZ-CNTs were larger than that of the pure SMZ. And with the increased carboxylated group presence in f-CNTs, the amount of particles remaining in suspension was higher.

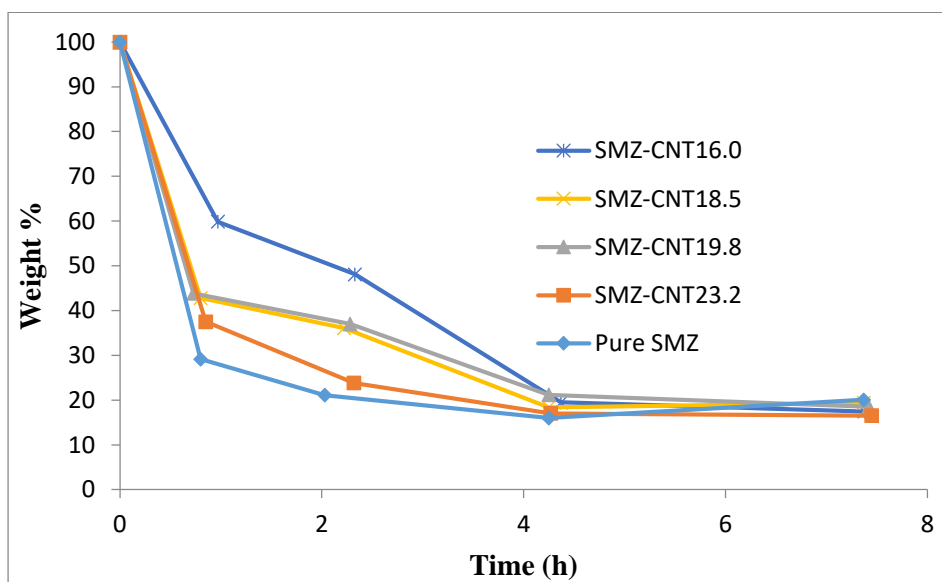


Figure 4.8 Weight percentage of stabilized drug particles in suspension for Pure SMZ, SMZ-CNT_{23.2}, SMZ-CNT_{19.8}, SMZ-CNT_{18.5} and SMZ-CNT_{16.0}.

The settling rate was computed as a function of time for all systems and presented in Figure 4.9. It was evident that the settling rate increased rapidly within the first half hour and then dropped. It was found that settling rate of SMZ-CNTs were slower than that of the pure SMZ. And with the increased carboxylated group presence in f-CNTs, the settling

rate was slower. The rate of settling was the slowest for SMZ-CNT_{16.0} and fastest for pure SMZ. In all cases, f-CNTs was effective in lowering the settling rate.

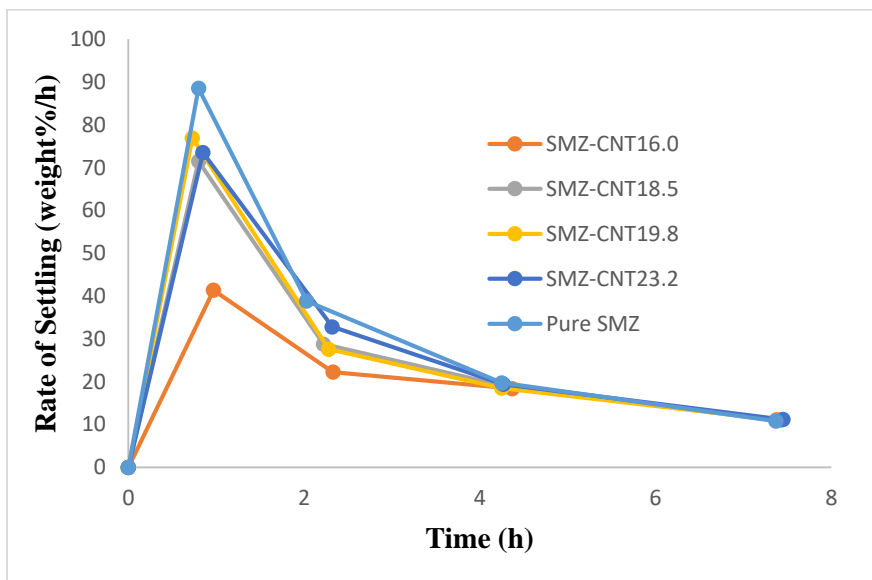


Figure 4.9 Rate of settling as a function of time for Pure SMZ, SMZ-CNT_{23.2}, SMZ-CNT_{19.8}, SMZ-CNT_{18.5} and SMZ-CNT_{16.0}.

4.4 Conclusion

The integration of anti-solvent synthesis of micron-scale particles, their stabilization using f-CNTs was accomplished. It has been found that the f-CNTs were capable of inhibiting particle growth and stabilize the drug particles during anti-solvent precipitation. Compared to pure drug, incorporating f-CNTs provide both steric stabilization and electrostatic stabilization to prevent aggregation. With the increase in carboxylated group, the electrostatic stabilization increases which lead to the particles size decreased and rate of settling slowed.

REFERENCES

1. Mitragotri, S., Immunization without Needles. *Nature Reviews Immunology* **2005**, *5*, 905.
2. Mitragotri, S., *Recent Development in Needle-Free Drug Delivery Frontiers of Engineering*. . 2005; Vol. 38.
3. Jain, K. K., Drug Delivery Systems - an Overview. In *Drug Delivery Systems*, Jain, K. K., Ed. Humana Press: Totowa, NJ, 2008; pp 1-50.
4. Chien, Y. W., Oral Drug Delivery and Delivery System. In *Novel Drug Delivery Systems*, 1992; pp 139-196.
5. Rowland, M., Influence of Route of Administration on Drug Availability. *Journal of Pharmaceutical Sciences* **1972**, *61* (1), 70-74.
6. Brown, M. B.; Martin, G. P.; Jones, S. A.; Akomeah, F. K., Dermal and Transdermal Drug Delivery Systems: Current and Future Prospects. *Drug Delivery* **2006**, *13* (3), 175-187.
7. Brown, M. B.; Traynor, M. J.; Martin, G. P.; Akomeah, F. K., Transdermal Drug Delivery Systems: Skin Perturbation Devices. In *Drug Delivery Systems*, Jain, K. K., Ed. Humana Press: Totowa, NJ, 2008; pp 119-139.
8. Beck-Broichsitter, M.; Gauss, J.; Packhaeuser, C. B.; Lahnstein, K.; Schmehl, T.; Seeger, W.; Kissel, T.; Gessler, T., Pulmonary Drug Delivery with Aerosolizable Nanoparticles in an Ex Vivo Lung Model. *International Journal of Pharmaceutics* **2009**, *367* (1), 169-178.
9. Seppälä O. P.; Herrala, J.; Hedman, J.; Alanko, K.; Liipo, K.; Terho, E.; Pietinalho, A.; Nyholm, J. E.; Nieminen, M. M., The Bronchoprotective Efficacy of Salbutamol Inhaled from a New Metered-Dose Powder Inhaler Compared with a Conventional Pressurized Metered-Dose Inhaler Connected to a Spacer. *Respiratory Medicine* **1998**, *92* (3), 578-583.
10. Pierigè F.; Serafini, S.; Rossi, L.; Magnani, M., Cell-Based Drug Delivery. *Advanced Drug Delivery Reviews* **2008**, *60* (2), 286-295.
11. Wischke, C.; Schwendeman, S. P., Principles of Encapsulating Hydrophobic Drugs in PLA/PLGA Microparticles. *International Journal of Pharmaceutics* **2008**, *364* (2), 298-327.
12. Yasuji, T.; Takeuchi, H.; Kawashima, Y., Particle Design of Poorly Water-Soluble Drug Substances Using Supercritical Fluid Technologies. *Advanced Drug Delivery Reviews* **2008**, *60* (3), 388-398.
13. Hodgson, J., Admet—Turning Chemicals into Drugs. *Nature Biotechnology* **2001**, *19*, 722.

14. Merisko-Liversidge, E.; Liversidge, G. G.; Cooper, E. R., Nanosizing: A Formulation Approach for Poorly-Water-Soluble Compounds. *European Journal of Pharmaceutical Sciences* **2003**, *18* (2), 113-120.
15. Rxlist. <https://www.rxlist.com/cipro-iv-drug.htm> (accessed May 28, 2018).
16. Rxlist. <https://www.rxlist.com/taxotere-drug.htm> (accessed July 19, 2018).
17. Kesisoglou, F.; Panmai, S.; Wu, Y., Nanosizing - Oral Formulation Development and Biopharmaceutical Evaluation. *Advanced Drug Delivery Reviews* **2007**, *59* (7), 631-644.
18. Fuhrman, L., Jr., Ansel's Pharmaceutical Dosage Forms and Drug Delivery Systems, 8th Edition. *American Journal of Pharmaceutical Education* **2006**, *70* (3), 71.
19. Sanganwar, G. P.; Sathigari, S.; Babu, R. J.; Gupta, R. B., Simultaneous Production and Co-Mixing of Microparticles of Nevirapine with Excipients by Supercritical Antisolvent Method for Dissolution Enhancement. *European Journal of Pharmaceutical Sciences* **2010**, *39* (1), 164-174.
20. Merisko-Liversidge, E.; Liversidge, G. G., Nanosizing for Oral and Parenteral Drug Delivery: A Perspective on Formulating Poorly-Water Soluble Compounds Using Wet Media Milling Technology. *Advanced Drug Delivery Reviews* **2011**, *63* (6), 427-440.
21. Muller, R. H.; Moschwitz, J.; Bushrab, F. N., *Manufacturing of Nanoparticles by Milling and Homogenization Techniques*. 2006.
22. Akkar, A.; Müller, R. H., Intravenous Itraconazole Emulsions Produced by Solemuls Technology. *European Journal of Pharmaceutics and Biopharmaceutics* **2003**, *56* (1), 29-36.
23. Kipp, J. E., The Role of Solid Nanoparticle Technology in the Parenteral Delivery of Poorly Water-Soluble Drugs. *International Journal of Pharmaceutics* **2004**, *284* (1-2), 109-122.
24. Ward, G. H.; Schultz, R. K., Process-Induced Crystallinity Changes in Albuterol Sulfate and Its Effect on Powder Physical Stability. *Pharmaceutical Research* **1995**, *12* (5), 773-779.
25. Willart, J. F.; De Gusseme, A.; Hemon, S.; Odou, G.; Danede, F.; Descamps, M., Direct Crystal to Glass Transformation of Trehalose Induced by Ball Milling. *Solid State Communications* **2001**, *119* (8), 501-505.
26. Maulding, H. V.; Tice, T. R.; Cowsar, D. R.; Fong, J. W.; Pearson, J. E.; Nazareno, J. P., Biodegradable Microcapsules: Acceleration of Polymeric Excipient Hydrolytic Rate by Incorporation of a Basic Medicament. *Journal of Controlled Release* **1986**, *3* (1), 103-117.
27. Suzuki, K.; Price, J. C., Microencapsulation and Dissolution Properties of a Neuroleptic in a Biodegradable Polymer, Poly(D,L-Lactide). *Journal of Pharmaceutical Sciences* **1985**, *74* (1), 21-24.

28. Sawalha, H. I. M.; Purwanti, N.; Rinzema, A.; Schroën, C. G. P. H.; Boom, R. M., Poly lactide Microspheres Prepared by Premix Membrane Emulsification - Effects of Solvent Removal Rate. *Journal of Membrane Science* **2008**, *310* (1-2), 484-493.
29. Xia, D.; Quan, P.; Piao, H.; Piao, H.; Sun, S.; Yin, Y.; Cui, F., Preparation of Stable Nitrendipine Nanosuspensions Using the Precipitation–Ultrasonication Method for Enhancement of Dissolution and Oral Bioavailability. *European Journal of Pharmaceutical Sciences* **2010**, *40* (4), 325-334.
30. Zimmermann, A.; Elema, M. R.; Hansen, T.; Müllertz, A.; Hovgaard, L., Determination of Surface-Adsorbed Excipients of Various Types on Drug Particles Prepared by Antisolvent Precipitation Using Hplc with Evaporative Light Scattering Detection. *Journal of Pharmaceutical and Biomedical Analysis* **2007**, *44* (4), 874-880.
31. Chan, H. K.; Kwok, P. C. L., Production Methods for Nanodrug Particles Using the Bottom-up Approach. *Advanced Drug Delivery Reviews* **2011**, *63* (6), 406-416.
32. Desai, C.; Meng, X.; Yang, D.; Wang, X.; Akkunuru, V.; Mitra, S., Effect of Solvents on Stabilization of Micro Drug Particles. *Journal of Crystal Growth* **2011**, *314* (1), 353-358.
33. Meng, X.; Chen, Y.; Chowdhury, S. R.; Yang, D.; Mitra, S., Stabilizing Dispersions of Hydrophobic Drug Molecules Using Cellulose Ethers During Anti-Solvent Synthesis of Micro-Particulates. *Colloids and Surfaces B: Biointerfaces* **2009**, *70* (1), 7-14.
34. Zhu, W.; Romanski, F. S.; Meng, X.; Mitra, S.; Tomassone, M. S., Atomistic Simulation Study of Surfactant and Polymer Interactions on the Surface of a Fenofibrate Crystal. *European Journal of Pharmaceutical Sciences* **2011**, *42* (5), 452-461.
35. Meng, X.; Yang, D.; Keyvan, G.; Michniak-Kohn, B.; Mitra, S., Synthesis and Immobilization of Micro-Scale Drug Particles in Cellulosic Films. *Colloids and Surfaces B: Biointerfaces* **2011**, *86* (1), 181-188.
36. Hiremath, P. S.; Saha, R. N., Controlled Release Hydrophilic Matrix Tablet Formulations of Isoniazid: Design and in Vitro Studies. *AAPS PharmSciTech* **2008**, *9* (4), 1171-1178.
37. Weber, M.; Thies, M. C., Understanding the Res Process. In *Supercritical Fluid Technology in Materials Science and Engineering: Synthesis, Properties, and Applications*, 2002; pp 387-437.
38. Young, T. J.; Johnson, K. P.; Pace, G. W.; Mishra, A. K., Phospholipid-Stabilized Nanoparticles of Cyclosporine a by Rapid Expansion from Supercritical to Aqueous Solution. *AAPS PharmSciTech* **2009**, *5* (1), E11-E11.
39. Marchisio, D. L.; Rivautella, L.; Barresi, A. A., Design and Scale-up of Chemical Reactors for Nanoparticle Precipitation. *AIChE Journal* **2006**, *52* (5), 1877-1887.

40. Matteucci, M. E.; Hotze, M. A.; Johnston, K. P.; Williams, R. O., Drug Nanoparticles by Antisolvent Precipitation: Mixing Energy Versus Surfactant Stabilization. *Langmuir* **2006**, 22 (21), 8951-8959.
41. Martin, T. M.; Bandi, N.; Shulz, R.; Roberts, C. B.; Kompella, U. B., Preparation of Budesonide and Budesonide-Pla Microparticles Using Supercritical Fluid Precipitation Technology. *AAPS PharmSciTech* **2002**, 3 (3), E18-E18.
42. Shekunov, B. Y.; Baldyga, J.; York, P., Particle Formation by Mixing with Supercritical Antisolvent at High Reynolds Numbers. *Chemical Engineering Science* **2001**, 56 (7), 2421-2433.
43. Foldvari, M.; Bagonluri, M., Carbon Nanotubes as Functional Excipients for Nanomedicines: I. Pharmaceutical Properties. *Nanomedicine* **2008**, 4 (3), 173-82.
44. Foldvari, M.; Bagonluri, M., Carbon Nanotubes as Functional Excipients for Nanomedicines: Ii. Drug Delivery and Biocompatibility Issues. *Nanomedicine* **2008**, 4 (3), 183-200.
45. Chen, K.; Mitra, S., Incorporation of Functionalized Carbon Nanotubes into Hydrophobic Drug Crystals for Enhancing Aqueous Dissolution. *Colloids and Surfaces B: Biointerfaces* **2018**.
46. Prato, M.; Kostarelos, K.; Bianco, A., Functionalized Carbon Nanotubes in Drug Design and Discovery. *Accounts of Chemical Research* **2008**, 41 (1), 60-68.
47. Jain, A. K.; Dubey, V.; Mehra, N. K.; Lodhi, N.; Nahar, M.; Mishra, D. K.; Jain, N. K., Carbohydrate-Conjugated Multiwalled Carbon Nanotubes: Development and Characterization. *Nanomedicine* **2009**, 5 (4), 432-42.
48. Valery, N. K.; Haiqing, P.; Wilbur, E. B.; Yunming, Y. Method for Functionalizing Carbon Nanotubes Utilizing Peroxides. US20067125533, 2006.
49. Tour, J. M.; Hudson, J. L.; Dyke, C. R.; Stephenson, J. J. Functionalization of Carbon Nanotubes in Acidic Media. US20050280876, 2005.
50. Valery, N. K.; Enrique, V. B.; Daneesh, M.; Laura, P. P. Carbon Nanotube Reinforced Thermoplastic Polymer Composites Achieved through Benzoyl Peroxide Initiated Interfacial Bonding to Polymer Matrices. WO20066116547, 2006.
51. Ford, W. T.; Qin, S. Polymers Grafted to Carbon Nanotubes. US20087414088, 2008.
52. Tour, J. M.; Bahr, J. L.; Yang, J. Process for Making Polymers Comprising Derivatized Carbon Nanotubes and Compositon Thereof. US20077304103, 2007.
53. Yang, Z.; Zhang, Y.; Yang, Y.; Sun, L.; Han, D.; Li, H.; Wang, C., Pharmacological and Toxicological Target Organelles and Safe Use of Single-Walled Carbon Nanotubes as Drug Carriers in Treating Alzheimer Disease. *Nanomedicine: Nanotechnology, Biology and Medicine* **2010**, 6 (3), 427-441.

54. Zhang, Z. Y.; Xu, X. C., Nondestructive Covalent Functionalization of Carbon Nanotubes by Selective Oxidation of the Original Defects with K₂FeO₄. *Applied Surface Science* **2015**, *346*, 520-527.
55. Mattson, M. P.; Haddon, R. C.; Rao, A. M., Molecular Functionalization of Carbon Nanotubes and Use as Substrates for Neuronal Growth. *Journal of Molecular Neuroscience* **2000**, *14* (3), 175-182.
56. Dai L.; M., L. K. Asymmetric End-Functionalization of Carbon Nanotubes. WO2007061431, 2007.
57. Eguíluz, M.; Gutiérrez, A.; Gutierrez, F.; González-Domínguez, J. M.; Ansón-Casaos, A.; Hernández-Ferrer, J.; Ferreyra, N. F.; Martínez, M. T.; Rivas, G., Covalent Functionalization of Single-Walled Carbon Nanotubes with Polytyrosine: Characterization and Analytical Applications for the Sensitive Quantification of Polyphenols. *Analytica Chimica Acta* **2016**, *909*, 51-59.
58. Zhu, Y.; Chen, K.; Yi, C.; Mitra, S.; Barat, R., Dry Reforming of Methane over Palladium–Platinum on Carbon Nanotube Catalyst. *Chemical Engineering Communications* **2018**, *205* (7), 888-896.
59. Jia, N.; Lian, Q.; Shen, H.; Wang, C.; Li, X.; Yang, Z., Intracellular Delivery of Quantum Dots Tagged Antisense Oligodeoxynucleotides by Functionalized Multiwalled Carbon Nanotubes. *Nano Lett* **2007**, *7* (10), 2976-80.
60. Lucente-Schultz, R. M.; Moore, V. C.; Leonard, A. D.; Price, B. K.; Kosynkin, D. V.; Lu, M.; Partha, R.; Conyers, J. L.; Tour, J. M., Antioxidant Single-Walled Carbon Nanotubes. *J Am Chem Soc* **2009**, *131* (11), 3934-41.
61. Zhu, J.; Yudasaka, M.; Zhang, M.; Iijima, S., Dispersing Carbon Nanotubes in Water: A Noncovalent and Nonorganic Way. *The Journal of Physical Chemistry B* **2004**, *108* (31), 11317-11320.
62. Georgakilas, V.; Tzitzios, V.; Gournis, D.; Petridis, D., Attachment of Magnetic Nanoparticles on Carbon Nanotubes and Their Soluble Derivatives. *Chemistry of Materials* **2005**, *17* (7), 1613-1617.
63. Amadou, N.; Pierre, B.; Alain, P.; Marc, D.; Jérôme, B.; Christelle, V.; Katia, G.; Bernard, L., *Noncovalent Functionalization of Single-Wall Carbon Nanotubes for the Elaboration of Gas Sensor Dedicated to Btx Type Gases: The Case of Toluene*. 2016.
64. Gordon, R. G.; Farmer, D. B. Noncovalent Functionalization of Carbon Nanotubes. WO/2008/085183, 2008.
65. Chen, Y.; Wei, W.; Zhu, Y.; Luo, J.; Liu, X., Noncovalent Functionalization of Carbon Nanotubes Via Co-Deposition of Tannic Acid and Polyethyleneimine for Reinforcement and Conductivity Improvement in Epoxy Composite. *Composites Science and Technology* **2019**, *170*, 25-33.

66. Stoddart, J. F.; Star, A.; Liu, Y.; Ridvan, L. Noncovalent Functionalization of Nanotubes. US20077220818, 2007.
67. Chen, J.; Liu, H. Polymer and Method for Using the Polymer for Solubilizing Nanotubes. US20077244407, 2007.
68. Wise, K. E.; Park, C.; Kang, J. H.; Siochi, E. J.; Harrison, J. S. Nanocomposites Issues De Dispersions Stables De Nanotubes De Carbone Contenus Dans Des Matrices Polymères Faisant Appel À Des Interactions De Dispersion. WO/2008/073153, 2008.
69. Kim, O. K.; Je, J.; Baldwin, J. W.; Kooi, S.; Pehrsson, P. E.; Buckley, L. J., Solubilization of Single-Wall Carbon Nanotubes by Supramolecular Encapsulation of Helical Amylose. *J Am Chem Soc* **2003**, *125* (15), 4426-7.
70. Guo, Z.; Sadler, P. J.; Tsang, S. C., Immobilization and Visualization of DNA and Proteins on Carbon Nanotubes. *Advanced Materials* **1999**, *10* (9), 701-703.
71. Zheng, M.; Jagota, A.; Semke, E. D.; Diner, B. A.; McLean, R. S.; Lustig, S. R.; Richardson, R. E.; Tassi, N. G., DNA-Assisted Dispersion and Separation of Carbon Nanotubes. *Nat Mater* **2003**, *2* (5), 338-342.
72. Vigolo, B.; Penicaud, A.; Coulon, C.; Sauder, C.; Pailler, R.; Journet, C.; Bernier, P.; Poulin, P., Macroscopic Fibers and Ribbons of Oriented Carbon Nanotubes. *Science* **2000**, *290* (5495), 1331-4.
73. Italia, J. L.; Yahya, M. M.; Singh, D.; Ravi Kumar, M. N. V., Biodegradable Nanoparticles Improve Oral Bioavailability of Amphotericin B and Show Reduced Nephrotoxicity Compared to Intravenous Fungizone®. *Pharmaceutical Research* **2009**, *26* (6), 1324-1331.
74. Prow, T. W.; Grice, J. E.; Lin, L. L.; Faye, R.; Butler, M.; Becker, W.; Wurm, E. M. T.; Yoong, C.; Robertson, T. A.; Soyer, H. P.; Roberts, M. S., Nanoparticles and Microparticles for Skin Drug Delivery. *Advanced Drug Delivery Reviews* **2011**, *63* (6), 470-491.
75. Nair, L. S.; Laurencin, C. T., Biodegradable Polymers as Biomaterials. *Progress in Polymer Science* **2007**, *32* (8), 762-798.
76. Azqhandi, M. H. A.; Farahani, B. V.; Dehghani, N., Encapsulation of Methotrexate and Cyclophosphamide in Interpolymer Complexes Formed between Poly Acrylic Acid and Poly Ethylene Glycol on Multi-Walled Carbon Nanotubes as Drug Delivery Systems. *Materials Science and Engineering: C* **2017**, *79*, 841-847.
77. Yang, S.; Guo, W.; Lin, Y.; Deng, X.; Wang, H.; Sun, H.; Liu, Y.; Wang, X.; Wang, W.; Chen, M.; Huang, Y.; Sun, Y., Biodistribution of Pristine Single-Walled Carbon Nanotubes *In Vivo*. *The Journal of Physical Chemistry C* **2007**, *111* (48), 17761-17764.
78. Martincic, M.; Tobias, G., Filled Carbon Nanotubes in Biomedical Imaging and Drug Delivery. *Expert Opinion on Drug Delivery* **2015**, *12* (4), 563-581.

79. Tao Yang; Wu, Z.; Wang, P.; Mu, T.; Qin, H.; Zhu, Z.; Wang, J.; Sui, L., A Large-Inner-Diameter Multi-Walled Carbon Nanotube-Based Dual-Drug Delivery System with Ph-Sensitive Release Properties. *Journal of Materials Science: Materials in Medicine* **2017**, *28* (110).
80. Cao, X.; Tao, L.; Wen, S.; Hou, W.; Shi, X., Hyaluronic Acid-Modified Multiwalled Carbon Nanotubes for Targeted Delivery of Doxorubicin into Cancer Cells. *Carbohydrate Research* **2015**, *405*, 70-77.
81. Kaur, S.; Mehra, N. K.; Jain, K.; Jain, N. K., Development and Evaluation of Targeting Ligand-Anchored Cnts as Prospective Targeted Drug Delivery System. *Artificial Cells, Nanomedicine, and Biotechnology* **2017**, *45* (2), 242-250.
82. Reddy, S. T.; Rehor, A.; Schmoekel, H. G.; Hubbell, J. A.; Swartz, M. A., *In Vivo* Targeting of Dendritic Cells in Lymph Nodes with Poly(Propylene Sulfide) Nanoparticles. *Journal of Controlled Release* **2006**, *112* (1), 26-34.
83. Yang, F.; Fu, D. L.; Long, J.; Ni, Q. X., Magnetic Lymphatic Targeting Drug Delivery System Using Carbon Nanotubes. *Medical Hypotheses* **2008**, *70* (4), 765-767.
84. Yang, F.; Hu, J.; Yang, D.; Long, J.; Luo, G.; Jin, C.; Yu, X.; Xu, J.; Wang, C.; Ni, Q.; Fu, D., Pilot Study of Targeting Magnetic Carbon Nanotubes to Lymph Nodes. *Nanomedicine* **2009**, *4* (3), 317-330.
85. Liu, Y.; Ng, K. Y.; Lillehei, K. O., Cell-Mediated Immunotherapy: A New Approach to the Treatment of Malignant Glioma. *Cancer Control* **2003**, *10* (2), 138-147.
86. Zheng, L.; Wu, S.; Tan, L.; Tan, H.; Yu, B., Chitosan-Functionalised Single-Walled Carbon Nanotube-Mediated Drug Delivery of Snx-2112 in Cancer Cells. *J Biomater Appl* **2016**, *31* (3), 379-86.
87. Liu, Z.; Fan, A. C.; Rakhra, K.; Sherlock, S.; Goodwin, A.; Chen, X.; Yang, Q.; Felsher, D. W.; Dai, H., Supramolecular Stacking of Doxorubicin on Carbon Nanotubes for *in Vivo* Cancer Therapy. *Angewandte Chemie International Edition* **2009**, *48* (41), 7668-7672.
88. Li, J.; Pant, A.; Chin, C. F.; Ang, W. H.; Ménard-Moyon, C.; Nayak, T. R.; Gibson, D.; Ramaprabhu, S.; Panczyk, T.; Bianco, A.; Pastorin, G., *In Vivo* Biodistribution of Platinum-Based Drugs Encapsulated into Multi-Walled Carbon Nanotubes. *Nanomedicine: Nanotechnology, Biology and Medicine* **2014**, *10* (7), 1465-1475.
89. Han, H.; Mann, A.; Ekstein, D.; Eyal, S., Breaking Bad: The Structure and Function of the Blood-Brain Barrier in Epilepsy. *Aaps j* **2017**, *19* (4), 973-988.
90. Costa, P. M.; Bourgognon, M.; Wang, J. T. W.; Al-Jamal, K. T., Functionalised Carbon Nanotubes: From Intracellular Uptake and Cell-Related Toxicity to Systemic Brain Delivery. *Journal of Controlled Release* **2016**, *241*, 200-219.

91. Tan, J. M.; Foo, J. B.; Fakurazi, S.; Hussein, M. Z., Release Behaviour and Toxicity Evaluation of Levodopa from Carboxylated Single-Walled Carbon Nanotubes. *Beilstein journal of nanotechnology* **2015**, *6*, 243-253.
92. Al-Jamal, K. T.; Gherardini, L.; Bardi, G.; Nunes, A.; Guo, C.; Bussy, C.; Herrero, M. A.; Bianco, A.; Prato, M.; Kostarelos, K.; Pizzorusso, T., Functional Motor Recovery from Brain Ischemic Insult by Carbon Nanotube-Mediated Sirna Silencing. *Proceedings of the National Academy of Sciences* **2011**, *108* (27), 10952.
93. Zhao, D.; Alizadeh, D.; Zhang, L.; Liu, W.; Farrukh, O.; Manuel, E.; Diamond, D. J.; Badie, B., Carbon Nanotubes Enhance CpG Uptake and Potentiate Antiglioma Immunity. *Clin Cancer Res* **2011**, *17* (4), 771-82.
94. Klumpp, C.; Kostarelos, K.; Prato, M.; Bianco, A., Functionalized Carbon Nanotubes as Emerging Nanovectors for the Delivery of Therapeutics. *Biochimica et Biophysica Acta (BBA) - Biomembranes* **2006**, *1758* (3), 404-412.
95. Harrison, B. S.; Atala, A., Carbon Nanotube Applications for Tissue Engineering. *Biomaterials* **2007**, *28* (2), 344-353.
96. Fabbro, C.; Ali-Boucetta, H.; Ros, T. D.; Kostarelos, K.; Bianco, A.; Prato, M., Targeting Carbon Nanotubes against Cancer. *Chemical Communications* **2012**, *48* (33), 3911-3926.
97. Sitharaman, B.; Shi, X.; Walboomers, X. F.; Liao, H.; Cuijpers, V.; Wilson, L. J.; Mikos, A. G.; Jansen, J. A., *In Vivo* Biocompatibility of Ultra-Short Single-Walled Carbon Nanotube/Biodegradable Polymer Nanocomposites for Bone Tissue Engineering. *Bone* **2008**, *43* (2), 362-370.
98. Shi, X.; Sitharaman, B.; Pham, Q. P.; Liang, F.; Wu, K.; Edward Billups, W.; Wilson, L. J.; Mikos, A. G., Fabrication of Porous Ultra-Short Single-Walled Carbon Nanotube Nanocomposite Scaffolds for Bone Tissue Engineering. *Biomaterials* **2007**, *28* (28), 4078-4090.
99. Martinelli, V.; Cellot, G.; Toma, F. M.; Long, C. S.; Caldwell, J. H.; Zentilin, L.; Giacca, M.; Turco, A.; Prato, M.; Ballerini, L.; Mestroni, L., Carbon Nanotubes Promote Growth and Spontaneous Electrical Activity in Cultured Cardiac Myocytes. *Nano Letters* **2012**, *12* (4), 1831-1838.
100. Nayak, T. R.; Jian, L.; Phua, L. C.; Ho, H. K.; Ren, Y.; Pastorin, G., Thin Films of Functionalized Multiwalled Carbon Nanotubes as Suitable Scaffold Materials for Stem Cells Proliferation and Bone Formation. *ACS Nano* **2010**, *4* (12), 7717-7725.
101. Li, X.; Liu, H.; Niu, X.; Yu, B.; Fan, Y.; Feng, Q.; Cui, F. Z.; Watari, F., The Use of Carbon Nanotubes to Induce Osteogenic Differentiation of Human Adipose-Derived Mscs in Vitro and Ectopic Bone Formation in Vivo. *Biomaterials* **2012**, *33* (19), 4818-4827.
102. Moon, H. K.; Lee, S. H.; Choi, H. C., *In Vivo* near-Infrared Mediated Tumor Destruction by Photothermal Effect of Carbon Nanotubes. *ACS Nano* **2009**, *3* (11), 3707-3713.

103. Zhou, F.; Wu, S.; Wu, B.; Chen, W. R.; Xing, D., Mitochondria-Targeting Single-Walled Carbon Nanotubes for Cancer Photothermal Therapy. *Small* **2011**, *7* (19), 2727-2735.
104. Zhou, F.; Wu, S.; Yuan, Y.; Chen, W. R.; Xing, D., Mitochondria-Targeting Photoacoustic Therapy Using Single-Walled Carbon Nanotubes. *Small* **2012**, *8* (10), 1543-1550.
105. Zhou, F.; Xing, D.; Ou, Z.; Wu, B.; Resasco, D. E.; Chen, W. R., Cancer Photothermal Therapy in the near-Infrared Region by Using Single-Walled Carbon Nanotubes. *Journal of Biomedical Optics* **2009**, *14* (2), 021009-021009-7.
106. Keefer, E. W.; Botterman, B. R.; Romero, M. I.; Rossi, A. F.; Gross, G. W., Carbon Nanotube Coating Improves Neuronal Recordings. *Nature Nanotechnology* **2008**, *3* (7), 434-439.
107. Lee, H. J.; Park, J.; Yoon, O. J.; Kim, H. W.; Lee, D. Y.; Kim, D. H.; Lee, W. B.; Lee, N. E.; Bonventre, J. V.; Kim, S. S., Amine-Modified Single-Walled Carbon Nanotubes Protect Neurons from Injury in a Rat Stroke Model. *Nature Nanotechnology* **2011**, *6* (2), 121-125.
108. Liu, Z.; Sun, X.; Nakayama-Ratchford, N.; Dai, H., Supramolecular Chemistry on Water-Soluble Carbon Nanotubes for Drug Loading and Delivery. *ACS Nano* **2007**, *1* (1), 50-56.
109. Feazell, R. P.; Nakayama-Ratchford, N.; Dai, H.; Lippard, S. J., Soluble Single-Walled Carbon Nanotubes as Longboat Delivery Systems for Platinum(IV) Anticancer Drug Design. *Journal of the American Chemical Society* **2007**, *129* (27), 8438-8439.
110. Liu, Z.; Chen, K.; Davis, C.; Sherlock, S.; Cao, Q.; Chen, X.; Dai, H., Drug Delivery with Carbon Nanotubes for in Vivo Cancer Treatment. *Cancer Research* **2008**, *68* (16), 6652-6660.
111. Yang, D.; Yang, F.; Hu, J.; Long, J.; Wang, C.; Fu, D.; Ni, Q., Hydrophilic Multi-Walled Carbon Nanotubes Decorated with Magnetite Nanoparticles as Lymphatic Targeted Drug Delivery Vehicles. *Chemical Communications* **2009**, (29), 4447-4449.
112. Pastorin, G.; Wu, W.; Wieckowski, S.; Briand, J. P.; Kostarelos, K.; Prato, M.; Bianco, A., Double Functionalisation of Carbon Nanotubes for Multimodal Drug Delivery. *Chemical Communications* **2006**, (11), 1182-1184.
113. Li, J.; Yap, S. Q.; Chin, C. F.; Tian, Q.; Yoong, S. L.; Pastorin, G.; Ang, W. H., Platinum(IV) Prodrugs Entrapped within Multiwalled Carbon Nanotubes: Selective Release by Chemical Reduction and Hydrophobicity Reversal. *Chemical Science* **2012**, *3* (6), 2083-2087.
114. Ali-Boucetta, H.; Al-Jamal, K. T.; McCarthy, D.; Prato, M.; Bianco, A.; Kostarelos, K., Multiwalled Carbon Nanotube-Doxorubicin Supramolecular Complexes for Cancer Therapeutics. *Chemical Communications* **2008**, *8* (4), 459-461.
115. Benincasa, M.; Pacor, S.; Wu, W.; Prato, M.; Bianco, A.; Gennaro, R., Antifungal Activity of Amphotericin B Conjugated to Carbon Nanotubes. *ACS Nano* **2011**, *5* (1), 199-208.

116. Wu, W.; Wieckowski, S.; Pastorin, G.; Benincasa, M.; Klumpp, C.; Briand, J. P.; Gennaro, R.; Prato, M.; Bianco, A., Targeted Delivery of Amphotericin B to Cells by Using Functionalized Carbon Nanotubes. *Angewandte Chemie International Edition* **2005**, *44* (39), 6358-6362.
117. Shah, M.; Agrawal, Y., Carbon Nanotube: A Novel Carrier for Sustained Release Formulation. *Fullerenes, Nanotubes and Carbon Nanostructures* **2012**, *20* (8), 696-708.
118. Pantarotto, D.; Partidos, C. D.; Hoebeke, J.; Brown, F.; Kramer, E.; Briand, J. P.; Muller, S.; Prato, M.; Bianco, A., Immunization with Peptide-Functionalized Carbon Nanotubes Enhances Virus-Specific Neutralizing Antibody Responses. *Chemistry & Biology* **2003**, *10* (10), 961-966.
119. Pantarotto, D.; Partidos, C. D.; Graff, R.; Hoebeke, J.; Briand, J.-P.; Prato, M.; Bianco, A., Synthesis, Structural Characterization, and Immunological Properties of Carbon Nanotubes Functionalized with Peptides. *Journal of the American Chemical Society* **2003**, *125* (20), 6160-6164.
120. McDevitt, M. R.; Chattopadhyay, D.; Kappel, B. J.; Jaggi, J. S.; Schiffman, S. R.; Antczak, C.; Njardarson, J. T.; Brentjens, R.; Scheinberg, D. A., Tumor Targeting with Antibody-Functionalized, Radiolabeled Carbon Nanotubes. *Journal of Nuclear Medicine* **2007**, *48* (7), 1180-1189.
121. Podesta, J. E.; Al-Jamal, K. T.; Herrero, M. A.; Tian, B.; Ali-Boucetta, H.; Hegde, V.; Bianco, A.; Prato, M.; Kostarelos, K., Antitumor Activity and Prolonged Survival by Carbon-Nanotube-Mediated Therapeutic Sirna Silencing in a Human Lung Xenograft Model. *Small* **2009**, *5* (10), 1176-1185.
122. Lacerda, L.; Russier, J.; Pastorin, G.; Herrero, M. A.; Venturelli, E.; Dumortier, H.; Al-Jamal, K. T.; Prato, M.; Kostarelos, K.; Bianco, A., Translocation Mechanisms of Chemically Functionalised Carbon Nanotubes across Plasma Membranes. *Biomaterials* **2012**, *33* (11), 3334-3343.
123. Charbgoon, F.; Behmanesh, M.; Nikkhah, M., Enhanced Reduction of Single-Wall Carbon Nanotube Cytotoxicity in Vitro: Applying a Novel Method of Arginine Functionalization. *Biotechnology and Applied Biochemistry* **2015**, *62* (5), 598-605.
124. Mallakpour, S.; Zadehnazari, A., Effect of Amino Acid-Functionalization on the Interfacial Adhesion and Behavior of Multi-Walled Carbon Nanotubes/Poly(Amide-Imide) Nanocomposites Containing Thiazole Side Unit. *Journal of Polymer Research* **2013**, *20* (7), 1-12.
125. Tan, J. M.; Arulselvan, P.; Fakurazi, S.; Ithnin, H.; Hussein, M. Z., A Review on Characterizations and Biocompatibility of Functionalized Carbon Nanotubes in Drug Delivery Design. *Journal of Nanomaterials* **2014**, *2014*, 20.
126. Milosavljevic, V.; Krejcova, L.; Guran, R.; Buchtelova, H.; Wawrzak, D.; Richtera, L.; Heger, Z.; Kopel, P.; Adam, V., Exceptional Release Kinetics and Cytotoxic Selectivity of

Oxidised Mwcnts Double-Functionalised with Doxorubicin and Prostate-Homing Peptide. *Colloids and Surfaces B: Biointerfaces* **2017**, 156, 123-132.

127. Kumar, M.; Sharma, G.; Misra, C.; Kumar, R.; Singh, B.; Katare, O. P.; Raza, K., N-Desmethyl Tamoxifen and Quercetin-Loaded Multiwalled Cnts: A Synergistic Approach to Overcome Mdr in Cancer Cells. *Materials Science and Engineering: C* **2018**, 89, 274-282.
128. Lohan, S.; Raza, K.; Mehta, S. K.; Bhatti, G. K.; Saini, S.; Singh, B., Anti-Alzheimer's Potential of Berberine Using Surface Decorated Multi-Walled Carbon Nanotubes: A Preclinical Evidence. *International Journal of Pharmaceutics* **2017**, 530 (1), 263-278.
129. Li, J.; Yap, S. Q.; Yoong, S. L.; Nayak, T. R.; Chandra, G. W.; Ang, W. H.; Panczyk, T.; Ramaprabhu, S.; Vashist, S. K.; Sheu, F.-S.; Tan, A.; Pastorin, G., Carbon Nanotube Bottles for Incorporation, Release and Enhanced Cytotoxic Effect of Cisplatin. *Carbon* **2012**, 50 (4), 1625-1634.
130. Park, T. J.; Kim, Y. S.; Hwang, T.; Govindaiah, P.; Choi, S. W.; Kim, E.; Won, K.; Lee, S. H.; Kim, J. H., Preparation and Characterization of Heparinized Multi-Walled Carbon Nanotubes. *Process Biochemistry* **2012**, 47 (1), 113-118.
131. Li, R.; Wu, R.; Zhao, L.; Hu, Z.; Guo, S.; Pan, X.; Zou, H., Folate and Iron Difunctionalized Multiwall Carbon Nanotubes as Dual-Targeted Drug Nanocarrier to Cancer Cells. *Carbon* **2011**, 49 (5), 1797-1805.
132. Spizzirri, U. G.; Hampel, S.; Cirillo, G.; Nicoletta, F. P.; Hassan, A.; Vittorio, O.; Picci, N.; Iemma, F., Spherical Gelatin/Cnts Hybrid Microgels as Electro-Responsive Drug Delivery Systems. *International Journal of Pharmaceutics* **2013**, 448 (1), 115-122.
133. Liu, X.; Gurel, V.; Morris, D.; Murray, D. W.; Zhitkovich, A.; Kane, A. B.; Hurt, R. H., Bioavailability of Nickel in Single-Wall Carbon Nanotubes. *Advanced Materials* **2007**, 19 (19), 2790-2796.
134. Poland, C. A.; Duffin, R.; Kinloch, I.; Maynard, A.; Wallace, W. A. H.; Seaton, A.; Stone, V.; Brown, S.; MacNee, W.; Donaldson, K., Carbon Nanotubes Introduced into the Abdominal Cavity of Mice Show Asbestos-Like Pathogenicity in a Pilot Study. *Nature Nanotechnology* **2008**, 3, 423.
135. Sato, Y.; Yokoyama, A.; Shibata, K. I.; Akimoto, Y.; Ogino, S. I.; Nodasaka, Y.; Kohgo, T.; Tamura, K.; Akasaka, T.; Uo, M.; Motomiya, K.; Jeyadevan, B.; Ishiguro, M.; Hatakeyama, R.; Watari, F.; Tohji, K., Influence of Length on Cytotoxicity of Multi-Walled Carbon Nanotubes against Human Acute Monocytic Leukemia Cell Line Thp-1 in Vitro and Subcutaneous Tissue of Rats in Vivo. *Molecular BioSystems* **2005**, 1 (2), 176-182.
136. Jia, G.; Wang, H.; Yan, L.; Wang, X.; Pei, R.; Yan, T.; Zhao, Y.; Guo, X., Cytotoxicity of Carbon Nanomaterials: Single-Wall Nanotube, Multi-Wall Nanotube, and Fullerene. *Environmental Science & Technology* **2005**, 39 (5), 1378-1383.

137. Pacurari, M.; Yin, X. J.; Zhao, J.; Ding, M.; Leonard, S. S.; Schwegler-Berry, D.; Ducatman, B. S.; Sbarra, D.; Hoover, M. D.; Castranova, V.; Vallyathan, V., Raw Single-Wall Carbon Nanotubes Induce Oxidative Stress and Activate Mapks, Ap-1, Nf-Kappab, and Akt in Normal and Malignant Human Mesothelial Cells. *Environ Health Perspect* **2008**, *116* (9), 1211-7.
138. Wang, L.; Luanpitpong, S.; Castranova, V.; Tse, W.; Lu, Y.; Pongrakhananon, V.; Rojanasakul, Y., Carbon Nanotubes Induce Malignant Transformation and Tumorigenesis of Human Lung Epithelial Cells. *Nano Letters* **2011**, *11* (7), 2796-2803.
139. Pulskamp, K.; Diabat é S.; Krug, H. F., Carbon Nanotubes Show No Sign of Acute Toxicity but Induce Intracellular Reactive Oxygen Species in Dependence on Contaminants. *Toxicology Letters* **2007**, *168* (1), 58-74.
140. Kagan, V. E.; Konduru, N. V.; Feng, W.; Allen, B. L.; Conroy, J.; Volkov, Y.; Vlasova, I. I.; Belikova, N. A.; Yanamala, N.; Kapralov, A.; Tyurina, Y. Y.; Shi, J.; Kisin, E. R.; Murray, A. R.; Franks, J.; Stolz, D.; Gou, P.; Klein-Seetharaman, J.; Fadeel, B.; Star, A.; Shvedova, A. A., Carbon Nanotubes Degraded by Neutrophil Myeloperoxidase Induce Less Pulmonary Inflammation. *Nature Nanotechnology* **2010**, *5*, 354.
141. Takagi, D.; Homma, Y.; Hibino, H.; Suzuki, S.; Kobayashi, Y., Single-Walled Carbon Nanotube Growth from Highly Activated Metal Nanoparticles. *Nano Letters* **2006**, *6* (12), 2642-2645.
142. Wu, Z.; Wang, Z.; Yu, F.; Thakkar, M.; Mitra, S., Variation in Chemical, Colloidal and Electrochemical Properties of Carbon Nanotubes with the Degree of Carboxylation. *Journal of Nanoparticle Research* **2017**, *19* (1), 16.
143. Allegri, M.; Perivoliotis, D. K.; Bianchi, M. G.; Chiu, M.; Pagliaro, A.; Koklioti, M. A.; Trompeta, A.-F. A.; Bergamaschi, E.; Bussolati, O.; Charitidis, C. A., Toxicity Determinants of Multi-Walled Carbon Nanotubes: The Relationship between Functionalization and Agglomeration. *Toxicology Reports* **2016**, *3*, 230-243.
144. Thorat, A. A.; Dalvi, S. V., Liquid Antisolvent Precipitation and Stabilization of Nanoparticles of Poorly Water Soluble Drugs in Aqueous Suspensions: Recent Developments and Future Perspective. *Chemical Engineering Journal* **2012**, *181-182*, 1-34.
145. Gao, Y.; Li, L. B.; Zhai, G., Preparation and Characterization of Pluronic/Tpgs Mixed Micelles for Solubilization of Camptothecin. *Colloids and Surfaces B: Biointerfaces* **2008**, *64* (2), 194-199.
146. Singh, D.; Bedi, N.; Tiwary, A. K., Enhancing Solubility of Poorly Aqueous Soluble Drugs: Critical Appraisal of Techniques. *Journal of Pharmaceutical Investigation* **2017**.
147. Wong, S. M.; Kellaway, I. W.; Murdan, S., Enhancement of the Dissolution Rate and Oral Absorption of a Poorly Water Soluble Drug by Formation of Surfactant-Containing Microparticles. *International Journal of Pharmaceutics* **2006**, *317* (1), 61-68.

148. Kakran, M.; Sahoo, N. G.; Tan, I. L.; Li, L., Preparation of Nanoparticles of Poorly Water-Soluble Antioxidant Curcumin by Antisolvent Precipitation Methods. *Journal of Nanoparticle Research* **2012**, *14* (3), 757.
149. Lonare, A. A.; Patel, S. R., Antisolvent Crystallization of Poorly Water Soluble Drugs. *International Journal of Chemical Engineering and Applications* **2013**, *4* (5), 337-341.
150. Wang, Z.; Wu, Z.; Benedetto, G. D.; Zunino III, J. L.; Mitra, S., Microwave Synthesis of Highly Oxidized and Defective Carbon Nanotubes for Enhancing the Performance of Supercapacitors. *Carbon* **2015**, *91*, 103-113.
151. Wu, Z.; Hamilton, R. F.; Wang, Z.; Holian, A.; Mitra, S., Oxidation Debris in Microwave Functionalized Carbon Nanotubes: Chemical and Biological Effects. *Carbon* **2014**, *68* (Supplement C), 678-686.
152. Bolton, B. A.; Prasad, P. N., Laser Raman Investigation of Pharmaceutical Solids: Griseofulvin and Its Solvates. *Journal of Pharmaceutical Sciences* **1981**, *70* (7), 789-793.
153. Macchione, M.; Biglione, C.; Strumia, M., Design, Synthesis and Architectures of Hybrid Nanomaterials for Therapy and Diagnosis Applications. *Polymers* **2018**, *10* (5), 527.
154. Bhise, K.; Sau, S.; Alsaab, H.; Kashaw, S. K.; Tekade, R. K.; Iyer, A. K., Nanomedicine for Cancer Diagnosis and Therapy: Advancement, Success and Structure–Activity Relationship. *Therapeutic Delivery* **2017**, *8* (11), 1003-1018.
155. Vashist, A.; Kaushik, A.; Vashist, A.; Sagar, V.; Ghosal, A.; Gupta, Y. K.; Ahmad, S.; Nair, M., Advances in Carbon Nanotubes–Hydrogel Hybrids in Nanomedicine for Therapeutics. *Advanced Healthcare Materials* **2018**, *7* (9), 1701213.
156. Wulan, P. P.; Wulandari, H.; Ulwan, S. H.; Purwanto, W. W.; Mulia, K., Modification of Carbon Nanotube's Dispersion Using Cetyltrimethyl Ammonium Bromide (Ctab) as Cancer Drug Delivery. *AIP Conference Proceedings* **2018**, *1933* (1), 030008.
157. Rezaei, S. J. T.; Hesami, A.; Khorramabadi, H.; Amani, V.; Malekzadeh, A. M.; Ramazani, A.; Niknejad, H., Pt(II) Complexes Immobilized on Polymer-Modified Magnetic Carbon Nanotubes as a New Platinum Drug Delivery System. *Applied Organometallic Chemistry* **2018**, *32* (7), e4401.
158. Tan, J.; Saifullah, B.; Kura, A.; Fakurazi, S.; Hussein, M., Incorporation of Levodopa into Biopolymer Coatings Based on Carboxylated Carbon Nanotubes for Ph-Dependent Sustained Release Drug Delivery. *Nanomaterials* **2018**, *8* (6), 389.
159. Chae, S.; Kim, D.; Lee, K. J.; Lee, D.; Kim, Y. O.; Jung, Y. C.; Rhee, S. D.; Kim, K. R.; Lee, J. O.; Ahn, S.; Koh, B., Encapsulation and Enhanced Delivery of Topoisomerase I Inhibitors in Functionalized Carbon Nanotubes. *ACS Omega* **2018**, *3* (6), 5938-5945.
160. Ryu, T. K.; Kim, S. E.; Kim, J. H.; Moon, S. K.; Choi, S. W., Biodegradable Uniform Microspheres Based on Solid-in-Oil-in-Water Emulsion for Drug Delivery: A Comparison

- of Homogenization and Fluidic Device. *Journal of Bioactive and Compatible Polymers* **2014**, 29 (5), 445-457.
161. Wang, Y.; Zhu, L. H.; Chen, A. Z.; Xu, Q.; Hong, Y. J.; Wang, S. B., One-Step Method to Prepare Plla Porous Microspheres in a High-Voltage Electrostatic Anti-Solvent Process. *Materials* **2016**, 9 (5), 368.
 162. Imchalee, R.; Charoenchaitrakool, M., Gas Anti-Solvent Processing of a New Sulfamethoxazole–L-Malic Acid Cocrystal. *Journal of Industrial and Engineering Chemistry* **2015**, 25, 12-15.
 163. Singh, C.; Tiwari, V.; Mishra, C. P.; Shankar, R.; Sharma, D.; Jaiswal, S., Fabrication of Cefpodoxime Proxetil Nanoparticles by Solvent Anti-Solvent Precipitation Method for Enhanced Dissolution. *International Journal of Research in Pharmaceutical and Nano Sciences* **2015**, 4 (4), 18.
 164. Park, M. W.; Yeo, S. D., Antisolvent Crystallization of Carbamazepine from Organic Solutions. *Chemical Engineering Research and Design* **2012**, 90 (12), 2202-2208.
 165. Pachuau, L., *Application of Nanocellulose for Controlled Drug Delivery*. 2017.
 166. Bharti, C.; Nagaich, U.; Pal, A.; Gulati, N., Mesoporous Silica Nanoparticles in Target Drug Delivery System: A Review. *International Journal of Pharmaceutical Investigation* **2015**, 5 (3), 124-133.
 167. Du, A. W.; Stenzel, M. H., Drug Carriers for the Delivery of Therapeutic Peptides. *Biomacromolecules* **2014**, 15 (4), 1097-1114.
 168. Sim, T.; Lim, C.; Lee, J. W.; Kim, D. W.; Kim, Y.; Kim, M.; Choi, S.; Choi, H. G.; Lee, E. S.; Kim, K. S.; Kang, W.; Oh, K. T., Characterization and Pharmacokinetic Study of Itraconazole Solid Dispersions Prepared by Solvent-Controlled Precipitation and Spray-Dry Methods. *Journal of Pharmacy and Pharmacology* **2017**, 69 (12), 1707-1715.
 169. Kalepu, S.; Nekkanti, V., Insoluble Drug Delivery Strategies: Review of Recent Advances and Business Prospects. *Acta Pharmaceutica Sinica B* **2015**, 5 (5), 442-453.
 170. Al-Hamidi, H.; Edwards, A. A.; Mohammad, M. A.; Nokhodchi, A., To Enhance Dissolution Rate of Poorly Water-Soluble Drugs: Glucosamine Hydrochloride as a Potential Carrier in Solid Dispersion Formulations. *Colloids and Surfaces B: Biointerfaces* **2010**, 76 (1), 170-178.
 171. Loftsson, T.; Brewster, M. E., Pharmaceutical Applications of Cyclodextrins. 1. Drug Solubilization and Stabilization. *Journal of Pharmaceutical Sciences* **1996**, 85 (10), 1017-1025.
 172. Cavallaro, G.; Grillo, I.; Gradzielski, M.; Lazzara, G., Structure of Hybrid Materials Based on Halloysite Nanotubes Filled with Anionic Surfactants. *The Journal of Physical Chemistry C* **2016**, 120 (25), 13492-13502.

173. Lazzara, G.; Cavallaro, G.; Panchal, A.; Fakhrullin, R.; Stavitskaya, A.; Vinokurov, V.; Lvov, Y., An Assembly of Organic-Inorganic Composites Using Halloysite Clay Nanotubes. *Current Opinion in Colloid & Interface Science* **2018**, *35*, 42-50.
174. Lisuzzo, L.; Cavallaro, G.; Lazzara, G.; Milioto, S.; Parisi, F.; Stetsyshyn, Y., Stability of Halloysite, Imogolite, and Boron Nitride Nanotubes in Solvent Media. *Applied Sciences* **2018**, *8* (7), 1068.
175. Yu, Z.; Johnston, K. P.; Williams, R. O., Spray Freezing into Liquid Versus Spray-Freeze Drying: Influence of Atomization on Protein Aggregation and Biological Activity. *European Journal of Pharmaceutical Sciences* **2006**, *27* (1), 9-18.
176. Tho, I.; Liepold, B.; Rosenberg, J.; Maegerlein, M.; Brandl, M.; Fricker, G., Formation of Nano/Micro-Dispersions with Improved Dissolution Properties Upon Dispersion of Ritonavir Melt Extrudate in Aqueous Media. *European Journal of Pharmaceutical Sciences* **2010**, *40* (1), 25-32.
177. Pinto-Cocozza, E., Particle Size Reduction for Investigational New Drugs. *Pharmaceutical Technology* **2017**, *41* (6), 24-27.
178. Shariare, M. H.; Sharmin, S.; Jahan, I.; Reza, H. M.; Mohsin, K., The Impact of Process Parameters on Carrier Free Paracetamol Nanosuspension Prepared Using Different Stabilizers by Antisolvent Precipitation Method. *Journal of Drug Delivery Science and Technology* **2018**, *43*, 122-128.
179. Hu, J.; Dong, Y.; Ng, W. K.; Pastorin, G., Preparation of Drug Nanocrystals Embedded in Mannitol Microcrystals Via Liquid Antisolvent Precipitation Followed by Immediate (on-Line) Spray Drying. *Advanced Powder Technology* **2018**, *29* (4), 957-963.
180. Sinha, B.; Müller, R. H.; Möschwitzer, J. P., Bottom-up Approaches for Preparing Drug Nanocrystals: Formulations and Factors Affecting Particle Size. *International Journal of Pharmaceutics* **2013**, *453* (1), 126-141.
181. Meng, X.; Yang, D.; Keyvan, G.; Michniak-Kohn, B.; Mitra, S., Synthesis and Immobilization of Micro-Scale Drug Particles in Presence of B-Cyclodextrins. *Colloids and Surfaces B: Biointerfaces* **2012**, *92*, 213-222.
182. Chen, Y.; Mitra, S., Fast Microwave-Assisted Purification, Functionalization and Dispersion of Multi-Walled Carbon Nanotubes. *Journal of Nanoscience and Nanotechnology* **2008**, *8* (11), 5770-5775.
183. Ain-Ai, A.; Gupta, P. K., Effect of Arginine Hydrochloride and Hydroxypropyl Cellulose as Stabilizers on the Physical Stability of High Drug Loading Nanosuspensions of a Poorly Soluble Compound. *International Journal of Pharmaceutics* **2008**, *351* (1), 282-288.
184. Mersmann, A., Crystallization and Precipitation. *Chemical Engineering and Processing: Process Intensification* **1999**, *38* (4), 345-353.

185. Allen, L. V.; Popovich, N. G.; Ansel, H. C., *Ansel's Pharmaceutical Dosage Forms and Drug Delivery Systems*. Ninth ed.; 2012.